AD 296 122

ELECTRICAL ENGINEERING DEPARTMENT
UNIVERSITY OF MINNESOTA
INSTITUTE OF TECHNOLOGY

FINAL REPORT
Task II
January 1, 1961 to July 31, 1962

Study of Noise in Semiconductors and Semiconductor Devices

Volume II of two volumes

Contract DA 36-039 sc-85374
D.A. Proj. No. 3A99-21-001

PLACED BY U. S. ARMY SIGNAL CORPS ENGINEERING LABORATORY
FORT MONMOUTH, NEW JERSEY

REGENTS OF THE UNIVERSITY OF MINNESOTA
MINNEAPOLIS, MINNESOTA

"ASTIA Availability Notice: Qualified requestors may obtain copies of this report from ASTIA. ~~Foreign announcement or dissemination of this report by ASTIA is limited.~~" FOR OTS per 12 Feb 62

AD _____ Accession No. _____
Univ. of Minnesota, Minneapolis 14, Minn.
"STUDY OF NOISE IN SEMICONDUCTORS AND SEMICONDUCTOR DEVICES."
Final Report, 1 January 1961 to 31 July 1962
Volume Two, Task II
130 pp. -illus. - graphs
Contract DA 36-039 SC85374 (Task II)
DA Proj. No. 3A99-21-001
Unclassified Report
Final Report summarizing the theoretical and experimental work on tunnel diode mixers.

Unclassified

1. Semiconductor Noise
2. Contract DA36-039 SC85374 (Task II)

AD _____ Accession No. _____
Univ. of Minnesota, Minneapolis 14, Minn.
"STUDY OF NOISE IN SEMICONDUCTORS AND SEMICONDUCTOR DEVICES."
Final Report, 1 January 1961 to 31 July 1962
Volume Two, Task II
130 pp. -illus. - graphs
Contract DA 36-039 SC85374 (Task II)
DA Proj. No. 3A99-21-001
Unclassified Report
Final Report summarizing the theoretical and experimental work on tunnel diode mixers

Unclassified

1. Semiconductor Noise
2. Contract DA36-039 SC85374 (Task II)

AD _____ Accession No. _____
Univ. of Minnesota, Minneapolis 14, Minn.
"STUDY OF NOISE IN SEMICONDUCTORS AND SEMICONDUCTOR DEVICES."
Final Report, 1 January 1961 to 31 July 1962
Volume Two, Task II
130 pp. -illus. - graphs
Contract DA 36-039 SC85374 (Task II)
DA Proj. No. 3A99-21-001
Unclassified Report
Final Report summarizing the theoretical and experimental work on tunnel diode mixers,

Unclassified

1. Semiconductor Noise
2. Contract DA36-039 SC85374 (Task II)

AD _____ Accession No. _____
Univ. of Minnesota, Minneapolis 14, Minn.
"STUDY OF NOISE IN SEMICONDUCTORS AND SEMICONDUCTOR DEVICES."
Final Report, 1 January 1961 to 31 July 1962
Volume Two, Task II
130 pp. -illus. - graphs
Contract DA 36-039 SC85374 (Task II)
DA Proj. No. 3A99-21-001
Unclassified Report
Final Report summarizing the theoretical and experimental work on tunnel diode mixers.

Unclassified

1. Semiconductor Noise
2. Contract DA36-039 SC85374 (Task II)

AD _____ Accession No. _____ Univ. of Minnesota, Minneapolis 14, Minn. "STUDY OF NOISE IN SEMICONDUCTORS AND SEMICONDUCTOR DEVICES." Final Report, 1 January 1961 to 31 July 1962 Volume Two, Task II 130 pp. -illus. - graphs Contract DA 36-039 SC85374 (Task II) DA Proj. No. 3A99-21-001 Unclassified Report Final Report summarizing the theoretical and experimental work on tunnel diode mixers.	Unclassified 1. Semiconductor Noise 2. Contract DA36-039 SC85374 (Task II)	AD _____ Accession No. _____ Univ. of Minnesota, Minneapolis 14, Minn. "STUDY OF NOISE IN SEMICONDUCTORS AND SEMICONDUCTOR DEVICES." Final Report, 1 January 1961 to 31 July 1962 Volume Two, Task II 130 pp. -illus. - graphs Contract DA 36-039 SC85374 (Task II) DA Proj. No. 3A99-21-001 Unclassified Report Final Report summarizing the theoretical and experimental work on tunnel diode mixers	Unclassified 1. Semiconductor Noise 2. Contract DA36-039 SC85374 (Task II)
AD _____ Accession No. _____ Univ. of Minnesota, Minneapolis 14, Minn. "STUDY OF NOISE IN SEMICONDUCTORS AND SEMICONDUCTOR DEVICES." Final Report, 1 January 1961 to 31 July 1962 Volume Two, Task II 130 pp. -illus. - graphs Contract DA 36-039 SC85374 (Task II) DA Proj. No. 3A99-21-001 Unclassified Report Final Report summarizing the theoretical and experimental work on tunnel diode mixers,	Unclassified 1. Semiconductor Noise 2. Contract DA36-039 SC85374 (Task II)	AD _____ Accession No. _____ Univ. of Minnesota, Minneapolis 14, Minn. "STUDY OF NOISE IN SEMICONDUCTORS AND SEMICONDUCTOR DEVICES." Final Report, 1 January 1961 to 31 July 1962 Volume Two, Task II 130 pp. -illus. - graphs Contract DA 36-039 SC85374 (Task II) DA Proj. No. 3A99-21-001 Unclassified Report Final Report summarizing the theoretical and experimental work on tunnel diode mixers.	Unclassified 1. Semiconductor Noise 2. Contract DA36-039 SC85374 (Task II)

Study of Noise in Semiconductor and Semiconductor Devices

Final Report

January 1, 1961 to July 31, 1962

The object of this investigation is the study of noise in semiconductors and semiconductor devices and the theoretical interpretation of the results.

Volume II of two volumes

Task II

Contract No. DA 36-039 sc-85374

D.A. Proj. No. 3A99-21-001

A. van der Ziel, Chief Investigator

Table of Contents

Table of Contents (continued)

List of Illustrations

List of Illustrations (continued)

I. Abstract

This study is to investigate the noise in tunnel diode mixers emphasising on the correlation between the high-frequency noise and the intermediate-frequency noise. Methods of optimization of the tunnel diode mixer operation are discussed with respect to the noise figure, available gain and stability, etc. The similar study is extended to the double sideband mixers.

In Chapter I a historical survey of mixers is briefly mentioned. The advantages of using tunnel diode for mixing and the experimental data of the tunnel diode mixers reported by others are illustrated.

In Chapter II the tunnel diode mixer is represented by a simple two-port network equivalent circuit in terms of the parameters I_{eo}, I_{el}, g_o and g_1. From the equivalent circuit, the expressions are derived for the input conductance, the output conductance and the available gain. It is found that the input and output conductances are not always positive and that an available gain larger than unity is possible for tunnel diode mixers.

In Chapter III the noise theory for shot noise only is derived. The noise figure is minimized by varying the signal conductance. Due to the interaction of the high-frequency noise and the intermediate-frequency noise a correlation term exists. Properly operating the

tunnel diode by making use of the correlation term, a partial noise cancellation can be achieved.

In Chapter IV the total system noise figure for both positive and negative output conductance of the mixer are studied. It is shown that feedback from a capacitance in the anode lead of a triode or from an inductance in the cathode lead of a triode can give a low-noise conductance for the output of the tunnel diode mixer. The noise figure of the mixer plus the i.f. stage with feedback from an inductance in the cathode lead are derived. The noise figure and power gain of the tunnel diode mixer plus a grounded grid amplifier have been calculated. The stability of these circuits is also discussed.

In Chapter V a graphical method as well as an experimental method for determining the sign of the parameters I_{eo}, I_{el}, g_o and g_1 of the tunnel diode mixer are illustrated. Other possible methods are also mentioned. A method has been devised to determine the current amplification factor of the tunnel diode mixer by using two noise diodes.

In Chapter VI the conditions required for displaying the I-V curve of the tunnel diode are given. I-V curves of different types of tunnel diodes are traced and investigated. A method is given to extend the results of

tunnel diode mixing for one particular tunnel diode to other diodes. Noise in different types of tunnel diodes is measured in the positive conductance regions.

In Chapter VII operation of the tunnel diode mixer is discussed with the help of seven theoretical figures and two modes of operation are given. Theoretical analysis was done on the tunnel diode mixer for different types of tunnel diodes at different operating conditions. The effect of the local oscillator voltage amplitude and the signal conductance on the tunnel diode mixer operation are discussed.

In Chapter VIII the experimental tunnel diode mixer and the noise measurement equipment are described. Experimental results are obtained and the noise measurement method is illustrated. A comparison with the theoretical results is made. Good agreement with the theory and the importance of the correlation term between the high-frequency and the intermediate-frequency are noted.

In Chapter IX the equivalent circuit, available gain and noise figure F of a double side band mixer are derived. The factor (F-1) of the double side band mixer is more than 3 dB better than that of a single side band mixer.

Chapters X and XI give conclusions and recommendations respectively.

The final results obtained in this research are:

1) Correlation between intermediate-frequency noise and high-frequency noise is important.

2) Low noise and high gain do not go together. The best tunnel diode mixers are of the back diode type.

3) It is not recommended to use tunnel diodes with a large negative resistance region. If one does so, nevertheless, circuiting can be designed that gives stability at low additional noise.

4) Approximate evaluation of the mixer operation can be made directly from the I-V characteristic of the device.

II. Purpose

The purpose of Volume II of this report is to give a summary of the progress made on Task II of this project during the period January 1, 1961 to July 31, 1962.

The contract calls for an investigation to determine the cause and effect of the noise that occurs in semiconductors and semiconductor devices when dc current is flowing through the sample or device.

Task II was a study of noise properties of tunnel diode mixers and was divided as follows:

(a) A theoretical investigation of the noise and of the correlation between the direct noise signal and the converted high-frequency noise at the output of the device; an examination of the effect of the operating conditions on the noise performance.

(b) An experimental determination of the noise performance in the various operating regions; a determination of the noise figure and the parameters involved.

III. Communications and Reports

During the contract period, the project engineer Mr. P. Newman of the Evans Signal Corps Laboratory visited the University of Minnesota to discuss the progress on the project; the most recent visit was on May 23, 1962.

Dr. A. van der Ziel attended the 1961 International Solid State Circuits Conference, February 15-17, 1961 and the 1962 International Solid State Circuits Conference, February 14-16, 1962 at Philadelphia, Pennsylvania.

List of Publications:

Shi-fang Lo, "Noise in Tunnel Diode Mixers," Proc. IRE 49, 1688-1689, Nov. (1961).

Shi-fang Lo, Ph.D. thesis entitled "Noise in Tunnel Diode Mixers," University of Minnesota, July 1962.

IV. General Outline of Work Accomplished, Task II

I. Introduction

The mixer is a device which converts a signal from one frequency to another. Any nonlinear element such as a vacuum tube diode, triode, pentode, crystal diode or tunnel diode can be used as a mixing element in the mixer. Owing to the limitation of the transit time effects, the vacuum tube is used as a mixer only in the lower frequency part of the microwave region below 1000 Mc or so. The crystal diode, on the other hand, has a narrow junction, the transit time effects are small and can be neglected even in the microwave region. During the World War II numerous investigations and improvements were made on the microwave crystal mixer, which became superior to the vacuum tube mixer.[1,2] Since the crystal diode is a passive element, no mixer gain can be obtained. This is undesirable as far as the total system noise is concerned.

In 1957, the tunnel diode was first mentioned publicly. The negative resistance portion of the tunnel diode current-voltage characteristic leads to the possibilities of mixing with gain and self-excitation mixing without the local oscillator voltage. Also the tunnel diode is tolerant to nuclear radiation and suitable for wide temperature range and high-frequency

applications.[3,4] Several papers have been published on the subject of the tunnel diode mixer using different theoretical approaches and experimental techniques.[5-14] A noise figure theory for the tunnel diode mixer was also derived here independently in late 1959. It agrees quite well with refs. 6 and 8 but deviates a little from 5 due to the approximations made in 5. The deviation has been reported in refs. 9 and 11. From both the theoretical and experimental results reported, the tunnel diode mixer can have power gain greater than unity and also the noise figure is usually better than that of the crystal diode mixer. A measured UHF noise figure of 2.8 dB and power gain of 22.7 dB when converting from a signal frequency of 210 Mc to an intermediate frequency of 30 Mc at a rather low impedance level is given in ref. 5. In ref. 12 a conversion gain of 5 dB was measured at a signal frequency of 3000 Mc using a 30 Mc intermediate frequency. The best measured noise figure obtained in ref. 13 is 3 dB at a signal frequency of 1200 Mc using a 30 Mc intermediate frequency with a high but unstable gain.

The impressive performance of the tunnel diode mixer makes it a worthwhile topic of investigation. The purpose of this study is to understand and optimize the tunnel diode mixer with respect to stability, power gain, noise figure, the effects of the input and output

terminations, the bias and the local oscillator voltage, etc. The emphasis will be on the identification of the noise sources and the measurement of the correlation between the signal frequency component noise and the intermediate frequency component noise. Several intermediate frequency amplifiers with high input conductance and small noise contribution are introduced for the cases when the output conductance of the mixer is negative.

II. Mixer Circuits

A. Conductance Matrix

It is true that the mixer is a nonlinear device, but the nonlinearity is only important to the local oscillator voltage and the interaction with the signals. The relation of the small signals at the input, output, image and all the side bands can still be represented by a set of linear equations.

Suppose a dc bias and a local oscillator voltage is applied to the nonlinear element. The conductance of this element will be a function of time and varies periodically with the local oscillator voltage. If a time reference can be assumed such that the instantaneous conductance of the nonlinear element g(t) is an even function, the Fourier series representation of g(t) is

$$g(t) = g_o + 2g_1 \cos\omega_h t + 2g_2 \cos 2\omega_h t + \cdots\cdots \qquad (2.1)$$

where ω_h is the local oscillator frequency. The assumption of the time reference is true if the local oscillator harmonic voltages are zero or are correctly phased with respect to the fundamental. This assumption is believed to be a good approximation for the actual mixers.

If a small rf signal $V_{io}\cos(\omega_i t + \phi_i)$ and a small i.f. signal $V_{mo}\cos(\omega_m t + \phi_m)$ is applied to the mixing element having a conductance g(t), currents with all kinds of frequencies will exist. This can be seen by multiplying the rf and i.f. signals, respectively, by the g(t) of (2.1). The signals of interest at the particular frequencies can always be obtained by using tuned circuits. Suppose the frequency relation $\omega_i = \omega_h + \omega_m$ is used and the rf image and all the side bands are shorted out by ideal tuned circuits, the linear relations between these rf and i.f. quantities are

$$I_i = g_o V_i + g_1 V_m$$

$$I_m = g_1 V_i + g_o V_m \qquad (2.2)$$

They can be expressed in matrix form as

$$\begin{bmatrix} I_i \\ I_m \end{bmatrix} = Y \begin{bmatrix} V_i \\ V_m \end{bmatrix} \qquad (2.3)$$

where

$$Y = \begin{bmatrix} g_o & g_1 \\ g_1 & g_o \end{bmatrix} \qquad (2.4)$$

is the so called "conductance matrix" of the mixer. The subscripts i and m refer, respectively, to the rf and i.f. signals, where I and V are the complex rms values of the current and voltage. Equations (2.2) and (2.3) have the same form as the current-voltage relation of a two-port network, but now the input and output are at different frequencies and the g's are the coefficients of the Fourier components instead of a time independent conductance in the ordinary circuit analysis. Hence a mixer can be considered as a two-port network. A mixer, having signal current generator I_s and signal conductance g_s at the rf input and load conductance g_L at the i.f. output, is represented by a two-port network in Fig. 1.

The case for mixing on a higher harmonic or mixing on the fundamental using the frequency relations other than $\omega_i = \omega_h + \omega_m$ can be derived in a similar way.[15]

It is well known that the tunnel diode can be represented by an equivalent circuit which consists of a voltage dependent conductance g(V) in parallel with a junction barrier capacitance C, a series inductance L, and a series resistance R_s (Fig. 2). The above derivation applies to the tunnel diode only when the R_s, L and

C are negligible or if R_s is very small and the reactive elements are tuned out externally. The general equivalent circuit of a tunnel diode mixer including R_s, L and C is complicated but still can be derived in the similar way.[1,8]

B. Output Conductance

The output conductance of a mixer when a signal conductance g_s is connected to the input terminals can be obtained by substituting $I_i = - g_s V_i$ into (2.2). The output conductance g_{out} is given by

$$g_{out} = g_o - \frac{g_1^2}{g_o + g_s} \tag{2.5}$$

By substituting $y = g_{out} - g_o$, $x = g_s + g_o$, (2.5) can be written as

$$y = - \frac{g_1^2}{x} \tag{2.6}$$

which is a rectangular hyperbola in the second and fourth quadrant having the x and y axes as asymptotes and vertexes at $(-g_1, g_1)$ and $(g_1, -g_1)$ as shown in Fig. 3.

The dependence of g_{out} upon g_s will be considered for four separate cases. The g_{out} versus g_s curves can be obtained from Fig. 3 for each case by properly locating the g_{out} and g_s axes as shown in Table I.

Table I

Case	Location of g_s axis	Location of g_{out} axis
(a) $g_o > 0$; $g_o^2 > g_1^2$ (b) $g_o > 0$; $g_o^2 < g_1^2$	$y = -g_o$	$x = g_o$
(c) $g_o < 0$; $g_o^2 > g_1^2$ (d) $g_o < 0$; $g_o^2 < g_1^2$	$y = \lvert g_o \rvert$	$x = -\lvert g_o \rvert$

For convenience of later reference the g_{out} versus g_s curves are plotted separately in Fig. 4. Since the Friis' formula for stages in cascade is only applicable when the output conductance of the mixer is positive, the positive g_{out} regions are indicated by shaded areas.

C. Input Conductance

Analogous to the previous section, the input conductance of a mixer when a load conductance g_L is connected to the output terminals can be obtained by substituting $I_m = -g_L V_m$ into (2.2). The input conductance g_{in} is given by

$$g_{in} = g_o - \frac{g_1^2}{g_o + g_L} \qquad (2.7)$$

Equation (2.7) indicates that the input conductance is a function of load conductance and the mixer conductance matrix elements. Friis' formula does not put any condition on the input conductance of the mixer, so that g_{in} may have negative values. When g_{in} is negative, the signal conductance g_s must be chosen such that $(g_s + g_{in}) > 0$ for stable operation.

D. Available Gain

From the terminal conditions shown in Fig. 1, we have

$$I_i = I_s - g_s V_i \quad \text{and} \quad I_m = - g_L V_m \tag{2.8}$$

Substituting (2.8) into (2.2) and solving for V_m, we obtain

$$V_m = \frac{I_s g_1}{(g_o + g_s)(g_o + g_L) - g_1^2} \tag{2.9}$$

Thus, the power gain of the mixer is

$$G = \frac{\text{Power fed into load}}{\text{Power available at source}} = \frac{V_m V_m^* g_L}{I_s I_s^* / 4 g_s}$$

$$= \frac{4 g_s g_L g_1^2}{\left[(g_o + g_s)(g_o + g_L) - g_1^2\right]^2} \tag{2.10}$$

Where the I and V are complex rms values.

For convenience, the current amplification factor $F_c = g_1/(g_o + g_s)$ will be defined and derived here by

substituting $I_m = - g_L V_m$ into (2.9) and letting $g_L = \infty$. Then

$$I_m = -\left(\frac{g_1}{g_o + g_s}\right) I_s = - F_c I_s \qquad (2.11)$$

If $g_1^2 > g_o^2$, the mixer circuit is not unconditionally stable, since G can be made infinitely large by proper choice of g_s and g_L. In other words, under high gain conditions the mixer may have negative input conductance or negative output conductance or both. Also, under these conditions the mixer noise figure may not have the minimum value, as will be seen below.

If $g_1^2 < g_o^2$ and $g_o > 0$, the circuit is unconditionally stable and G can not exceed unity. This is the ordinary diode mixer case and will not be discussed here.[15,16]

If g_{out} is positive, G can be optimized by putting $g_L = g_{out}$, one then obtains the available gain

$$G_{av} = \frac{g_s}{g_{out}} \left(\frac{g_1}{g_o + g_s}\right)^2 = \frac{g_s g_1^2}{(g_o + g_s)(g_o^2 + g_o g_s - g_1^2)} \qquad (2.12)$$

It follows from the results of Sec. II B, that when $g_s = (g_s)_{opt}$,* the relation $g_{out} > 0$ is not always satisfied. If one keeps $g_s = (g_s)_{opt}$, the relation $g_{out} > 0$ is only

*In Chapter III we shall show that the noise figure of the mixer will have a minimum value if $g_s = (g_s)_{opt} = \sqrt{g_o^2 - 2 g_o g_1 I_{ei}/I_{eo} + g_1^2}$.

satisfied if g_o and g_1 meet certain requirements. Even if $g_{out} > 0$ when $g_s = (g_s)_{opt}$, then the available gain G_{av} may not be the optimum value at the same time. It should be mentioned that G_{av} may not exceed unity in some cases.

There are too many things involved to make a general study which concerns the optimum available gain ($g_L = g_{out} > 0$ of course) and the minimum noise figure when $g_s = (g_s)_{opt}$. An investigation of the special cases will be made later in Sec. VII E.

III. Noise Theory of a Tunnel Diode Mixer

Let a small pulse occur in the diode current between $t = \tau$ and $t = (\tau + d\tau)$. Developing this pulse into a Fourier series, we obtain an i.f. component $a\cos\omega_m(t - \tau)$ and an rf component $-a\cos\omega_1(t - \tau)$. The minus sign associated with the rf component is due to the current direction assigned to the rf component and the i.f. component as shown in Fig. 1. When the diode current is flowing in the same direction as the i.f. component, it must be in the opposite direction as the rf component.

If the input were also short-circuited, $a\cos\omega_m(t - \tau)$ would be the total i.f. noise current. But if the input is not short-circuited, an rf voltage is developed across the input and this gives an i.f. current by conversion. The rf component current $-a\cos\omega_1(t - \tau)$ corresponds to a

current generator I_s of $a\cos\omega_i(t - \tau)$ applied to the input (Fig. 1). The amplitude and direction of the converted i.f. current is $-aF_c$ which is determined by Eq. (2.11). The input phase angle $-\omega_i\tau$ is preserved when $\omega_m = \omega_i \pm \omega_h$ and changes sign when $\omega_m = \omega_h - \omega_i$.[15] Thus, the converted i.f. component current is

$$-aF_c\cos\left[\omega_m(t - \tau) \pm \omega_h\tau\right] \tag{3.1}$$

where the plus sign refers to $\omega_m = \omega_h \pm \omega_i$, the minus sign to $\omega_m = \omega_i - \omega_h$. We have neglected the circuit conductance g_c. Combining the two i.f. components $a\cos\omega_m(t - \tau)$ and (3.1), the square of the amplitude of the total i.f. noise current is

$$a^2\ (1 - 2F_c\cos\omega_h\tau + F_c{}^2) \tag{3.2}$$

The mean-square noise current can be found by taking averages over an ensemble and over equivalent instances τ. For shot noise only,

$$d(\overline{i_\tau{}^2}) = 2eI_{eq}(\tau)df\ \frac{d(\omega_h\tau)}{2\pi}\ (1 - 2F_c\cos\omega_h\tau + F_c{}^2) \tag{3.3}$$

The reason is an obvious one, for if we integrate this over a full cycle for the case that $F_c = 0$ and $I_{eq}(\tau) = I$ is independent of τ we must get Schottky's theorem $\overline{i^2} = \int_{-\pi}^{\pi} d(\overline{i_\tau{}^2}) = 2eIdf$.

We now integrate with respect to τ and bear in mind that

$$\frac{1}{2\pi}\int_{-\pi}^{\pi} I_{eq}(\tau)\, d(\omega_h \tau) = I_{eo} = \text{average value of } I_{eq}(\tau) \tag{3.4}$$

$$\frac{1}{2\pi}\int_{-\pi}^{\pi} I_{eq}(\tau)\cos\omega_h\tau\, d(\omega_h\tau) = I_{e1} = \text{one half of}$$

$$\text{the first Fourier component of } I_{eq}(\tau) \tag{3.5}$$

Hence

$$\overline{i_d^2} = \int_{-\pi}^{\pi} d(\overline{i_\tau^2}) = 2e\left[I_{eo}(1+F_c^2) - 2I_{e1}F_c\right] df \tag{3.6}$$

This is the mean-square value of the short-circuit i.f. noise current caused by the device. The signal source (conductance g_s) gives a mean-square short-circuit i.f. noise current

$$\overline{i_s^2} = 4kTg_s df \frac{g_1^2}{(g_o + g_s)^2} = 4kTg_s F_c^2 df \tag{3.7}$$

so that the noise figure F is

$$F = 1 + \frac{\overline{i_d^2}}{\overline{i_s^2}} = 1 + \frac{2eI_{eo}df}{4kTg_s df}\left(\frac{1 - 2F_c I_{e1}/I_{eo} + F_c^2}{F_c^2}\right) \tag{3.8}$$

which may be written as

$$F = 1 + \frac{e}{2kT}\frac{I_{eo}}{g_s}\left\{\frac{(g_s+g_o)^2 - 2g_1(g_s+g_o)I_{e1}/I_{eo} + g_1^2}{g_1^2}\right\} = 1$$

$$+ \frac{e}{2kT}\frac{I_{eo}}{g_s}\left\{\frac{g_s^2 + 2g_s(g_o - g_1 I_{e1}/I_{eo}) + (g_o^2 - 2g_o g_1 I_{e1}/I_{eo} + g_1^2)}{g_1^2}\right\} \tag{3.8a}$$

This may be rewritten as

$$F = 1 + \frac{e}{2kT}\frac{I_{eo}}{g_1^2}\left\{g_s + \frac{1}{g_s}\left(g_o^2 - 2g_o g_1 \frac{I_{e1}}{I_{eo}} + g_1^2\right) + 2\left(g_o - g_1 \frac{I_{e1}}{I_{eo}}\right)\right\} \tag{3.8b}$$

Differentiation with respect to g_s gives that F has a minimum value if

$$g_s = (g_s)_{opt} = \sqrt{g_o^2 - 2g_o g_1 \frac{I_{e1}}{I_{eo}} + g_1^2}\,, \tag{3.9}$$

unless $\left(g_o^2 - 2g_o g_1 \frac{I_{e1}}{I_{eo}} + g_1^2\right) < 0$

and

$$F = F_{min} = 1 + \frac{e}{2kT}\frac{I_{eo}}{g_1^2}\left\{2\sqrt{g_o^2 - 2g_o g_1 \frac{I_{e1}}{I_{eo}} + g_1^2} + 2\left(g_o - g_1 \frac{I_{e1}}{I_{eo}}\right)\right\} \tag{3.10}$$

The condition

$$\left(g_o^2 - 2g_o g_1 \frac{I_{e1}}{I_{eo}} + g_1^2\right) = \left(g_o - g_1 \frac{I_{e1}}{I_{eo}}\right)^2 + g_1^2\left\{1 - \left(\frac{I_{e1}}{I_{eo}}\right)^2\right\} \geq 0 \tag{3.9a}$$

is always satisfied since $\left|I_{e1}/I_{eo}\right| \leq 1$. To prove this, observe that $I_{eq}(\tau) \geq 0$ and hence

$$I_{el} \quad \frac{1}{2\pi} \int_{-\pi}^{\pi} I_{eq}(\tau) \cos\omega_h\tau \, d(\omega_h\tau) \quad \frac{1}{2\pi} \int_{-\pi}^{\pi} I_{eq}(\tau) \, d(\omega_h\tau)$$

$$= I_{eo}$$

The result leads to the well-known diode formula if applied to a vacuum tube diode mixer by changing a^2 into $e4kTg_m(\tau)df$ instead of $2eI_{eq}(\tau)df$.[15]

IV. Total System Noise Figure of a Receiver

A. Positive Mixer Output Conductance

If the output conductance of the mixer, g_{out}, is positive, the total system noise figure F_{tot} can be obtained by Friis' formula

$$F_{tot} = F + \frac{F_{i.f.} - 1}{G_{av}} \tag{4.1}$$

Here F is the noise figure of the mixer, G_{av} is the available gain of the mixer and $F_{i.f.}$ is the noise figure of the first i.f. stage. Since the gain of the first i.f. stage is usually large, the contribution to the total system noise figure from stages occurring after the first i.f. stage can be neglected. This is the reason that (4.1) contains only the noise figures of the mixer and the first i.f. stage. Equation (4.1) shows that the mixer available gain plays a very important role in determining the total system noise figure of a receiver. For better total system noise figure the mixer should have not only low noise figure but also high available gain

at the same time in order to reduce the noise contribution from the first i.f. stage.

If G_{av} is sufficiently large, $F_{tot} \simeq F$. Then F_{tot} can be minimized by minimizing F if G_{av} has not been affected much.

If the mixer available gain is less than unity (actually a power loss), the noise of the first i.f. stage might become important. We can best minimize F_{tot} by operating the mixer having minimum noise figure and maximum available gain at the same time, but this is not always possible. F_{tot} can approximately be minimized by minimizing F and taking the value of G_{av} that is obtained under that condition. Usually there is little difference between the value of F_{tot} that is thus obtained and the value obtained by minimizing (4.1) accurately.

It is understood that g_{out} is positive only under certain conditions which were discussed in Sec. II B.

B. Negative Mixer Output Conductance[17]

If the output conductance of the mixer is negative, the available gain of the mixer can not be defined. Therefore Friis' formula is no longer applicable. A general expression for F_{tot} if $g_{out} < 0$ is very difficult; especially since one has to satisfy the condition $(g_{out} + g_L) > 0$ in that case in order to have stability. In this section several topics concerning the tunnel diode

mixer output loading and its noise effect will be studied. Two low-noise load conductances and two total system noise figures of the tunnel diode mixer plus a special i.f. amplifier are discussed.

1. Loading the Tunnel Diode Mixer Output With a Low-Noise Load Conductance

It will be shown that feedback can provide a low-noise output load for a tunnel diode mixer. Two circuits will be discussed:

a. Feedback from a capacitance in the anode lead of a triode

The circuit is shown in Fig. 5a. It is easily demonstrated that the input admittance:

$$Y = \frac{I}{V} = j\omega \frac{C_1 C_2}{C_1 + C_2} + g_m \frac{C_1}{C_1 + C_2} = j\omega C + g \qquad (4.2)$$

The apparent input capacitance C can be removed by tuning, so that only the conductance g remains. By appropriate choice of C_1 and C_2 this conductance can vary between 0 and the transconductance g_m of the triode.

To determine the noise temperature T_n of g, we turn to Fig. 5b. The noise of the tube is represented by an emf $\sqrt{4kTR_n df}$ in series with the grid and a current generator $\sqrt{2eI_{eq} df}$ in parallel to the grid. The first term represents the tube noise and the second term the induced grid noise; both terms are considered to be

independent. It is easily demonstrated that the mean square value $\overline{i_n^2}$ of the noise current flowing in the lead short-circuiting the input is given as:

$$\overline{i_n^2} = 4kTR_n df g^2 + 2eI_{eq} df \qquad (4.3)$$

Equating $\overline{i_n^2} = 4kT_n g df$, one obtains for the noise temperature T_n of g:

$$T_n = TR_n g + \frac{eI_{eq}}{2kg} \qquad (4.4)$$

which has a minimum value;

$$(T_n)_{min} = 2\sqrt{TR_n \left(\frac{eI_{eq}}{2k}\right)} \text{ for } g = g_{opt} = \sqrt{\frac{eI_{eq}}{2kTR_n}} \qquad (4.5)$$

Taking representative values like R_n = 250 ohms, T = 300°K, I_{eq} = 5 μA at 30 Mc yield: T_n = 93°K at g_{opt} = 0.62 x 10^{-3} mhos, T_n = 104°K at g = 10^{-3} mhos and T_n = 300°K for g = 3.9 x 10^{-3} mhos. This example indicates that relatively "cool" loads can be obtained as long as the conductance does not exceed 10^{-3} mhos, but that the load becomes noisy if the conductance g becomes too large.

b. <u>Feedback from an inductance in the cathode lead of a triode</u>

The circuit is shown in Fig. 6a; C_{cg} may either be the cathode-grid capacitance or may be increased by adding an external capacitance, L_c is the cathode lead

inductance. A calculation shows that the input admittance is

$$Y = \frac{I}{V} = g + j\omega C = \frac{j\omega C_{cg}}{(1 - \omega^2 L_c C_{cg} + j\omega L_c g_m)} \qquad (4.6)$$

where

$$\omega C = \frac{\omega C_{cg}(1 - \omega^2 L_c C_{cg})}{(1 - \omega^2 L_c C_{cg})^2 + (\omega L_c g_m)^2} \; ;$$

$$g = \frac{\omega^2 L_c C_{cg} g_m}{(1 - \omega^2 L_c C_{cg})^2 + (\omega L_c g_m)^2} \; . \qquad (4.6a)$$

Equation (4.6) is valid under all load conditions except when the output is open-circuited. The apparent capacitance C can be eliminated by tuning, so that only the conductance g remains. For a certain value of L_c, g has an optimum value g_{opt}. Differentiating the expression for g shows that

$$g = g_{opt} = \frac{1}{2} g_m \frac{\omega C_{cg}}{(\sqrt{g_m^2 + \omega^2 C_{cg}^2} - \omega C_{cg})}$$

for

$$\omega L_c = \frac{1}{\sqrt{g_m^2 + \omega^2 C_{cg}^2}} \qquad (4.7)$$

As long as $\omega^2 C_{cg}^2 \ll g_m^2$, this expression reduces to:

$$g_{opt} \simeq \frac{1}{2} \omega C_{cg} \quad \text{for} \quad \omega L_c \simeq \frac{1}{g_m} \qquad (4.7a)$$

Taking $g_m = 10^{-2}$ mhos, f = 30 Mc; $C_{cg} = 10$ $\mu\mu$f, then $g \simeq 10^{-3}$ mhos at $L \simeq 0.5$ μh. At higher frequencies or for larger values of C_{cg} one can do considerably better.

To determine the noise temperature T_n of g, turn to Fig. 6b. The noise of the tube is represented by a noise current generator $i_a = \sqrt{4kTR_n df g_m^2}$ in parallel to L_c and a noise current generator $\sqrt{2eI_{eq}df}$ in parallel to C_{cg}; the latter term represents the induced grid noise. Both noise generators are considered to be independent.

It can be shown from Fig. 6b that the mean-square value $\overline{i_n^2}$ of the noise current flowing in the lead short-circuiting the input is given as:

$$\overline{i_n^2} = \frac{4kTR_n df(\omega^2 L_c C_{cg} g_m)^2 + 2eI_{eq}df\left[1 + (\omega L_c g_m)^2\right]}{\left[(1 - \omega^2 L_c C_{cg})^2 + (\omega L_c g_m)^2\right]} \qquad (4.8)$$

Equation (4.8) is also valid under all load conditions except when the output is open-circuited. Equating $\overline{i_n^2} = 4kT_n g df$, yields for the noise temperature T_n:

$$T_n = R_n T \omega^2 L_c C_{cg} g_m + \left(\frac{eI_{eq}}{2k}\right) \frac{\left[1 + (\omega L_c g_m)^2\right]}{\omega^2 L_c C_{cg} g_m} \qquad (4.9)$$

Considered as a function of L_c, T_n has a minimum value $(T_n)_{min}$:

$$(T_n)_{min} = 2\sqrt{R_n T\left(\frac{eI_{eq}}{2k}\right) + \left(\frac{eI_{eq}}{2k\omega C_{cg}}\right)^2}$$

$$\text{for } \omega^2 L_c C_{cg} g_m = \sqrt{\frac{eI_{eq}}{2k\left[R_n T + eI_{eq}/(2\omega^2 C_{cg}{}^2 k)\right]}} \qquad (4.10)$$

If $eI_{eq}/(2k\omega^2 C_{cg}{}^2) \ll R_n T$, this reduces to

$$(T_n)_{min} = 2\sqrt{R_n T\left(\frac{eI_{eq}}{2k}\right)} \text{ for } \omega^2 L_c C_{cg} g_m = \sqrt{\frac{eI_{eq}}{2kR_n T}} \qquad (4.10a)$$

Substituting into the expression for g of (4.6a) yields, if $\omega^2 L_c C_{cg} \ll 1$ and $(\omega L_c g_m)^2 \ll 1$

$$g = g_{opt} \simeq \sqrt{\frac{eI_{eq}}{2kTR_n}} \qquad (4.10b)$$

Substituting R_n = 250 ohms, C_{cg} = 10 μμf; I_{eq} = 5 μa at f = 30 Mc and T = 300°K yields $(T_n)_{min}$ = 98°K with g = 0.60 x 10^{-3} mhos for $L_c \simeq$ 0.17 μh.

The conditions for Eqs. (4.10a) and (4.10b) are satisfied within 10% compared with the exact expressions. Moreover, since I_{eq} is proportional to ω^2, the conditions are reasonably well satisfied over a reasonably wide frequency range. As a consequence the two cases discussed in this section give approximately equal results.

The result of our discussion is therefore that reasonably low equivalent noise temperatures can be obtained at 30 Mc for output load conductances up to about 10^{-3} mhos. Such low-noise load conductances may stabilise

tunnel diode mixers with negative output conductances and reduce the noise figure of mixer plus load.

2. Noise Figure of a Tunnel Diode Mixer with a Feedback I.F. Stage

We now consider the situation in which the low-noise output load is not made with the help of a separate stage, but in which the feedback is taken from the cathode lead of the first i.f. stage. The noise of the "low-noise load" is then correlated with the noise of the first i.f. stage so that both have to be taken into account together.

The circuit is shown in Fig. 7. The noise of the mixer stage is represented by a current generator $F_c \sqrt{4kTFg_s df}$ in parallel with the output conductance g_{out} of the mixer. Here F_c is the mixer current gain, F the mixer noise figure, g_s the source conductance; the output conductance, g_{out}, of the mixer may be negative. The noise of the i.f. stage is represented by a current generator $\sqrt{2eI_{eq}df}$ connected between grid and cathode and a current generator $i_a = \sqrt{4kTR_n g_m^2 df}$ between anode and cathode. The tuned circuit impedance is represented by the conductance g_c and the tuning is represented by the positive or negative capacitance C_1. L_c is the cathode inductance that supplies the feedback and C_{cg} is the (internal + external) capacitance between grid and cathode.

Introducing the following circuit parameters

$$Y_{in} = g_{out} + g_c + j\omega C_1 ; \; Y_{tot} = Y_{in} + \frac{Y_c Y_{cg}}{Y_c + Y_{cg} + g_m} \quad (4.11)$$

$$Y_2' = g_m \frac{Y_c}{Y_c + Y_{cg} + g_m}$$

where

$$Y_{cg} = j\omega C_{cg} \; ; \; Y_c = 1/(j\omega L_c) \quad (4.12)$$

one obtains the following contributions to the mean-square value of the noise current flowing in the short-circuited output lead:

a) Mixer noise: $$F_c^2 4kTFg_s df \left| \frac{Y_2'}{Y_{tot}} \right|^2 \quad (4.13)$$

b) The circuit noise: $$4kTg_c df \left| \frac{Y_2'}{Y_{tot}} \right|^2 \quad (4.14)$$

c) Induced grid noise:

$$2eI_{eq} \, df \left| \frac{Y_c + Y_{in}}{Y_c} \right|^2 \left| \frac{Y_2'}{Y_{tot}} \right|^2 \quad (4.15)$$

d) Tube noise:

$$4kTR_n df \left| Y_{in} + Y_{cg} + \frac{Y_{cg} Y_{in}}{Y_c} \right|^2 \left| \frac{Y_2'}{Y_{tot}} \right|^2 \quad (4.16)$$

The thermal noise of the source conductance g_s of the mixer gives a contribution

$$F_c^2 \, 4kTg_s df \left| \frac{Y_2'}{Y_{tot}} \right|^2 \quad (4.17)$$

to $\overline{i_n^2}$. Adding Eqs. (4.13) - (4.16) and dividing by (4.17) gives for the total noise figure F_{tot}, since $(e/2kT) \simeq 20$:

$$F_{tot} = F + \frac{1}{F_c^2 g_s} \left[g_c + 20\, I_{eq} (1 - \omega^2 L_c C_1)^2 + R_n \left\{ \omega C_{cg} + \omega C_1 (1 - \omega^2 L_c C_{cg}) \right\}^2 + (g_{out} + g_c)^2 \left\{ R_n (1 - \omega^2 L_c C_{cg})^2 + 20\, I_{eq} \omega^2 L_c^2 \right\} \right] \quad (4.18)$$

Since F, F_c and g_s are fixed, one has to choose C_1 and L_c such that F_{tot} is minimized.

It is now generally true that $20\, I_{eq} \ll R_n (\omega C_{cg})^2$. For taking the following representative values: $R_n = 250$ ohms, $I_{eq} = 5$ μA at f = 30 Mc, $C_{cg} = 10$ μμf, one obtains $R_n (\omega C_{cg})^2 = 9 \times 10^{-4}$ and $20\, I_{eq} = 10^{-4}$. Since I_{eq} and $(\omega C_{cg})^2$ both vary as ω^2, the inequality holds over a wide frequency range. Considered as a function of C_1, F_{tot} is practically minimized if

$$\omega C_{cg} + \omega C_1 (1 - \omega^2 L_c C_{cg}) = 0. \quad (4.19)$$

Substituting into Eq. (4.18), one obtains

$$F_{tot} = F + \frac{1}{F_c^2 g_s} \left[g_c + \frac{20\, I_{eq}}{(1 - \omega^2 L_c C_{cg})^2} + (g_{out} + g_c)^2 \left\{ R_n (1 - \omega^2 L_c C_{cg})^2 + 20\, I_{eq} \omega^2 L_c^2 \right\} \right] \quad (4.20)$$

If $(1 - \omega^2 L_c C_{cg}) \simeq 1$ and $20\, I_{eq} \omega^2 L_c^2 \ll R_n$, this expression may be written:

$$F_{tot} = F + \frac{1}{F_c^2 g_s} \left[g_c + 20\, I_{eq} + (g_{out} + g_c)^2 R_n \right] \qquad (4.20a)$$

which is independent of L_c. In first approximation one has therefore that the total noise figure F_{tot} is the same as without feedback; the only effect of the feedback then is that it dampe the output circuit of the mixer.

We still have to prove the above conditions. We saw in the previous section that a load conductance of about 10^{-3} mhos could be obtained at 30 Mc for C_{cg} = 10 µµf and L_c = 0.5 µh. If in addition R_n = 250 ohms and I_{eq} = 5 µA at 30 Mc, one obtains $(1 - \omega^2 L_c C_{cg}) = 0.82$ and $20\, I_{eq} \omega^2 L_c^2 / R_n = 3.6 \times 10^{-3}$ so that both conditions are reasonably well satisfied.

If g_{out} is negative, we have two possibilities:

a) We can take $g_c = - g_{out}$ to bring the circuit to its limit of stability. In that case, since $g_{out} = - |g_{out}|$

$$F_{tot} = F + \frac{1}{F_c^2 g_s} \left[|g_{out}| + 20\, I_{eq} \right] \qquad (4.21)$$

b) We can stabilise the circuit with the help of feedback so that the input conductance of the first i.f. stage equals $-g_{out}$. This brings the circuit also to the limit of its stability, but it has now lower noise, since it is given by Eq. (4.20a).

Substituting $g_c = 4 \times 10^{-5}$ mhos, $I_{eq} = 5$ μA, $g_{out} = -10^{-3}$ mhos and $R_n = 250$ ohms gives for the form between brackets in Eq. (4.20a) 3.7×10^{-4}, whereas the corresponding form between brackets in Eq. (4.21) is 11×10^{-4}. The damping of the output circuit with the help of feedback is thus superior.

The effect of the noise of the output load is often not very large, however. Taking representative values like $F_{min} = 4$, $F_c^2 = 0.5$, $g_s = 4 \times 10^{-3}$ mhos and $g_{out} = -10^{-3}$ mhos gives $F_{tot} = 4.55$ from (4.21) and $F_{tot} = 4.18$ from (4.20a). Large differences will be obtained if F_c is smaller.

3. Noise Figure and Power Gain of a Tunnel Diode Mixer Followed by a Grounded Grid I.F. Stage

Since the grounded grid stage has a high input conductance ($\simeq g_m$ over a wide frequency range), it will be useful to have a tunnel diode mixer followed by a grounded grid stage to satisfy the stability condition $(g_{out} + g_m) > 0$. The noise equivalent circuit of a tunnel diode mixer followed by a grounded grid i.f. stage is given in Fig. 8 where C_1 is the tuning capacitance. From Fig. 8 we obtain the corresponding mean-square noise current at the input from the various noise sources. The noise contribution of the output load of the grounded

grid stage is also included because of the nearly open-circuited input of the grounded grid stage this can not be ignored.

a) Mixer noise: $F4kTg_s df F_c^2$ (4.22)

b) Input circuit noise: $4kTg_c df$ (4.23)

c) Induced grid noise: $2eI_{eqi} df$ (4.24)

d) Tube noise: $4kTR_n df \left(\frac{\mu}{\mu + 1}\right)^2 (g_{out} + g_c)$ (4.25)

Where the factor $\left(\frac{\mu}{\mu + 1}\right)^2$ is due to the connection of the tube noise emf in the cathode lead instead of the grid lead.

e) Load conductance noise:

$$4kTg_L df \left[\frac{g_{out} + g_c + g_m(1 + 1/\mu)}{g_m(1 + 1/\mu)}\right]^2 \qquad (4.26)$$

Equation (4.26) can be obtained as follows: The current source $\sqrt{4kTg_L df}$ corresponds to a voltage $e_c = \sqrt{4kTg_L df} / g_m(1 + 1/\mu)$ at the input as shown in Fig. 8. The voltage e_c corresponds a current source of (4.26) in parallel with a conductance $\left[g_{out} + g_c + g_m(1 + 1/\mu)\right]$. This is correct since the input conductance of the grounded grid stage is $g_m(1 + 1/\mu)$ when the output is short-circuited.

The noise figure F_{tot} is therefore

$$F_{tot} = \frac{a) + b) + c) + d) + e)}{a)} = F$$

$$+ \frac{1}{g_s F_c^2}\left[20 I_{eqi} + g_c + \left(\frac{\mu}{\mu+1}\right)^2 R_n (g_{out} + g_c)^2 \right]$$

$$+ \frac{1}{g_s F_c^2} \cdot \left[g_L \left\{ \frac{g_{out} + g_c + g_m(1 + 1/\mu)}{g_m(1 + 1/\mu)} \right\}^2 \right] \qquad (4.27)$$

Where I_{eqi} represents the induced grid noise, R_n the tube noise, μ the amplification factor of the triode, g_c the input tuned circuit conductance, g_m the tube transconductance, whereas F, g_s, F_c, g_{out} and g_L have the usual meaning.

The last term in (4.27) is not negligible. For since

$$\left[g_{out} + g_c + g_m(1 + 1/\mu) \right]^2 \Big/ \left[g_m(1 + 1/\mu) \right]^2$$

is usually near unity, loading the output circuit of the grounded grid stage has about as much effect upon the noise figure of the mixer as loading the output circuit of the mixer directly.

If the output of the mixer had been loaded by the conductance $g_c = - g_{out}$ (we assume here g_{out} to be negative) and the same triode had been used in a cascode

circuit, the noise figure would have been:

$$F_{tot} = F + \frac{1}{g_s F_c^2} \left(20\, I_{eq} + |g_{out}| \right) \qquad (4.28)$$

and the circuit would be at its limit of stability.

As an example take $I_{eqi} = 5\ \mu A$ at 30 Mc, $g_{out} = -10^{-3}$ mhos, $R_n = 250$ ohms, $g_m = 10^{-2}$ mhos, $(1 + 1/\mu) = 1$, $g_c = 0.5 \times 10^{-4}$ mhos in Eq. (4.27) and $g_L = 4 \times 10^{-4}$ mhos, then the factor between brackets in Eq. (4.27) has the value 7×10^{-4} whereas the factor between brackets in Eq. (4.28) has the value 11×10^{-4}. The two forms between brackets are practically equal if $R_n |g_{out}|^2 = |g_{out}|$ or $|g_{out}| = 1/R_n$.

The grounded grid i.f. stage thus gives less contribution to the noise figure than the damping $|g_{out}|$, and in addition stabilises the circuit.

The power gain of this combination is defined as the ratio of the power $V_2 V_2^* g_L$ delivered to the load g_L to the available power $I_{ms} I_{ms}^*/4g_s$ of the signal source at the input of the mixer. Here the current generator I_{ms} in parallel with a conductance g_s represents the mixer signal source. Then $I_s = F_c I_{ms}$ by using the definition of the current amplification F_c of the mixer.

In calculating the voltage V_2 developed across g_L due to a current surce I_s at the input of the grounded grid stage, the equivalent circuit shown in Fig. 9 applies.

The following equations can be written:

$$I_1 = g_m(1 + \tfrac{1}{\mu})V_1 - \frac{g_m}{\mu} V_2 \qquad (4.29)$$

$$I_2 = - g_m(1 + \tfrac{1}{\mu})V_1 + \frac{g_m}{\mu} V_2 \qquad (4.30)$$

$$I_1 = I_s - g_{out}V_1 \qquad (4.31)$$

$$I_2 = - g_L V_2 \qquad (4.32)$$

From Eqs. (4.29) - (4.32), V_2 can be obtained.

$$V_2 = \left[\frac{g_m(\mu + 1)}{D} \right] I_s \qquad (4.33)$$

where $D = g_m(\mu + 1)g_L + g_m g_{out} + \mu g_L g_{out}$ (4.33a)

Putting $I_s = F_c I_{ms}$, the power delivered to the load is

$$V_2 V_2^* g_L = \left[\frac{g_m(\mu + 1)}{D} \right]^2 I_{ms} I_{ms}^* F_c^2 g_L \qquad (4.34)$$

Then the power gain of a tunnel diode mixer followed by a grounded grid stage is obtained by dividing (4.34) by the available power $I_{ms}I_{ms}^*/4g_s$ of the mixer signal source.

$$G = \left[\frac{g_m(\mu + 1)}{D} \right]^2 4g_s g_L F_c^2 \qquad (4.35)$$

where D is given by (4.33a). Equation (4.35) can be written as

$$G = \frac{4g_L g_s}{\left[g_L\left(1 + \frac{g_{out}}{g_m}\frac{\mu}{\mu+1}\right) + \frac{g_{out}}{\mu+1}\right]^2}\left(\frac{g_1}{g_o + g_s}\right)^2 \qquad (4.36)$$

Since we assume g_{out} to be negative, G will become infinitely large if g_L is chosen such that the form between the brackets in the denominator of (4.36) is zero, i.e.,

$$g_L = -\frac{g_{out}}{\mu+1} \cdot \frac{1}{1 + \frac{g_{out}}{g_m}\left(\frac{\mu}{\mu+1}\right)} \qquad (4.37)$$

As an example, take $g_{out} = -10^{-3}$ mhos, $\mu = 30$ and $g_m = 10^{-2}$ mhos, then $g_L \simeq 3.6 \times 10^{-5}$ mhos. This small value of g_L will lead to small bandwidth and reduce the magnitude of the input conductance of the grounded grid i.f. stage. Suppose we take $g_L = 4 \times 10^{-4}$ mhos, then $g_L >> \frac{|g_{out}|}{\mu+1}$ and G of (4.36) can be approximately written as

$$G \simeq \frac{4g_s}{g_L}\left(\frac{g_1}{g_o + g_s}\right)^2 \qquad (4.38)$$

which may still have a reasonable value. Hence this is a reasonable "safe" circuit unless g_L is chosen too small.

V. Parameters of a Tunnel Diode Mixer

It becomes obvious by examining the expressions for the noise figure, available gain and output conductance, etc., that both the magnitude and the sign of the parameters I_{eo}, I_{el}, g_o and g_1 play a very important role

in determining the operation of a tunnel diode mixer. A properly chosen set of parameters will give the optimum results. The parameters I_{eo} and I_{e1} are Fourier components of the instantaneous equivalent shot noise current $I_{eq}(t)$, and g_o and g_1 are Fourier components of the instantaneous conductance g(t) of the tunnel diode, defined by the equations

$$I_{eq}(t) = I_{eo} + 2I_{e1}\cos\omega_h t + 2I_{e2}\cos 2\omega_h t + \ldots\ldots \quad (5.1)$$

$$g(t) = g_o + 2g_1\cos\omega_h t + 2g_2\cos 2\omega_h t + \ldots\ldots \quad (5.2)$$

These parameters are a function of the dc bias, the local oscillator voltage amplitude and the shape of the current-voltage curve of the tunnel diode as shown in Fig. 10 and Eqs. (5.1) and (5.2). A number of different ways can be used to determine them, e.g., (i) Match the current-voltage curve by a mathematical equation and calculate the parameters by Fourier analysis with the aid of digital computers.[18,19] (ii) Determine the parameters from i.f. measurements of g_{out} and I_{eq} as a function of the signal conductance g_s.[20] (iii) The parameters g_o, g_1, g_2, etc., can be determined by the measured data of Fourier components of the tunnel diode current because of their close relationship.[21] Two methods, used in this report, involving only the noise measurement equipments and a graphical analysis, will be illustrated.

A. Graphical Method

As we know from the previous chapters, when the dc bias and the local oscillator voltage is applied to a tunnel diode, the equivalent shot noise current I_{eq} and the conductance g will vary periodically with the local oscillator voltage. These periodic functions (i.e., I_{eq} vs. $\omega_h t$ and g vs. $\omega_h t$) for a given set of I_{eq} - V curve, g-V curve, dc bias and local oscillator voltage can be easily obtained as shown in Fig. 10. Making a Fourier analysis for these functions, the parameters are determined. For the particular case of Fig. 10, the signs of the parameters are all positive.

Similarly, the magnitudes and the signs of the parameters under other operating conditions can be found.

The signs of the parameters are rather important in tunnel diode mixer operation. It will be very useful if a sign rule is available for each specified operating condition. Unfortunately, the I_{eq}-V and g-V curves can hardly be defined precisely except by actual pictures or rigorous mathematical equations. Also the signs of the parameters sometimes are so critical that it will be different by a slight change in the I_{eq}-V curve, the g-V curve, the dc bias or the local oscillator voltage amplitude. Therefore the most reliable way is to determine the signs of the parameters for each individual case.

From the Fourier series definitions of (5.1) and (5.2) and the graphical analysis experience, the effects of the shape of the I_{eq}-V and the g-V curves on the parameters can be concluded. Suppose the tunnel diode is biased at the vicinity of the valley point for small I_{eo} and the I_{eq}-V and the I-V curves coincide in this operating region as shown in Fig. 10.

If the negative resistance region of the I-V curve does not exist and the curve rises very steeply to the right of the valley point, large values of I_{el}, which means large noise correlation, can be obtained. But at the same time g_1 will be smaller than g_o which is undesirable for it leads to a gain less than unity. It is the ideal case for the ordinary diode mixer.

If the negative resistance region to the left of the valley point is very pronounced, then g_1 will be larger than g_o with smaller I_{el} and larger I_{eo}. This is undesirable, for smaller I_{el} means smaller correlation and larger I_{eo} means larger background noise.

From the above statements, it is clear that an idealized I-V curve which could satisfy the conditions of large I_{el}/I_{eo}, large g_1, small g_o/g_1 and small I_{eo} (i.e., low noise, high gain mixer) at the same time, can not be defined.

B. Experimental Method

From Eqs. (3.6) and (3.7), the equivalent shot noise current at the output of the tunnel diode mixer is

$$I_{eq} = I_{eo}(1 + F_c^2) - 2I_{el}F_c + \frac{2kT}{e} g_s F_c^2 \qquad (5.3)$$

where $F_c = g_1/(g_o + g_s)$. Equation (5.3) indicates that $I_{eq} = I_{eo}$ when the input is short-circuited. Using the noise measurement techniques described in Chapter VIII and the method of measuring F_c, the parameters I_{eo}, I_{el}, or the correlation term $2I_{el}F_c$ can then be determined from (5.3)

To develop a method of measuring F_c, we refer to Fig. 11. The output terminals 22' are connected to the preamplifier of the noise measurement equipment. g_{ω_1} and g_{ω_2} are the tuned circuit conductances at frequencies ω_1 and ω_2 respectively. When there is a signal conductance g_s which will be included in g_{ω_1}. i_{d1} and i_{d2} are the rms values of noise diode currents at the input and output respectively. I_{eq1} and I_{eq2} are the equivalent saturated noise diode currents at the input and output respectively. From the network theory, we have

$$I_1 = (g_o + g_{\omega_1})V_1 + g_1 V_2$$

$$I_2 = g_1 V_1 + (g_o + g_{\omega_2})V_2 \qquad (5.4)$$

Suppose there is a noise diode current i_{d1} flowing into the input terminals, only the voltage component of ω_1 will exist because the input is tuned to the input frequency ω_1. If the output is short-circuited, the intermediate-frequency current is

$$I_2 = i_{d1} \left(\frac{g_1}{g_o + g_{\omega_1}}\right) \tag{5.5}$$

If the short circuit is removed, this current will flow into the parallel combination of the output conductance of the mixer g_{out} and the load conductance g_L. The voltage developed across the output terminals will be proportional to the output short-circuited current I_2. Since the output terminals are connected to the preamplifier of the noise measurement equipment, the deflection on the square law detector will be proportional to the square of I_2.

Similarly, when the noise diode current i_{d1} is removed and if the noise diode current i_{d2} is allowed to flow into the parallel combination of the output conductance of the mixer g_{out} and the load conductance g_L, the deflection on the square law detector will be proportional to the square of i_{d2}. If we adjust i_{d2} until the deflections on the square law detector due to i_{d1} and i_{d2} are the same, then we know i_{d2} must equal to I_2 of (5.5) and obtain

$$F_c = \frac{g_1}{g_o + g_{\omega_1}} = \frac{i_{d2}}{i_{d1}} = \sqrt{\frac{2eI_{eq2}df}{2eI_{eq1}df}} = \sqrt{\frac{I_{eq2}}{I_{eq1}}} \qquad (5.6)$$

VI. Characteristics of Tunnel Diodes

A. Current-Voltage Curves

1. I-V Curve Tracer[4,22,23]

The circuit diagram of the tunnel diode I-V curve tracer is illustrated in Fig. 12.

The total dc resistance, R_T, seen by the tunnel diode is the sum of the tunnel diode series resistance R_S, R_2, R_1 in parallel with the dc source resistance. R_S should be less than the absolute value of the negative resistance, R, of the tunnel diode in order to avoid switching. This can be explained by drawing two load lines with the slope $-1/R_T$ passing through the peak point and the valley point of the I-V curve.

The total ac resistance, R_T', seen by the tunnel diode is the sum of R_S, R_2 and R_1 in parallel with the ac source resistance. R_T' should be greater than L/RC to avoid oscillation. Here L is the total circuit inductance including the tunnel diode inductance and C is the total circuit capacitance including the tunnel diode capacitance. The condition can be obtained by setting the self-resonant frequency $f_{xo} = \frac{1}{2\pi}\sqrt{\frac{1}{LC} - \frac{1}{R^2C^2}}$ larger than the resistive cut-off frequency $f_{ro} = \frac{1}{2\pi RC}\sqrt{\frac{R}{R_T} - 1}$ of the tunnel diode.

The variable resistance R_1 in the circuit is provided for the adjustment of the total dc and ac resistance to satisfy the above two conditions: (i) $R_T < R$, (ii) $L/RC < R_T'$.

Displaying the I-V curve of tunnel diode on the oscilloscope is not always an easy task especially for those diodes having higher peak current values. For higher peak current values means smaller R, which makes the dis-- playable region smaller. The total circuit inductance should be kept at a minimum. If the inductance L is greater than R^2C the displayable region will not exist.

2. I-V Curves of the Tunnel Diodes

The I-V curves of eight types of tunnel diodes are shown in Figs. 13 and 14. The upper half of each picture is the forward voltage characteristic and the lower half is the reverse voltage characteristic. These pictures were taken using our sample No. 1 of each type. From now on unless otherwise stated all the tunnel diodes are our sample No. 1. The shape of the I-V curve of the same type tunnel diode may be quite different from one sample to another and so is the noise of the tunnel diode. Therefore a complete knowledge of the I-V curve and the noise of each tunnel diode is necessary before any further theoretical and experimental investigation becomes useful.

A comparison of (a) and (d) of Fig. 13 will indicate the I-V curves have almost the same shape but the two vertical (current) scales differ. Suppose these two tunnel diodes show full shot noise and have I-V curves of exactly the same shape. If they both are operated with the same bias and local oscillator voltage as tunnel diode mixers, the same noise figure and available gain will be obtained except at different impedance levels. The one that has the lower current value will operate on the higher impedance level. This can be seen by evaluating the change of the parameters I_{eo}, I_{el}, g_o and g_1 which determine the mixer operation.

The I-V curves of Figs. 13 and 14 covered a wide range of peak currents, valley currents and different I-V curve shapes. From the discussion in the last paragraph, the theoretical and experimental results of the mixer operation of any one of the tunnel diodes in Figs. 13 and 14 can be extended to other tunnel diodes having the same shape of I-V curve but a different current scale or voltage scale or even if both scales differ. The dc bias and the local oscillator peak amplitude should be changed in accordance with the voltage scale involved. Unfortunately, a tunnel diode that has the same shape of I-V curve in a larger voltage scale will operate as a mixer at a higher impedance level with the same available gain but higher noise figure.

B. Noise in the Tunnel Diodes

Noise measurements have been made on the tunnel diodes at 30 Mc for different bias points. The result indicates that the behavior of the noise could be different from one diode to another even in the same type of tunnel diode. For convenience, the experimental result will be outlined in several voltage regions. No specific data or physical reasons are given here because the purpose of this approximate measurement is to assist in the understanding of the background noise of the mixer and the selection of the tunnel diode for better mixer operation.

1. Small Reverse and Forward Voltage Region

A theoretical noise expression $I_{eq} = I \coth (eV/2kT)$ was derived.[24,25] The result of our approximate noise measurement for different types of tunnel diodes showed the tendency to agree with the theoretical expression. Owing to the high conductance value associated with the tunnel diode near the origin, the accuracy of the measurement is poor without using step-up transformers. Therefore no detailed comparison between the measured data and the theoretical expression was made. In order to have a general idea about the noise magnitude of the different type of tunnel diodes in this voltage region, a simple mathematical manipulation will be performed. To evaluate the noise at the origin ($V = 0$, $I = 0$) using l 'Hospital's rule, we have

$$\lim_{V \to 0} I_{eq} = (2kT/e) \left(\frac{dI}{dV}\right)_{V=0}$$

It shows the steeper the slope near the origin the higher the noise will be. Therefore Fig. 14(d) indicates the tunnel diode GE 4JF2-BD-7 will have very small noise near the origin.

2. Negative Resistance Region

No measurement was made.

3. The Region From the Valley Point Voltage Up to About 450 mV

GE 1N2939 shows about 20% higher than full shot noise.

Philco 1N3353 shows about 25% higher than full shot noise.

GE 4JF2-BD-2 sample No. 1 shows about 20% higher than full shot noise but sample No. 2 shows a little less than full shot noise.

GE 4JF2-BD-3, -4, and -7 all show less than full shot noise.

VII. Theoretical Analysis of Tunnel Diode Mixers

In this chapter, the tunnel diode mixers are mainly studied when the tunnel diode is biased in the vicinity of the valley point for its low I_{eo} value (i.e., low background noise), large noise correlation and stable operation. Under this bias condition, if the peak local

oscillator voltage is in the range of 140-220 mV, all the parameters I_{eo}, I_{el}, g_o and g_1 are positive as shown in Fig. 10. The operating condition when the tunnel diode is biased near the peak point is also discussed briefly.

A. Theoretical Curves

The parameters I_{eo}, I_{el}, g_o and g_1 which describe the tunnel diode mixer operation, are not independent to each other since they are derived from the same portion of the I-V curve. But they have no simple relations among them, either. Each Fourier component of the instantaneous conductance can be expressed by a series of all the Fourier components of the instantaneous current,[21] but this relation does not help to reduce the number of parameters required to describe the mixer operation. Therefore it is difficult to plot any theoretical curve in terms of the parameters without modifications.

Suppose two new variables $\alpha = I_{el}/I_{eo}$ and $x = g_o/g_1$ are defined. Substituting these variables into the theoretical expressions for $(g_s)_{opt}$, F_{min} and G_{av}, etc., all these quantities in some different forms can then be plotted versus α with x as the parameters as shown in Figs. 15-21. In those figures we always assume the signal conductance g_s is optimized for minimum mixer noise figure, i.e., $g_s = (g_s)_{opt}$ and $F = F_{min}$ and the output is matched when $g_{out} > 0$, i.e., $g_L = g_{out}$. Also the effects of the

conductance of the input and output tuned circuits are neglected. The figures cover the range of $0 \leq \alpha \leq 1$, $0.4 \leq x \leq 1$ which is most interested in our case.

It is our aim to achieve high gain, low noise and also stable operation. According to Figs. 21 and 16 large α and small x are desirable for large values of G_{av} and small values of $(F_{min} - 1)/(e/2kT)(I_{eo}/g_1)$. It is also understandable that small I_{eo} and large g_1 are preferred for low noise figure. Figures 17 and 20 show that the output and input conductances are positive only for certain values of α and x. In this region $G_{av} \lesssim 1$ at most. If higher gain is wanted, then either the output conductance or the input conductance or both must be negative. In case the negative value occurs its absolute value should be made as small as possible in order to maintain stability, i.e., $(g_{out} + g_L) > 0$ and $\left[(g_s)_{opt} + g_{in}\right] > 0$.

B. Tunnel Diode Mixer Operation

From Figs. 15-21, we concluded that large α, small x and small I_{eo}/g_1 are preferred for low noise, high gain mixer operation. However, there is a stability problem associated with the small x. Unfortunately no ideal I-V curve can be found to satisfy all the above requirements simultaneously because the conditions for obtaining large α contradict those for small x. Therefore using the actual I-V curve of the tunnel diode for mixer operation, one

can obtain either large α or small x but not both. Two possible ways of operating the tunnel diode as a mixer can be stated as follows:

1. Emphasize obtaining large α accompanied by the undesirable large x. I_{eo}/g_1 can be made small by choosing a small value of I_{eo}. The tunnel diode mixer will have a small gain or even a loss but has no stability problem.

These conditions can be satisfied by using proper local oscillator amplitude and biasing in the vicinity of the valley point of the I-V curve or other portion of the I-V curve with a similar characteristic.

A detailed analysis will be made in the next section.

2. Emphasize obtaining small x accompanied with an undesirable small α. I_{eo}/g_1 can be made small by choosing a large value of g_1. The tunnel diode mixer will operate with high gain but will have a negative input or output conductance or both may be negative. Proper terminations at both input and output are necessary to avoid unstable operation. Friis' formula cannot be applied in calculating the system noise figure of the mixer plus the i.f. amplifier if the output conductance is negative.

This case will be obtained by using proper local oscillator amplitude and biasing in the vicinity of the peak point of the I-V curve because only at the peak point the conductance changes rapidly from large positive value to large negative value or vice versa.

It should be noted that Figs. 15 - 21 are plotted for all positive parameter values. Is it correct to draw any conclusion from them for the case having bias point in the vicinity of the peak point?

It was mentioned in Chapter V that the signs of the parameters will be different if different bias and local oscillator voltage is used. If the tunnel diode is biased in the vicinity of the peak point at room temperature,* the signs of I_{eo}, I_{e1}, g_o and g_1 will be "+", "-", "+" and "-" respectively for most I-V characteristics and local oscillator voltage amplitudes except under some extreme conditions. For example: I_{eo} = 1.15 mA, I_{e1} = -0.18 mA, $g_o = 2.4 \times 10^{-3}$ mhos and $g_1 = -6.6 \times 10^{-3}$ mhos are obtained by applying a bias of 63 mV and a peak local oscillator voltage of 44 mV to a GE ZJ56 1 mA germanium tunnel diode.[26] The signs of I_{e1} and g_1 are changed compared with the corresponding ones for the case of biasing in the vicinity of the valley point.

Let us examine $(g_s)_{opt}$ of (3.9) and Fig. 15, F_{min} of (3.10) and Fig. 16, g_{out} of (2.5) and Fig. 17, g_{in} of (2.7) and Fig. 20 and G_{av} of (2.12) and Fig. 21, the parameters I_{e1} and g_1 always occur in the form of g_1^2 or the product of I_{e1} and g_1. Therefore the negative signs have no effect on Figs. 15 - 17, 20, 21 and the parameters can be replaced by their absolute values. Since

*At low temperature the sign of I_{e1} may be different because the I_{eq} - V curve depends on temperature.

$(g_s)_{opt} > 0$, Fig. 19 has no sign problem. But the F_c of (2.11) and Fig. 18 will be negative if $g_1 < 0$. Finally we can say that the conclusion which is made from Figs. 15-21, is valid for biasing in the vicinity of the peak point.

Two optimum operating regions concluded from those theoretical curves have also been found experimentally by Klapper, et al.[27]

C. Theoretical Analysis and Results

1. Procedure

The I-V curve is displayed on the oscilloscope and a picture taken. The picture of the I-V curve is then enlarged. From the enlarged I-V curve, the g-V curve is plotted and a graphical analysis as shown in Fig. 10 is made. Using Fourier series analysis, the parameters I_{eo}, I_{el}, g_o and g_1 of the tunnel diode mixer operation can be determined. Finally, one evaluates the parameters $\alpha = I_{el}/I_{eo}$, $x = g_o/g_1$, and I_{eo}/g_1 and then reads the noise figure, available gain, etc., from Figs. 15-21.

2. Remarks

a) Full shot noise is assumed for the theoretical analysis since there is a lack of the exact information about the noise in tunnel diodes.

b) The noise figure of the i.f. amplifier, $F_{i.f.} = 1.30$, is used for calculating the total system noise.

c) The data obtained from the theoretical curves may differ slightly from those calculated by direct

substitution into the proper equations due to the accuracy limitation of the curves.

d) The I-V and g-V curves, on which the graphical analysis is based, were reduced to a smaller size as shown in Figs. 22-24 to fit the report.

e) The I-V curves of sample No. 1 of GE 1N2939 and GE 4JF2-BD-2 are slightly different from their sample No. 2 respectively as shown in Figs. 13(a), 13(b), 22 and 23.

f) Owing to the similarity of the right portion of the I-V curves in Figs. 13(c), 14(a) and 14(d) an approximation was made as shown in Fig. 24. This approximation can be justified by the time saved, the difficulty of making an exact graphical and Fourier analysis and the difference among the I-V curves of the same type of tunnel diode.

The only serious possibility of error occurs under remark a). If there is not full shot noise, then there are two possibilities:

(i) I and I_{eq} differ by a constant amount. Then I_{eo} is not equal to the average value of the tunnel diode current but I_{el} is determined correctly.

(ii) The difference between I and I_{eq} depends on the voltage. Then the "calculated" values of both I_{eo} and I_{el} will differ from their actual values.

Correct values could be determined by making a Fourier analysis of $I_{eq}(t)$, which can be done after $I_{eq}(V)$

has been determined. This is usually not done in this report since the error made by putting $I_{eq}(t) = I(t)$ is often not very large in the voltage range from 100 mV to 500 mV which is most interested in our study. Compare however, Chapter VI section B and Fig. 10.

3. Results

The theoretical results are shown in the following five tables. It is just like what we predicted: high available gain and low noise figure can not be obtained at the same time. The best system noise figure, F_{tot}, is 3 dB as shown in Table VI. From the data of $(g_s)_{opt}$, g_{in} and g_{out} given in the tables, the circuit should be quite stable.

The tables also give measured data. In this section we deal only with the calculated values. The actual comparison between the theoretical and the experimental data will be made in Chapter VIII.

Table II

RESULTS OF TUNNEL DIODE MIXER OPERATION

USING GE 1N2939 (SAMPLE NO. 2)

	Theoretical	Measured
Bias	360	360
Peak Local-Oscillator Amplitude	160	(160)
I_{eo}	0.224	0.270
I_{el}	0.089	0.078
g_o	3.52	
g_1	4.10	
$\alpha = I_{el}/I_{eo}$	0.40	
$x = g_o/g_1$	0.86	
I_{eo}/g_1	0.0546	
$(g_s)_{opt}$	4.2	
F_{min}	4.3 (6.3 dB)	6.2 (7.9 dB)
g_{out}	1.34	
F_c	0.53	0.50
g_{in}	0.06	
G_{av}	0.88	
$\frac{(F_{i.f.} - 1)}{G_{av}}$	0.34	
F_{tot}	4.6 (6.6 dB)	

Unless otherwise noted all the conductance, current and voltage values are given in millimhos, mA and mV respectively.

Table III

RESULTS OF TUNNEL DIODE MIXER OPERATION

USING GE 4JF2-BD-2 (SAMPLE NO. 2)

	Theoretical				Measured
Bias	312.5	312.5	312.5	312.5	312.5
Peak Local-Oscillator Amplitude	140	160	180	200	(200)
I_{eo}	0.0906	0.123	0.175	0.235	0.230
I_{e1}	0.0235	0.0472	0.087	0.130	0.123
g_o	1.19	1.84	2.77	3.46	
g_1	1.53	2.26	3.29	4.17	
$\alpha = I_{e1}/I_{eo}$	0.26	0.38	0.50	0.56	
$x = g_o/g_1$	0.78	0.82	0.84	0.83	
I_{eo}/g_1	0.0592	0.0545	0.0532	0.0564	
$(g_s)_{opt}$	1.68	2.30	3.08	3.65	
F_{min}	4.8 (6.8 dB)	4.2 (6.2 dB)	3.7 (5.7 dB)	3.6 (5.6 dB)	3.4 (5.3 dB)
g_{out}	0.367	0.610	0.905	1.04	
F_c	0.53	0.54	0.56	0.59	0.62
gin	-0.22	-0.25	-0.21	-0.42	
G_{av}	1.25	1.10	1.07	1.22	
$\frac{F_{i.f.} - 1}{G_{av}}$	0.24	0.27	0.28	0.25	
F_{tot}	5.1 (7.1 dB)	4.4 (6.4 dB)	4.0 (6.0 dB)	3.9 (5.9 dB)	

Unless otherwise noted all the conductance, current and voltage values are given in millimhos, mA and mV respectively.

Table IV

RESULTS OF TUNNEL DIODE MIXER OPERATION

USING GE 4JF2-BD-3

	Theoretical			Measured	Theoretical
Bias	300	300	300	300	300
Peak Local-Oscillator Amplitude	160	180	200	(200)	220
I_{eo}	0.0394	0.0734	0.132	0.130	0.208
I_{el}	0.0238	0.0538	0.106	0.102	0.175
g_o	1.14	2.34	3.63		4.61
g_l	1.29	2.52	3.81		4.77
$\alpha = I_{el}/I_{eo}$	0.60	0.73	0.81		0.84
$x = g_o/g_l$	0.83	0.93	0.95		0.97
I_{eo}/g_l	0.0306	0.0292	0.0345		0.0437
$(g_s)_{opt}$	1.08	1.79	2.30		2.67
F_{min}	2.4 (3.8 dB)	2.1 (3.2 dB)	2.0 (3.0 dB)	2.46 (3.9 dB)	2.2 (3.4 dB)
g_{out}	0.393	0.806	1.14		1.43
F_c	0.58	0.61	0.65	0.58	0.66
g_{in}	0.0645	0.328	0.533		0.786
G_{av}	0.88	0.81	0.81		0.78
$\frac{F_{i.f.} - 1}{G_{av}}$	0.34	0.37	0.37		0.39
F_{tot}	2.7 (4.3 dB)	2.44 (3.9 dB)	2.4 (3.8 dB)		2.6 (4.1 dB)

Unless otherwise noted all the conductance, current and voltage values are given in millimhos, mA and mV respectively.

Table V

RESULTS OF TUNNEL DIODE MIXER OPERATION

USING GE 4JF2-BD-4

	Theoretical	Measured
Bias	300	300
Peak Local-Oscillator Amplitude	200	(200)
I_{eo}	0.126	0.095
I_{e1}	0.111	0.072
g_o	3.74	
g_1	3.71	
$\alpha = I_{e1}/I_{eo}$	0.88	
$x = g_o/g_1$	1.01	
I_{eo}/g_1	0.0340	
$(g_s)_{opt}$	1.82	
F_{min}	1.8 (2.6 dB)	2.4 (3.8 dB)
g_{out}	1.21	
F_c	0.67	0.58
g_{in}	0.89	
G_{av}	0.67	
$\frac{F_{i.f.} - 1}{G_{av}}$	0.45	
F_{tot}	2.3 (3.6 dB)	

Unless otherwise noted all the conductance, current and voltage values are given in millimhos, mA and mV respectively.

Table VI

RESULTS OF TUNNEL DIODE MIXER OPERATION

USING GE 4JF2-BD-7

	Theoretical	Measured	
Bias	300	300	35
Peak Local-Oscillator Amplitude	200	(200)	(200)*
I_{eo}	0.120	0.085	0.093
I_{e1}	0.116	0.074	0.083
g_o	3.80		
g_1	3.66		
$\alpha = I_{e1}/I_{eo}$	0.97		
$x = g_o/g_1$	1.04		
I_{eo}/g_1	0.0328		
$(g_s)_{opt}$	1.0		
F_{min}	1.45 (1.6 dB)	2.1 (3.2 dB)	1.95 (2.9 dB)
g_{out}	1.0		
F_c	0.76	0.67	0.70
g_{in}	1.0		
G_{av}	0.58		
$(F_{i.f.} - 1)/G_{av}$	0.52		
F_{tot}	2.0 (3.0 dB)		

Unless otherwise noted all the conductance, current and voltage values are given in millimhos, mA and mV respectively.

*Adjust the peak local-oscillator amplitude to approximately 200 mV until the average dc diode current reads -0.120 mA.

D. Effects of the Local Oscillator Voltage

If one biases in the vicinity of the valley point of the tunnel diode and the peak local oscillator amplitude is 140 mV or higher, the following can be concluded from Tables III and IV.

1. α increases as the local oscillator voltage increases since the current rises very rapidly near 450-500 mV. Keeping the graphical and Fourier analysis in mind, this can be explained as follows: The effect of the current values in the negative conductance region and to the left of the bias point is to decrease α. On the other hand, the effect of the high current values to the right of the bias point (near 450-500 mV) is to increase α. The effect of the relatively small current in the negative conductance region will become negligible when the local oscillator voltage swings deeper into the high current region. Hence when the local oscillator voltage reaches the high current region, α will be dominated by the high current values and will increase as the local oscillator voltage increases.

Large α is preferred for the low noise figure.

2. x increases somewhat as the local oscillator voltage increases. The differential conductance $g = dI/dV$ increases very rapidly near 450-500 mV, but the ratio $x = g_o/g_1$ changes much more slowly. This can

be explained in a manner similar to part 1 of this section. The effect of the negative conductance values to the left of the bias point is to decrease x; this is the only possible way one can make x less than unity. The high positive conductance values near 450-500 mV, to the right of the bias point, can make x close to unity but x will never be less than unity without the presence of a negative conductance region. Since the conductance values are so high near 450-500 mV, the effect of the negative conductance is small when the local oscillator voltage swings into this high positive conductance region. The negative conductance values may keep the value of x less than unity but cannot dominate it. Hence x will increase as the local oscillator voltage increases. There is an exception in Table III where x decreases a little when the peak local oscillator amplitude increases from 180 mV to 200 mV. This exception can be attributed to the rather large negative conductance values near 100 mV and the constant g-V curve slope near 500 mV.

Small x is preferred for high mixer gain.

3. I_{eo}/g_1 decreases first as the local oscillator voltage increases since the rate of increase of I_{eo} is smaller than that for g_1. After passing a minimum value, I_{eo}/g_1 will increase as local oscillator voltage keeps increasing since now the rate of increase of

I_{eo} is larger than that for g_l. The quantity I_{eo}/g_l does not depend very strongly upon the local oscillator voltage, however.

Small I_{eo}/g_l is preferred for low noise figure.

G_{av} does not depends strongly upon local oscillator voltage amplitude. G_{av} has a shallow minimum and is larger than unity as shown in Table III but it decreases slightly with increasing local oscillator voltage amplitude and is smaller than unity as shown in Table IV. F_{min} and F_{tot} decrease with increasing local oscillator voltage amplitude in Table III but F_{min} passes through a shallow minimum and so does F_{tot} in Table IV. In both Tables III and IV, F_c increases slightly with local oscillator voltage amplitude and $(g_s)_{opt}$ increases strongly with local oscillator voltage amplitude as expected.

For better mixer operation a large local oscillator voltage should be used. In our examples, the peak amplitude of about 200 mV is optimum. The local oscillator voltage amplitude is not very critical for mixer operation as the results in the Tables III and IV show for the different local oscillator voltages. This is rather convenient for practical operation of tunnel diode mixers.

E. Effects of the Signal Conductance

F has its minimum value F_{min} for $g_s = (g_s)_{opt}$ and F_{tot} is often nearly optimized for the same value of g_s. This means that for $g_s \neq (g_s)_{opt}$ the noise figure will be worse. However, since the minimum is relatively shallow, F and F_{tot} will not deteriorate much as long as the deviation from $(g_s)_{opt}$ is not too large.

The available gain of the mixer, G_{av}, may depend very strongly upon the source conductance. This is especially the case if $g_{in} < 0$, since one can make $G_{av} \rightarrow \infty$ if $g_s \rightarrow |g_{in}|$.

In order to study the effects of larger deviations of the signal conductance g_s from $(g_s)_{opt}$ on the mixer noise figure F, the mixer available gain G_{av} and the total system noise figure F_{tot}, several theoretical curves are plotted for two specific cases:

1. The available mixer gain can be larger than unity and the output conductance of the mixer g_{out} is negative for some signal conductance values (see Fig. 25). For the same reason the input conductance g_{in} can be negative in this case.

2. The mixer available gain is always less than unity and the output conductance of the mixer is positive for all the signal conductance values (see Fig. 26). In that case the input conductance g_{in} will be positive for all output load conductance values.

The total system noise figure is calculated by Friis' formula

$$F_{tot} = F + \frac{F_{i.f.} - 1}{G_{av}}$$

when the output conductance of the mixer is positive. In that case an i.f. amplifier noise figure $F_{i.f.} = 1.3$ will be assumed. The calculation of the total system noise figure is omitted for negative output conductance of the mixer. Since numerous kinds of i.f. amplifiers and the load conductances can be connected to the output of the mixer, it is difficult to give a general study of F_{tot} when the output conductance of the mixer is negative.

Figure 26 shows that the minimum noise figure and the maximum available gain of the mixer occur at the same signal conductance value if $G_{av} < 1$. But Fig. 25 shows that the signal conductance which gives the minimum noise figure is different from the signal conductance which is required for the maximum available gain if $G_{av} > 1$. This is generally true.

As said before, the valleys of the noise figure curves are rather flat. The noise figure will not deviate much from its minimum value if the signal conductance is chosen in the neighborhood of the minimum point. Since the output conductance of the mixer is also a function of the signal conductance, the signal conductance should

be chosen in the neighborhood of the minimum mixer noise figure such that a large mixer available gain and a desirable mixer output conductance can be obtained.

VIII. Measurement of Tunnel Diode Mixers

A. Equipment

1. Tunnel Diode Mixer

The circuit diagram is shown in Fig. 27. Several features are described briefly here.

a) The input signal is chosen at the comparatively low frequency of 63 Mc for easy tuning and for avoiding the possible interference of the local TV stations.

b) The 63 Mc tuned circuit at the input has an equivalent resistance of about 5 kohms and the 30 Mc tuned circuit at the output has about 2.5 kohms.* Both tuned circuits are practically short circuited for the undesirable frequency signals.

c) The tuned circuits are kept to a minimum number for getting sharp tuned circuit response.

d) The bias circuit has a low resistance and only contributes about 5 μA to the equivalent noise current of the system.

*The equivalent resistances of the tuned circuits are determined by the method given on p. 56 of van der Ziel's NOISE, Prentice Hall, 1954.

e) The local oscillator voltage is coupled with a small low-impedance loop tuned at its frequency. The coupled circuit has negligible effect on the noise of the system.

2. Noise Measurement Equipment

The block diagram is shown in Fig. 28.

a) Cascode preamplifier--see Fig. 29.

b) Modified NC 109 receiver--the automatic volume control is disconnected and the output signal is taken from the i.f. stage through a cathode follower employing a 6922 tube.

c) I.F. amplifier--it consists of a 6AG5 tuned stage and two cathode follower stages with 6AH6 and 6AH7 tubes.

B. Method

1. Determination of the Noise of the Tunnel Diode Mixer--we refer to Fig. 27.

Consider the circuit to the left of point A as the mixer whose noise equivalent circuit can be represented by a current generator $\sqrt{2eI_x df}$ in parallel with the output conductance g_{out} of the mixer. Consider the circuit to the right of A as the load whose noise equivalent circuit can be represented by a current generator $\sqrt{2eI_c df}$ in parallel with the equivalent resistance R_c.

a) Open the circuit at point A and take the galvanometer readings as follows (refer to Fig. 30):

(i) Short the input of the preamplifier. The reading:

$$M_1 = 4kTR_nBG^2 \qquad (8.1)$$

where G is the voltage amplification, and B is the bandwidth of the amplifier.

(ii) Remove the short circuit and let $I_{d2} = 0$. The reading:

$$M_2 = 4kTR_nBG^2 + 2eI_cR_c^2BG^2 \qquad (8.2)$$

(iii) Adjust I_{d2} until the reading $M_3 = 2M_2 - M_1$. Then:

$$M_3 = 4kTR_nBG^2 + 2eI_cR_c^2BG^2 + 2eI_{d2}R_c^2BG^2 \qquad (8.3)$$

and

$$I_c = I_{d2} \qquad (8.4)$$

(b) Connect the circuit at point A, take the galvanometer readings as follows (refer to Fig. 31):

(i) Short the input of the preamplifier. The reading:

$$M_1 = 4kTR_nBG^2 \qquad (8.5)$$

(ii) Remove the short circuit and let $I_{d2}' = 0$. The reading:

$$M_2 = 4kTR_nBG^2 + 2e(I_c + I_x)\,R^2BG^2 \qquad (8.6)$$

where R is the parallel combination of R_c and R_x.

(iii) Adjust I_{d2}' until the reading $M_3 = 2M_2 - M_1$. Then:

$$M_3 = 4kTR_n BG^2 + 2e(I_c + I_x)R^2BG^2 + 2eI_{d2}'R^2BG^2 \quad (8.7)$$

and

$$I_x = I_{d2}' - I_c = I_{d2}' - I_{d2} \quad (8.8)$$

2. Determination of I_{eo}, I_{el} and F_c -- we refer to Chapter V, section B.

C. Procedure

1. I_{eo} -- Short circuit the input of the mixer and bias the diode properly. Then adjust the local oscillator voltage amplitude until the dc average tunnel diode current reaches the required value. Under this condition the equivalent saturated noise diode current contributed by the tunnel diode is our measured I_{eo}; this can be compared with the average diode current itself, which is the "theoretical" I_{eo} value.

2. I_{eq}, defined by Eq. (8.9) -- Insert the theoretical optimized signal conductance $(g_s)_{opt}$ at the input of the mixer and bias the diode properly. Then adjust the local oscillator voltage amplitude until the dc average tunnel diode current reaches the required value. The equivalent saturated noise diode current due to the mixer is our measured I_{eq}.

3. F_c -- Under the same condition described in procedure 2 for measuring I_{eq}, a deflection will be shown on the square law detector. Adjust the filament voltage of the noise diode at the output of the mixer such that

the deflection on the square law detector is double. Record this equivalent saturated noise diode current I_{eq2} and turn the diode off. Repeat this for the noise diode at the input of the mixer to find I_{eq1}. Then $F_c = \sqrt{I_{eq2}/I_{eq1}}$.

4. I_{el} -- Substituting the measured I_{eo}, I_{eq} and F_c into the following equation

$$I_{eq} = I_{eo}(1 + F_c^2) - 2I_{el}F_c + \frac{2kT}{e}(g_s)_{opt}F_c^2 \qquad (8.9)$$

the measured I_{el} can be found. This can be compared with the "theoretical" I_{el} value determined from the (I,V) characteristic.

5. F_{min} -- It is determined by the ratio of I_{eq} to $(2kT/e)(g_s)_{opt}F_c^2$. Since all quantities are known, F_{min} can be determined.

D. Remark

The amplitude of the local oscillator voltage applied to the tunnel diode is not directly measured. The technique used to obtain the operating condition was given in procedure 2. Therefore the amplitude of the local oscillator voltages in the Tables II-VI are put in parentheses to distinguish these voltages from actually measured values.

E. Results and Conclusions

For each kind of tunnel diode, only the data of one operating condition which has the minimum noise figure,

were measured. The measured results are listed in Tables II-VI just next to the corresponding theoretical analysis results for convenience of comparison. A detailed comparison is also made here in this section.

Biasing in the vicinity of the valley point of the tunnel diode might lead to storage effects of injected minority carriers at microwave frequencies.[28] This would probably result in lower gain and higher noise at those frequencies. But the experimental results obtained by Sommers in the RCA Laboratory show that even in the valley point region the tunnel diode is still suitable for high-frequency applications.[29] Therefore this is not a series problem in normal tunnel diodes. It might be more serious for back diodes.

Owing to the similarity of the right and left portion of the I-V curve of Fig. 14(d) two cases are measured for GE 4JF2-BD-7 based on the same theoretical analysis. This is allowed because the left portion will look the same as the right portion, if one merely changes the direction of the current for the left portion. The bias is 300 mV in one case and 35 mV in another as shown in Table VI. This is designed to study the difference in mixer operation between the cases using the tunnel current region of the tunnel diode and using the excess and injected current region of the tunnel diode.

Table VII

COMPARISON OF THE THEORETICAL AND MEASURED I_{eo}, I_{el} AND F_c

	Table	Measured	Thecretical	Difference
I_{eo}	II	0.270	0.224	+ 21%
	III	0.230	0.235	- 2%
	IV	0.130	0.132	- 2%
	V	0.095	0.126	- 25%
	VI	0.085	0.120	- 29%
I_{el}	II	0.078	0.089	- 12%
	III	0.123	0.130	- 5%
	IV	0.102	0.106	- 4%
	V	0.072	0.111	- 35%
	VI	0.074	0.116	- 36%
F_c	II	0.50	0.53	- 6%
	III	0.62	0.59	+ 5%
	IV	0.58	0.65	- 11%
	V	0.58	0.67	- 13%
	VI	0.67	0.76	- 12%

Table VIII

COMPARISON OF THE THEORETICAL

AND MEASURED F_{min}

Table	Measured	Theoretical	Difference*
II	6.2	4.3	+ 44%
III	3.4	3.6	- 6%
IV	2.46	2.00	+ 23%
V	2.4	1.8	+ 33%
VI	2.1	1.45	+ 45%

*In Table II a major part of the difference comes from the discrepancy in I_{eo} between theory and measurement. If the measured I_{eo} value is used instead of the theoretical I_{eo} value in calculating the noise figure, we have a modified theoretical noise figure of 5.27 which agrees better to the measured result of 6.2. Then the difference reduces to + 18%.

In Table III the results agree well.

In Table IV a major part of the difference comes from the discrepancy in F_c between theory and measurement.

In Tables V and VI the difference comes from the combined effect of the discrepancies in I_{eo}, in I_{el} and in F_c between theory and measurement.

Our Philco 1N3353 sample No. 1 was very noisy. It has a measured I_{eo} = 0.215 mA when the bias is 300 mV and the dc average diode current is 0.132 mA after the local oscillator voltage is applied. No further investigation was made on this diode.

We may draw the following conclusions from Tables II to VIII:

1. The overall agreement between theory and measurement is reasonable.
2. Discrepancies between the calculated and measured values of I_{eo} and I_{el} can be accounted for by the fact that some tunnel diodes have less than full shot noise whereas others have more than full shot noise.
3. At the frequencies of measurement there is relatively little difference between operating the mixer in the forward direction and operating it in the back direction as shown in Table VI, i.e., no storage effect.
4. The best noise figures are obtained for back diodes, that is, diodes with a very small current maximum.

To demonstrate the importance and the relative magnitude of the correlation term, we make the following table from all the measured data. The mixer noise without correlation is determined by the sum of the tunnel diode noise at the mixer input and output terminals. The mixer noise with correlation is determined by the measured tunnel diode mixer noise, I_{eq}, corrected for input circuit noise,

$\frac{e}{2kT}(g_s)_{opt}F_c^2$. According to Eq. (8.9) the mixer noise with correlation can be represented by $\left[I_{eq} - \frac{e}{2kT}(g_s)_{opt}F_c^2\right]$ or $\left[I_{eo}(1+F_c^2) - 2I_{el}F_c\right]$. The former one is used here because it is directly measured.

Table IX

COMPARISON OF MIXER NOISE WITH AND WITHOUT CORRELATION

Table	Mixer Noise Without Correlation $I_{eo}(1+F_c^2)$	Mixer Noise With Correlation $I_{eq} - \frac{e}{2kT}(g_s)_{opt}F_c^2$
II	0.338	0.257
III	0.318	0.165
IV	0.174	0.056
V	0.127	0.044
VI	0.123	0.024

The discrepancy between the two columns is much larger than the experimental error. Hence in all our measurements it is absolutely essential that correlation is taken into account.

IX. Special Application--Radiometer[1,30-34]

Since the Johnson noise and the black body radiation are related, the noise measurement can be used as a tool to measure the microwave radiation from the sun and

moon, and the atmospheric absorption at several microwave frequencies. R. H. Dicke developed a very sensitive radiometer which is a modified superheterodyne receiver and is described in refs. 30 and 31. This device can also be used to calibrate the microwave noise source and to measure the temperature of an object referring to the standard thermal noise. The measurement techniques of the thermal radiation at microwave frequencies are different from those for monitoring a c.w. signal. A c.w. signal requires only a narrow i.f. band which will pass all the signal components but eliminates the unnecessary noise outside the band. Thermal radiation, on the other hand, is usually characterized by a very wide spectrum. Therefore a wide i.f. band receiver is required. Besides, the accuracy of the radiometer, determined by a simple theoretical model, is inversely proportional to the square root of the i.f. bandwidth. However, if the bandwidth is too great the noise of the i.f. amplifier will be higher. In the previous studies we always assumed the input tuned circuit has zero resistance at the image frequency. If we use a broad band tuned circuit which will have almost the same response at the input and image frequencies, two rf bands will convert to the i.f. If the input is not tuned but matched to the mixer the same situation will prevail. Therefore the receiver will detect

signals from two rf bands separated by twice the i.f. band and an rf band twice as wide as the i.f. amplifier bandwidth can be measured. Owing to the low noise and possible gain, the tunnel diode mixer can be used as the first stage of the radiometer. To minimize the noise arising from the local oscillator and the antenna mismatching a balanced mixer is preferred. The equivalent circuit, available gain and noise figure of the double sideband mixer which converts two rf bands to i.f., are given in the following section.

A. Equivalent Circuit

Let the current-voltage characteristic of the tunnel diode be given by

$$i = f(v) \tag{9.1}$$

Let us neglect the harmonics of the local oscillator voltage and let v be given by

$$v = V_o + V_h \cos\omega_h t \tag{9.2}$$

where V_o is the dc bias.

V_h is the fundamental peak amplitude of the local oscillator voltage.

Then the Fourier series representation of the instantaneous conductance of the tunnel diode becomes

$$g(t) = \frac{di}{dv} = g_o + 2g_1 \cos\omega_h t + 2g_2 \cos 2\omega_h t + \ldots. \tag{9.3}$$

Using subscripts i, m and k to refer, respectively, to rf input, i.f. output and rf image frequencies, we can denote the complex voltage and current rms values by V_i, V_m, V_k, I_i, I_m and I_k. The frequency relations are $\omega_i = \omega_h + \omega_m$, $\omega_k = \omega_h - \omega_m$, $\omega_i = 2\omega_h - \omega_k$ and $\omega_k = 2\omega_h - \omega_i$. If we multiply the instantaneous conductance g(t) of Eq. (9.3) by the rf input voltage $V_{io}\cos(\omega_i t + \phi_i)$, the i.f. output voltage $V_{mo}\cos(\omega_m t + \phi_m)$ and the rf image voltage $V_{ko}\cos(\omega_k t + \phi_k)$ respectively, the current with all kinds of frequencies will exist. Keeping the frequency relations in mind and selecting only those currents with input, output and image frequencies, we have the linear current-voltage relation

$$\begin{aligned} I_i &= g_o V_i + g_1 V_m + g_2 V_k^* \\ I_m &= g_1 V_i + g_o V_m + g_1 V_k^* \\ I_k^* &= g_2 V_i + g_1 V_m + g_o V_k^* \end{aligned} \tag{9.4}$$

where the asterisks (*) denote the complex conjugate quantities. The complex conjugate quantities are necessary because the phase angle changes sign when the image component is involved in the mixing process.

We assume the local oscillator harmonic voltages to be negligible is a good approximation for practical mixers. If the local oscillator harmonic voltages are not neglected,

the theoretical analysis will be very complicated. These harmonics will affect not only the instantaneous conductance but also the interaction between the input and image. Under the zero harmonics assumption, the only possible interaction between the input and image is via g_2 which is one half of the second Fourier component of g(t). This is clearly shown in Eq. (9.4).

B. Available Gain

The available gain expression is now derived based on the terminal conditions given in Fig. 32. Let the input of the mixer have a very broad response so that the input impedances at the frequencies ω_i and ω_k are equal.

If the output is short-circuited, the i.f. current due to a current source I at the input terminals can be found by substituting $V_m = 0$, $I = I_i + g_s V_i$ and $I_k^* = - g_s V_k^*$ into Eq. (9.4). We get

$$I_m = I \left(\frac{g_1}{g_o + g_2 + g_s}\right) \tag{9.5}$$

where I is the complex rms value of the current source.

Similarly, the i.f. output short-circuited current I_m due to a current source I at the image terminals can be found by substituting $V_m = 0$, $I = I_k + g_s V_k$ and $I_i = - g_s V_i$ into Eq. (9.4). We get

$$I_m^* = I \left(\frac{g_1}{g_o + g_2 + g_s}\right) \tag{9.6}$$

Equation (9.6) differs from (9.5) by a complex conjugate sign. This difference should be expected since the image terminal current and voltage enter into (9.4) as complex conjugate quantities.

From the mixer-terminal conditions as shown in Fig. 32, and suppressing the current generator, I, we have $I_i = - g_s V_i$, $I_k^* = - g_s V_k^*$ and $I_m = g_{out} V_m$. Substituting these conditions into Eq. (9.4), we get three homogeneous equations in V_i, V_m and V_k^*, the determinant of which must vanish in order to have solutions. Setting the determinant equal to zero, we have

$$g_{out} = g_o - \frac{2g_1^2}{g_o + g_2 + g_s} \tag{9.7}$$

This indicates that g_{out} has a greater tendency toward having a negative real part. This is not so surprising, for in this case <u>both</u> sidebands contribute to the negative term in (9.7).

The power gain of the mixer due to a current source I at the input terminals can be written as

$$G = \frac{\text{Power delivered to load conductance}}{\text{Available power of input signal source}}$$

$$= \frac{I_m I_m^* g_L / (g_{out} + g_L)^2}{I\, I^* / 4g_s} = 4 \left(\frac{g_1}{g_o + g_2 + g_s}\right)^2 \frac{g_s g_L}{(g_{out} + g_L)^2} \tag{9.8}$$

Suppose the mixer is operated in such a condition that g_{out} is positive. Then the available gain can be obtained by substituting $g_L = g_{out}$ into G of (9.8). Thus, the available gain

$$G_{av} = \frac{g_s g_1^2}{(g_o + g_2 + g_s)\left[g_o(g_o + g_2 + g_s) - 2g_1^2\right]} \tag{9.9}$$

Next, let us consider the available gain due to a current source I alone connected to the image terminals. The situation is quite similar to the case we just derived. The image and the output current relation is given by (9.6). The g_{out} of (9.7) is still applicable because all the terminal conditions are the same. The available gain will be exactly the same as G_{av} of (9.9).

It is now possible to optimize G_{av} as a function of g_s, and to obtain the maximum available gain $(G_{av})_{max}$ and the corresponding optimum source impedance $(g_s)_{max}$. Since we do not need these expressions in our discussion, this step will be omitted.

Does the expression (9.9) also hold for a wideband radiometer in which white noise is received in both sidebands? According to van der Ziel,[34] the effect of double sideband reception is that the noise signals in the two sidebands add quadratically in the output. Consequently, if the power gain is defined as

$$G = \frac{\text{Noise power delivered to the output load}}{\text{Total noise power available in both sidebands}}$$

one again obtains (9.9).

C. Noise Figure

The output short-circuited noise current is contributed by the following sources:

a) Input noise

$$\overline{a^2} = 4kTg_s df F_c'^2 \qquad (9.10)$$

where F_c' is the current amplification given by the term in the parenthesis of Eq. (9.5) or (9.6).

b) Image noise

$$\overline{b^2} = 4kTg_s df F_c'^2 \qquad (9.11)$$

c) Tunnel diode noise

A small pulse in the diode current at $t = \tau$ will give an i.f. output component $a\cos\omega_m(t - \tau)$, an rf input component $a\cos\omega_i(t - \tau)$ and an rf image component $a\cos\omega_k(t - \tau)$. Since both the input and image terminals are not short-circuited, there will be voltages developed across them. The input and image voltages will give, respectively, i.f. component currents,

$$-aF_c'\cos(\omega_m t - \omega_i\tau) = -aF_c'\cos\left[\omega_m(t-\tau) - \omega_h\tau\right] \qquad (9.12)$$

and

$$-aF_c'\cos(\omega_m t + \omega_k\tau) = -aF_c'\cos\left[\omega_m(t-\tau) + \omega_h\tau\right] \qquad (9.13)$$

Notice that the phase angle $\omega_k\tau$ of the rf image component changes sign in (9.13).

Combining these three i.f. currents Eqs. (9.12), (9.13) and $a\cos\omega_m(t - \tau)$, we have

$$a\,(1 - 2F_c'\cos\omega_h\tau)\,\cos\omega_m(t - \tau) \qquad (9.14)$$

The square of the amplitude of (9.14) is

$$a^2(1 + 2F_c'^2 - 4F_c'\cos\omega_h\tau + 2F_c'^2\cos 2\omega_h\tau) \qquad (9.15)$$

Since full shot noise is assumed, a^2 can be replaced by $2eI_{eq}(\tau)df$. $I_{eq}(\tau)$ is the instantaneous equivalent shot noise current of the tunnel diode. The mean-square noise current can be found by taking averages over an ensemble and over equivalent instances τ.

$$d(\overline{i_\tau^2}) = 2eI_{eq}(\tau)df\,\frac{d(\omega_h\tau)}{2\pi}\,(1 + 2F_c'^2 - 4F_c'\cos\omega_h\tau + 2F_c^2\cos 2\omega_h\tau) \qquad (9.16)$$

Hence the contribution of the tunnel diode noise is

$$\overline{c^2} = \int_{-\pi}^{\pi} d(\overline{i_\tau^2})$$

$$= 2e\left[I_{eo}(1 + 2F_c'^2) - 4F_c'I_{e1} + 2F_c'^2I_{e2}\right]df \qquad (9.17)$$

Consequently the double sideband noise figure F_{dsb} becomes

$$F_{dsb} = \frac{\overline{a^2} + \overline{b^2} + \overline{c^2}}{\overline{a^2} + \overline{b^2}}$$

$$= 1 + \frac{1}{2} \cdot \frac{e}{2kT} \cdot \frac{1}{g_s F_c'^2} \left[I_{eo}(1 + 2F_c'^2) - 4F_c' I_{e1} + 2F_c'^2 I_{e2} \right] \tag{9.18}$$

where the image noise is considered to be part of the signal source noise. Since the input and the image can be considered independent to each other,[34] no correlation needs to be taken into account.

The noise figure of the double sideband mixer is better than that of the single sideband mixer because not only the factor $\frac{1}{2}$ in front of the second term of Eq. (9.18) but also the form between the brackets can be made smaller by properly choosing the parameters I_{eo}, I_{e1}, I_{e2}, g_o, g_1, g_2 and the signal conductance g_s.

Let us investigate the possibility of full noise cancellation, i.e., $F_{dsb} = 1$. Referring to Eq. (9.18), it is the same to investigate the possibility for the form between the brackets of Eq. (9.18) to be zero. It is intuitively clear that this can not be the case. For Eq. (9.15), from which (9.18) is derived, is a quantity that is positive or zero. Hence (9.16) is positive or zero and, since (9.16) can not be zero for all values of $\omega_h \tau$, it follows immediately that (9.17) can not be negative or zero and hence it must be positive. Only in a limiting case it may happen that this ppsitive number goes to zero.

Nevertheless, it is instructive to prove this directly from the definitions of I_{eo}, I_{e1}, and I_{e2}. To do this, we solve for F_c' after setting the form between the brackets in (9.18) equal to zero. Then

$$F_c' = \frac{I_{e1}}{I_{eo} + I_{e2}} \pm \frac{\sqrt{8\left[2I_{e1}^2 - (I_{eo} + I_{e2})I_{eo}\right]}}{4(I_{eo} + I_{e2})} \qquad (9.19)$$

Since $F_c' = g_1/(g_o + g_2 + g_s)$ and is a real number as given in Eq. (9.5), therefore the condition $\left[2I_{e1}^2 - (I_{eo} + I_{e2})I_{eo}\right] \geq 0$ is required for Eq. (9.19) to have a real value. This condition can be rewritten as

$$\frac{2I_{e1}^2}{I_{eo}} \geq I_{eo} + I_{e2} \qquad (9.20)$$

If $I_{eq}(t) \geq 0$, it is not possible to satisfy the inequality sign of Eq. (9.20) and the equality sign can only hold in a limiting case. That means, full noise cancellation can not be obtained except under the ideal limiting condition which is very unlikely to occur.

The proof is given as follows. From the definition of $I_{eq}(t)$,

$$I_{eq}(t) = I_{eo} + 2I_{e1}\cos\omega_h t + 2I_{e2}\cos 2\omega_h t + \ldots. \qquad (9.21)$$

we have

$$I_{e2} = \frac{1}{2\pi}\int_{-\pi}^{\pi} I_{eq}(t)\cos 2\omega_h t \, d(\omega_h t)$$

$$= \frac{1}{2\pi}\int_{-\pi}^{\pi} I_{eq}(t)\left[2\cos^2\omega_h t - 1\right] d(\omega_h t) \qquad (9.22)$$

or

$$I_{e2} + I_{eo} = \frac{2}{2\pi} \int_{-\pi}^{\pi} I_{eq}(t)\cos^2\omega_h t \, d(\omega_h t) \qquad (9.23)$$

and also

$$I_{el} = \frac{1}{2\pi} \int_{-\pi}^{\pi} I_{eq}(t)\cos\omega_h t \, d(\omega_h t) \qquad (9.24)$$

or

$$\frac{2I_{el}^2}{I_{eo}} = \frac{2}{I_{el}} \left[\frac{1}{2\pi} \int_{-\pi}^{\pi} I_{eq}(t)\cos\omega_h t \, d(\omega_h t) \right]^2 \qquad (9.25)$$

Next it is observed that the following inequality holds:

$$\frac{1}{2\pi} \int_{-\pi}^{\pi} \frac{I_{eq}(t)}{I_{eo}} \left[\cos\omega_h t - \frac{1}{I_{eo}} \frac{1}{2\pi} \int_{-\pi}^{\pi} I_{eq}(t)\cos\omega_h t \, d(\omega_h t) \right]^2 d(\omega_h t) \geq 0 \qquad (9.26)$$

since $I_{eq} \geq 0$ and $I_{eo} \geq 0$ lead to a positive integrand. Only in the limiting case can the equal sign apply. Expanding Eq. (9.26), we have

$$\frac{1}{2\pi} \int_{-\pi}^{\pi} \frac{I_{eq}(t)}{I_{eo}} \cos^2\omega_h t \, d(\omega_h t) \geq \frac{1}{I_{eo}^2} \left[\frac{1}{2\pi} \int_{-\pi}^{\pi} I_{eq}(t)\cos\omega_h t \, d(\omega_h t) \right]^2 \qquad (9.27)$$

multiplying both sides of (9.27) by $2I_{eo}$ and comparing with the Eqs. (9.23) and (9.25), we have

$$I_{e2} + I_{eo} \geq \frac{2I_{el}^2}{I_{eo}} \qquad (9.28)$$

where the equal sign only holds in a limiting case. This contradicts the condition of Eq. (9.20) and proves that $F_{dsb} = 1$ is only an ideal limiting case.

The double sideband noise figure of (9.18) can be minimized by substituting $F_c = g_1/(g_o + g_2 + g_s)$ into Eq. (9.18) which can be written as

$$F_{dsb} = 1 + \frac{1}{2}\frac{e}{2kT}\frac{I_{eo}}{g_s g_1^2}\left\{(g_o + g_2 + g_s)^2 + 2g_1^2 - 4g_1(g_o + g_2 + g_s)I_{e1}/I_{eo} + 2g_1^2 I_{e2}/I_{eo}\right\} \tag{9.18a}$$

This may be rewritten as

$$F_{dsb} = 1 + \frac{1}{2}\frac{e}{2kT}\frac{I_{eo}}{g_1^2}\left\{g_s + \frac{1}{g_s}\left\{(g_o + g_2)^2 + 2g_1^2 - 4g_1(g_o + g_2)\frac{I_{e1}}{I_{eo}} + 2g_1^2\frac{I_{e2}}{I_{eo}}\right\} + 2(g_o + g_2 - 2g_1 I_{e1}/I_{eo})\right\} \tag{9.18b}$$

Differentiation with respect to g_s gives that F_{dsb} has a minimum value if

$$g_s = (g_s)_{opt} = \sqrt{(g_o + g_2)^2 + 2g_1^2 - 4g_1(g_o + g_2)I_{e1}/I_{eo} + 2g_1^2 I_{e2}/I_{eo}} \tag{9.29}$$

unless $(g_o + g_2)^2 + 2g_1^2 - 4g_1(g_o + g_2)I_{e1}/I_{eo} + 2g_1^2 I_{e2}/I_{eo} < 0$ and

$$F_{dsb} = (F_{dsb})_{min}$$

$$= 1 + \frac{1}{2}\frac{e}{2kT}\frac{I_{eo}}{2}\frac{}{g_1}\left[2\sqrt{(g_o+g_2)^2 + 2g_1^2 - 4g_1(g_o+g_2)I_{e1}/I_{eo} + 2g_1^2 I_{e2}/I_{eo}}\right.$$

$$\left. + 2(g_o + g_2 - 2g_1 I_{e1}/I_{eo})\right] \qquad (9.30)$$

The condition

$$(g_o+g_2)^2 + 2g_1^2 - 4g_1(g_o+g_2)(I_{e1}/I_{eo}) + 2g_1^2(I_{e2}/I_{eo})$$

$$= \left[(g_o+g_2)^2 - 2g_1(I_{e1}/I_{eo})\right]^2 + 2g_1^2\left[1 - (I_{e1}/I_{eo})^2\right]$$

$$+ 2g_1^2\left[(I_{e2}/I_{eo}) - (I_{e1}/I_{eo})^2\right] \geq 0 \qquad (9.29a)$$

is always satisfied since $(I_{e1}/I_{eo})^2 \leq 1$ and $(I_{e1}/I_{eo})^2 \leq (I_{e2}/I_{eo})$. The former was proved in Chapter III for Eq. (3.9a) and the latter can be obtained by subtracting $I_{eo} \geq I_{e1}^2/I_{eo}$ from Eq. (9.28).

V. Conclusions

1. Correlation between high-frequency noise and intermediate-frequency noise is important. It can not be neglected, especially not for back diode mixers.

2. No ideal current-voltage characteristic of the tunnel diode for a high gain, low noise mixer operation can be found.

3. The conditions for high gain and for low noise figure do not go together. Usually it is not worthwhile to design tunnel diode mixers with large gain.

4. Feedback from a capacitance in the anode lead or an inductance in the cathode lead of the first i.f. stage will damp out the negative output conductance of the mixer with slight improvement on the noise figure. A grounded-grid i.f. stage has the same characteristic.

5. The noise figure contribution from the mixer itself, i.e., the factor (F-1), is lowered more than 3 dB in double sideband mixing as compared with single sideband mixing.

6. In first approximation results can be deduced from static characteristic and can be extended to other characteristics by comparing their shapes.

7. Three possible operating regions of the tunnel diode can be distinguished.

(i) The vicinity of the valley point. This gives relatively low gain but also low noise.

(ii) The vicinity of the peak point. This can give high gain, but the noise is larger than under (i).

(iii) Operating at zero bias. This is especially useful in back diodes and leads to low noise operation as (i).

8. The peak local oscillator amplitude of about 200 mV is optimum. Its amplitude is not very critical on mixer operation.

9. The signal conductance should be chosen in the neighborhood of the optimized value $(g_s)_{opt}$ for minimum noise figure. If a compromise must be made, this should be done such that a larger mixer available gain and (or) a more desirable mixer output conductance is obtained.

10. The best noise figure is obtained for back diodes.

11. Operating back diodes in the backward region is recommended for microwave frequencies (operating on majority carriers and less trouble with burn-out).

VI. Recommendations for Further Work

1. It is recommended to measure the g-parameters (g_o, g_1, g_2, ...) of the device more accurately. This would allow a more accurate check of the optimum operation of the mixer.

2. It is recommended to carry out accurate power gain measurements on tunnel diode mixers which can be done by making two available power measurements. In particular means of optimizing the power gain as a function of the local oscillator signal should be studied, for in many applications it is highly desirable to have a stable gain.

3. It is recommended that a more detailed study be made of the minimum noise figure F_{min} as a function of the local oscillator voltage. The maximum in the power gain and the minimum in the noise figure are usually quite broad and it is often possible to find a good compromise for optimizing both.

4. The stability problem of tunnel diode mixers using diodes with a large negative conductance region requires further study. It should be noted, however, that such diodes do not give the same good noise performance as back diodes.

5. Further study of noise in tunnel diodes is indicated. This would allow to determine I_{eo} and I_{el} directly without any assumptions about the shot-noise character of the noise.

6. The work presented in this report should be extended to microwave frequencies. In particular the effect of the series of resistance of the diode upon the mixer performance at microwave frequencies should be studied.

7. A study should be made of the effect of the variable barrier capacitance upon the mixer performance at microwave frequencies.

8. A study should be made of possible storage effects in back diodes operated in the forward direction. Such effects, if present, might seriously deteriorate the gain and noise performance of the mixer at microwave frequencies.

9. A study should be made of the double sideband mixer for radiometer purposes. Here the conditions of low noise figure and a stable optimized power gain must be met simultaneously.

10. Backward diode mixers operated at zero bias have very low 1/f noise. A study should be made of the feasibility of replacing the tuned i.f. amplifier by a wideband video amplifier.

VII. Personnel Employed on Contract

	Man Months
A. van der Ziel (on leave from 1/1 - 6/15/61)	.70
Shi-fang Lo	17.167
Laboratory Technical Assistants	640.2 Man Hours

Curriculum Vitae

A. van der Ziel, B.A. 1930, M.A. 1933, Ph.D. 1934 (Physics and Mathematics), University of Groningen, the Netherlands; Research Fellow, N. V. Philips' Gloeilampenfabrieken, Eindhoven, the Netherlands, 1934-47; Associate Professor, Physics Department, University of British Columbia, Vancouver, Canada, 1947-50; Professor of Electrical Engineering, University of Minnesota, 1950-.

Shi-fang Lo, B.S. 1954, National Taiwan University, China; M.S. 1958, Ph.D. 1962, University of Minnesota; Teaching Assistant 1956-58, Instructor 1958-1960, Research Fellow 1961-1962, University of Minnesota.

BIBLIOGRAPHY

1. H. C. Torrey and C. A. Whitmer, CRYSTAL RECTIFIERS, M.I.T. Radiation Lab. Series 15, McGraw-Hill, New York, 1948.

2. R. V. Pound, MICROWAVE MIXERS, M.I.T. Radiation Lab. Series 16, McGraw-Hill, New York, 1948.

3. H. S. Sommers, Jr., "Tunnel Diodes as High-Frequency Devices," Proc. IRE 47, 1201-1206, July (1959).

4. I. A. Lesk, N. Halonyak, Jr., U. S. Davidsohn and M. W. Aarons, "Germanium and Silicon Tunnel Diodes--Design, Operation and Application," 1959 WESTON CONVENTION RECORD, Part 3.

5. K. K. N. Chang, G. H. Heilmeier and H. J. Prager, "Low-Noise Tunnel-Diode Down Converter Having Conversion Gain," Proc. IRE 48, 854-858, May (1960).

6. D. I. Breitzer, "Noise Figure of Tunnel-Diode Mixer," Proc. IRE 48, 935-936, May (1960).

7. J. C. Greene and E. W. Sard, "Experimental Tunnel-Diode Mixer," Proc. IRE 49, 350-351, Jan. (1961).

8. C. S. Kim, "Tunnel Diode Converter Analysis," General Electric Technical Information Series, No. R60ELS-102.

9. Don G. Peterson, "Tunnel-Diode Down Converters," Proc. IRE 49, 1225-1226, July (1961).

10. H. J. Prager and K. K. N. Chang, "The Effect of Large Pump Voltage on Tunnel Diode Down Converter Performance," RCA Review 22, 567-581, Sept. (1961).

11. Shih-fang Lo, "Noise in Tunnel Diode Mixers," Proc. IRE 49, 1688-1689, Nov. (1961).

12. C. S. Kim and J. E. Sparks, "Tunnel Diode Converters," Proc. Nat. Electronic Conf. 16, 791-800, (1960).

13. L. E. Dickens and C. R. Gneitling, "A Tunnel-Diode Amplifying Converter," IRE Trans., MIT-9, 99-100, Jan. (1961).

14. F. Sterzer and A. Fresser, "Stable Low-Noise Tunnel-Diode Frequency Converter," Proc. IRE 49, 1318, Aug. (1961).

Bibliography (continued)

15. A. van der Ziel, NOISE, Chapter 9, Prentice-Hall, Englewood Cliffs, N. J., 1954.

16. A. van der Ziel, SOLID STATE PHYSICAL ELECTRONICS, Prentice-Hall, Englewood Cliffs, N. J., 1957, pp. 264-267.

17. A. van der Ziel, NOISE, Chapter 10, Prentice-Hall, Englewood Cliffs, N. J., 1954.

18. H. J. Prager and K. K. N. Chang, "The Effect of Large Pump Voltage on Tunnel Diode Down Converter Performance," RCA Review, XXII, No. 3, 567-581, Sept. (1961).

19. F. Sterzer and A. Presser, "Stable Low-Noise Tunnel-Diode Frequency Converters," RCA Review XXIII, No. 1, 3-28, March (1962).

20. Fourth Quarterly Report, "Study of Noise in Semiconductors and Semiconductor Devices," Task II, April 1, 1961 to June 30, 1961, Contract DA 36-039 sc-85374, D.A. Proj. No. 3A99-21-001.

21. Bent Christensen, "Measurement of Tunnel-Diode Conductance Parameters," Proc. IRE 49, 1581, October (1961).

22. General Electric Tunnel Diode Manual, First Edition, p. 66, Sec. 7.1.

23. The General Radio Experimenter 34, Nos. 7 and 8, pp. 3-4, July-August (1960).

24. Fourth Quarterly Report, "Study of Noise in Semiconductors and Semiconductor Devices," pp. 15-17, April 1, 1961 to June 30, 1961, Contract DA 36-039 sc-85374, D.A. Proj. No. 3A99-21-001.

25. R. A. Pucel, "The Equivalent Noise Current of Esaki Diodes," Proc. IRE 49, 1080-1081, June (1961).

26. J. C. Greene, et al., "Eighth Quarterly Progress Report on Application of Semiconductor Diodes to Low-Noise Amplifiers, Harmonic Generators, and Fast-Acting TR Switches," Airborne Instruments Lab., Melville, N.Y., Report No. 4589-I-8; June 1960.

Bibliography (continued)

27. J. Klapper, A. Newton and B. Rabinovici, "Some Characteristics of Tunnel-Diode UHF Mixers," Proc. IRE 50, 479, April (1962).

28. A. van der Ziel, SOLID STATE PHYSICAL ELECTRONICS, Prentice-Hall, Englewood Cliffs, N.J., 1957, pp. 291-297.

29. Private communication.

30. R. H. Dicke, "The Measurement of Thermal Radiation at Microwave Frequencies," Rev. Sci. Instr. 17, 268-275, July (1946).

31. A. van der Ziel, NOISE, Prentice-Hall, Englewood Cliffs, N.J., 1954, pp. 83-86.

32. J. L. Lawson and G. E. Uhlenbeck, "Threshold Signals," M.I.T. Series 24, 103-108, McGraw-Hill, New York, 1950.

33. G. C. Southworth, "Microwave Radiation From the Sun," J. Frank. Inst., 239, 285-297, April (1945).

34. A. van der Ziel, NOISE, Prentice-Hall, Englewood Cliffs, N.J., 1954, pp. 253-254.

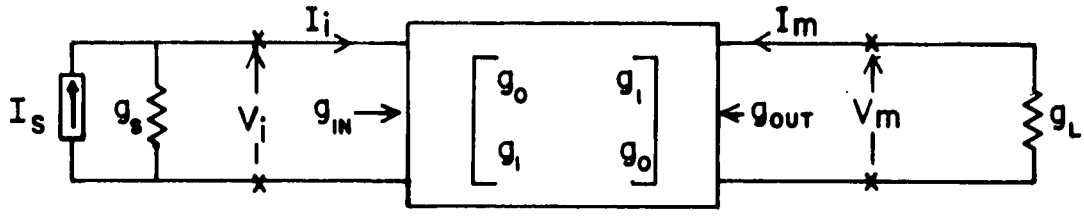

Fig. 1 Diode Mixer Considered as a Two-port Network

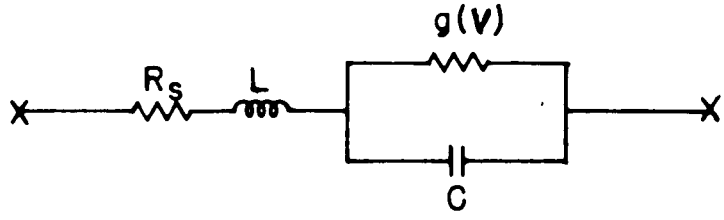

Fig. 2 Equivalent Circuit of a Tunnel Diode

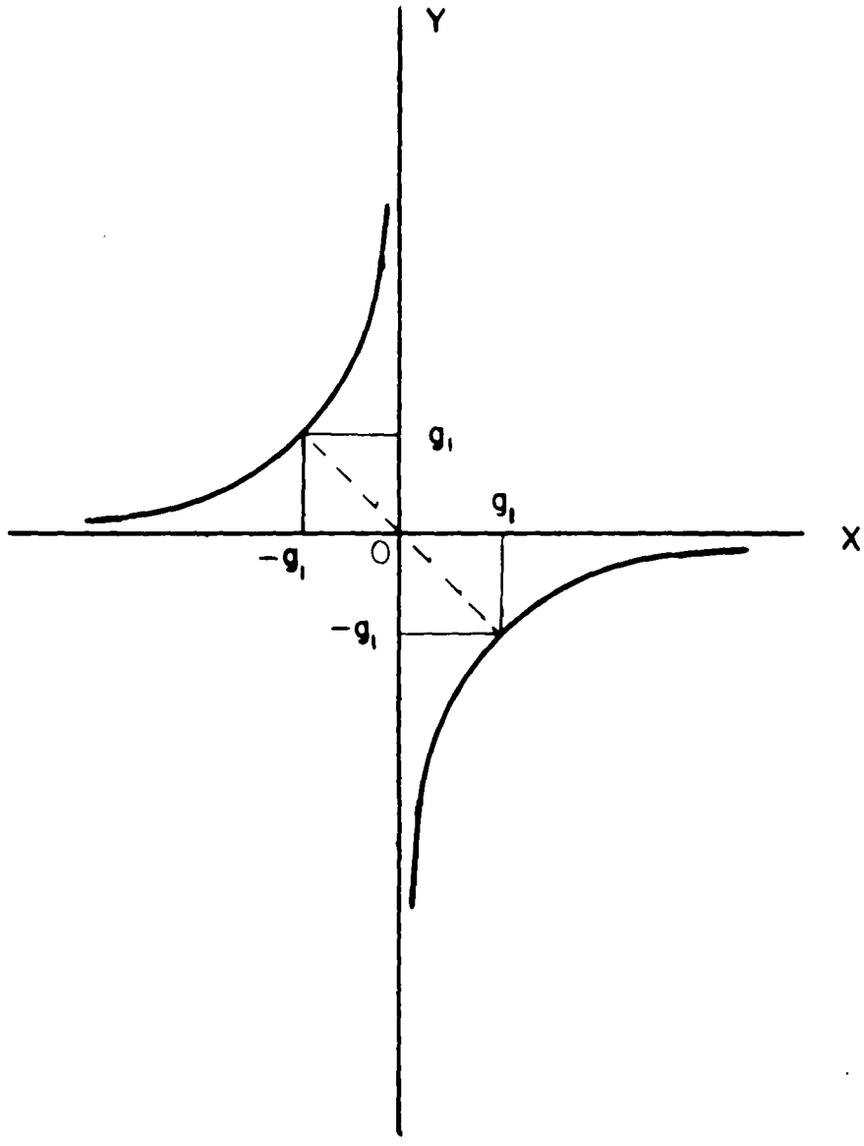

THE OUTPUT CONDUCTANCE OF A TUNNEL DIODE MIXER

Fig. 3

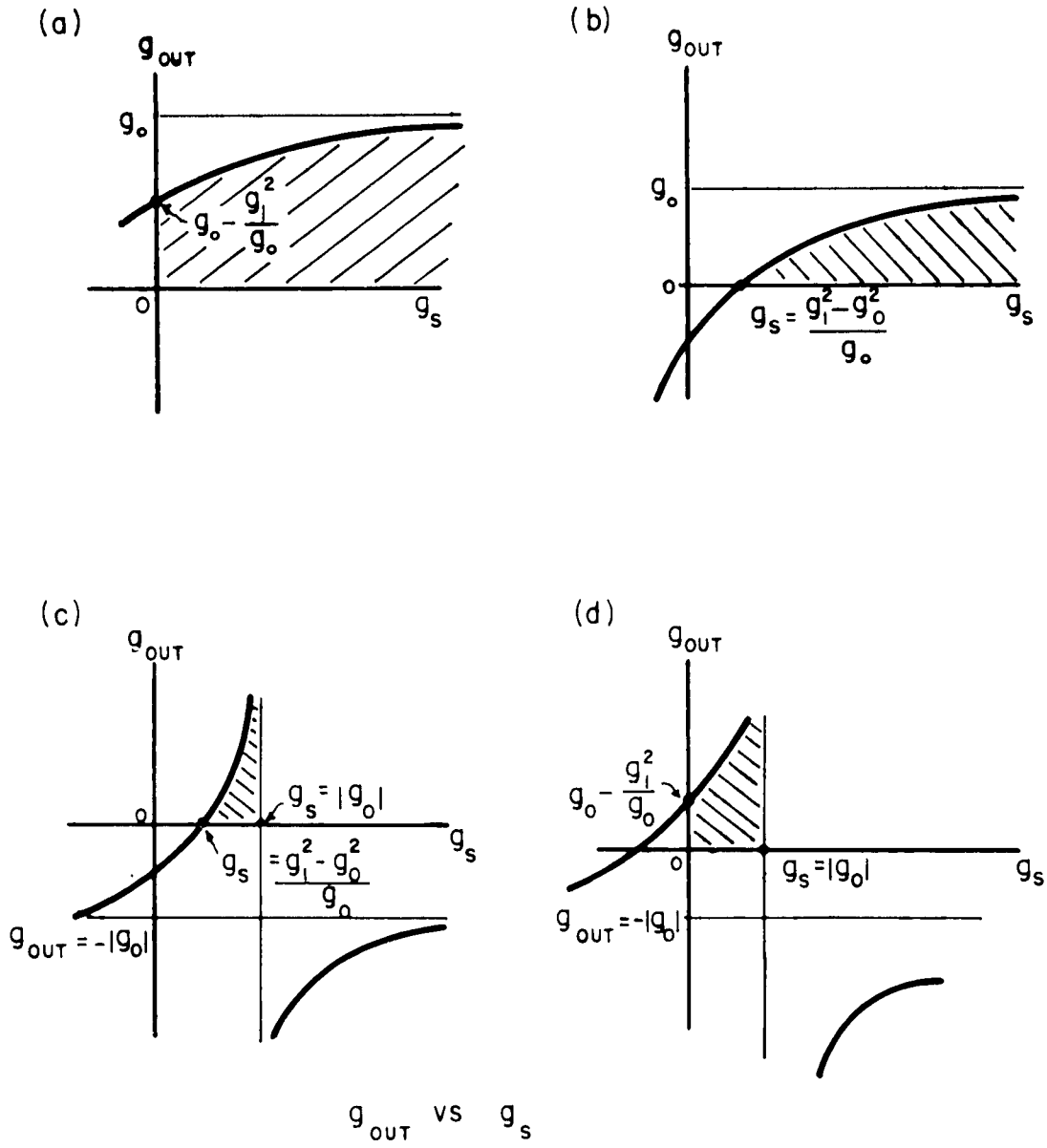

g_{OUT} vs g_s

For A Tunnel Diode Mixer

Fig. 4

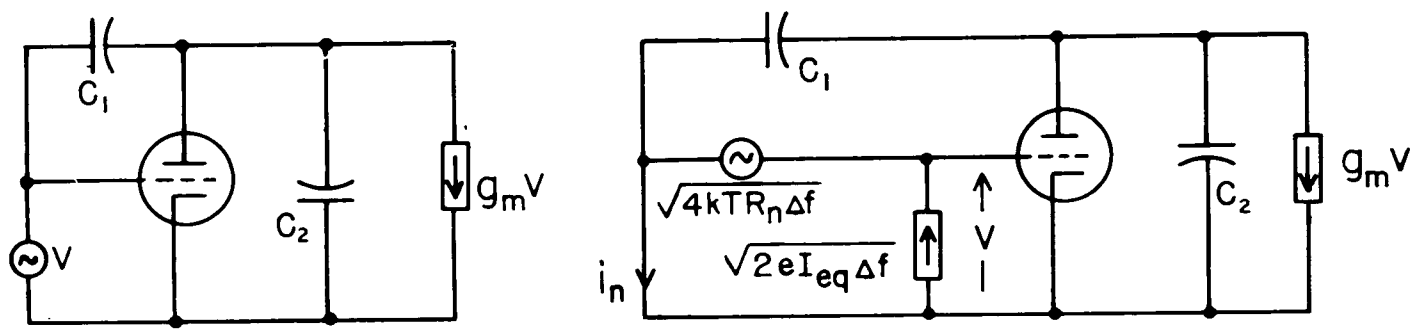

a) b)

Fig. 5

Feedback From A Capacitance In The Anode Lead Of A Triode

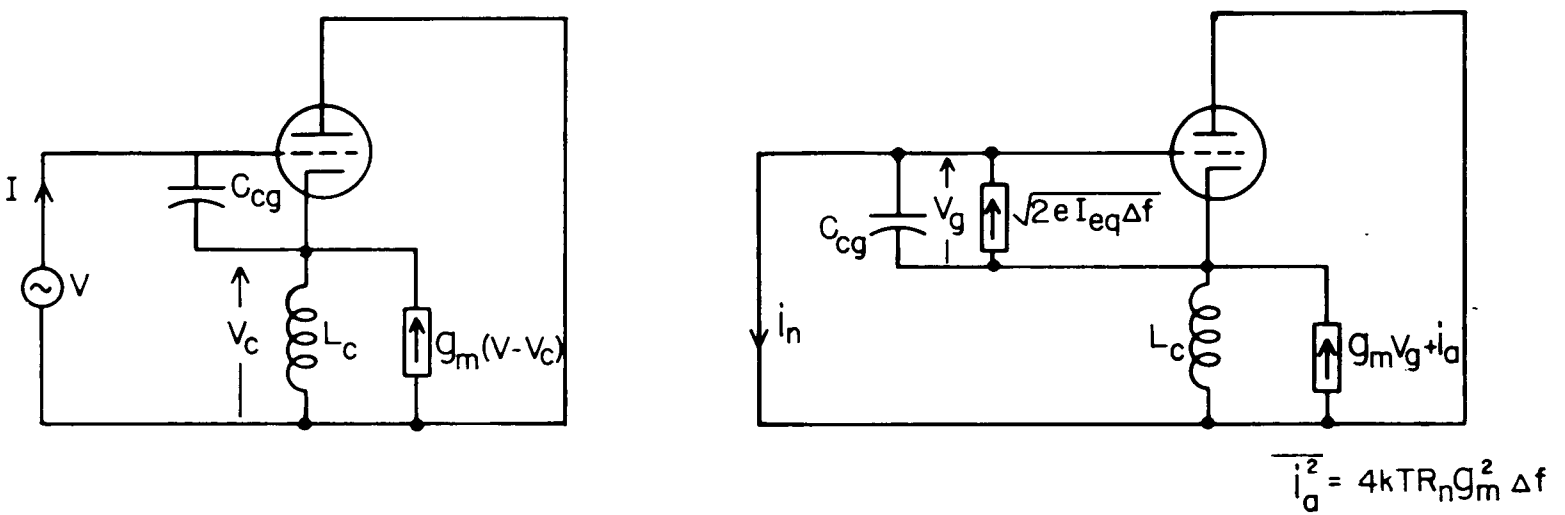

Feedback From An Inductance In The Cathode Lead Of A Triode

Fig. 6

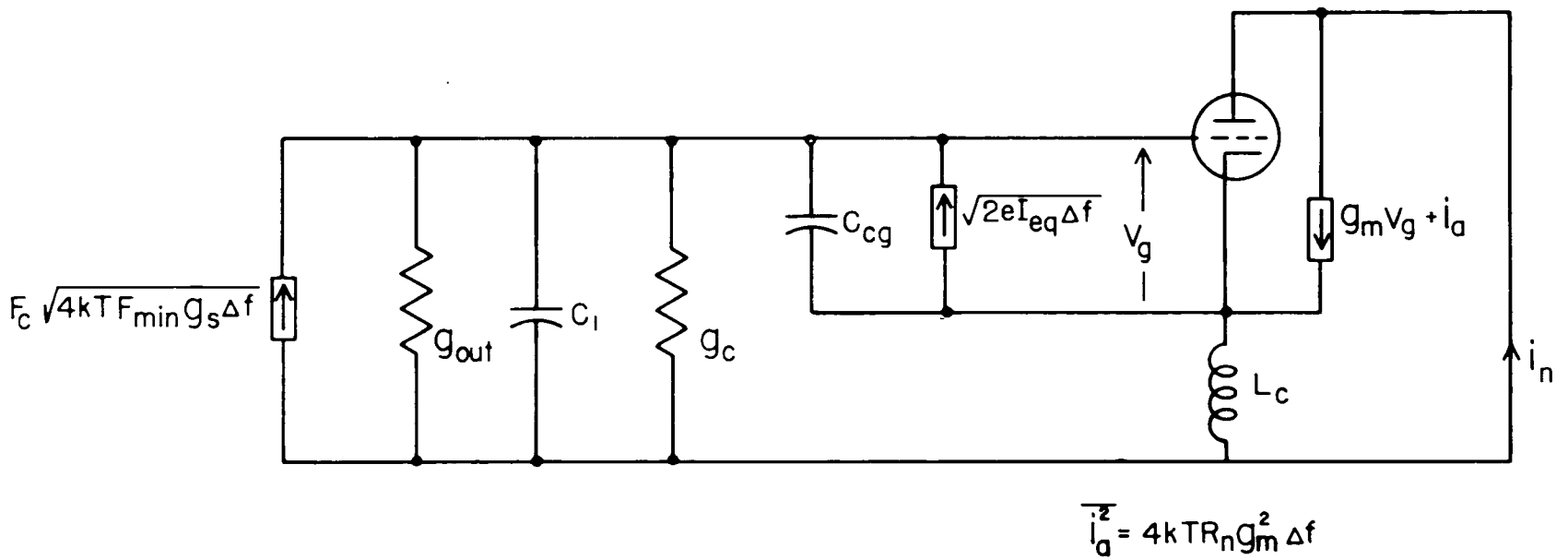

Noise Figure Of A Tunnel Diode Mixer With A Feedback i. f. Stage

Fig. 7

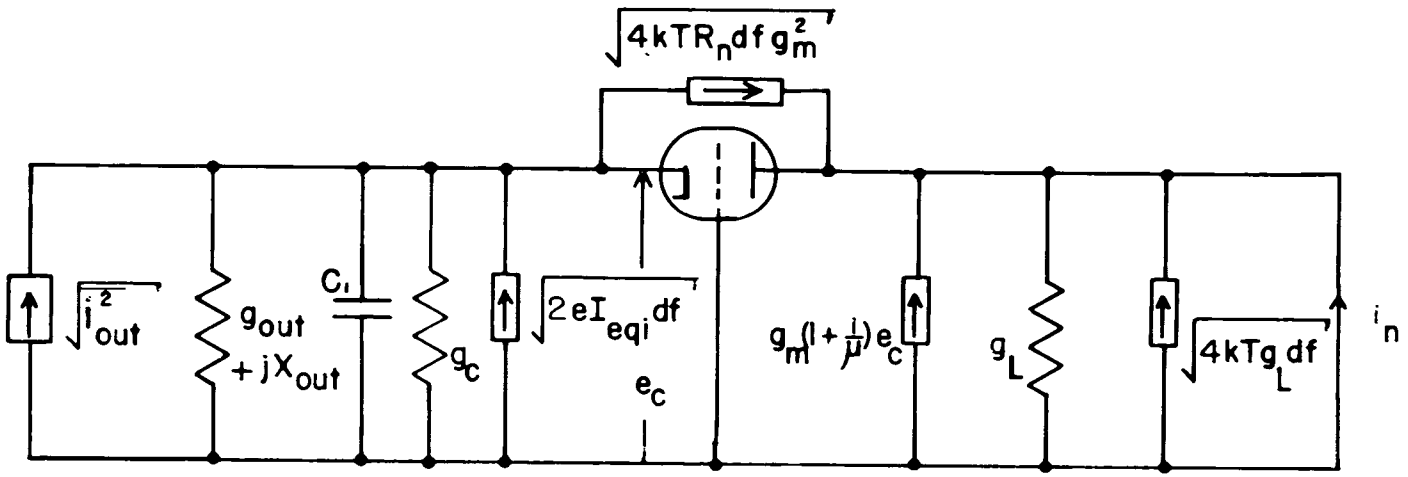

Fig. 8 Noise Figure of a Tunnel Diode Mixer Followed by a Grounded Grid I.F Stage

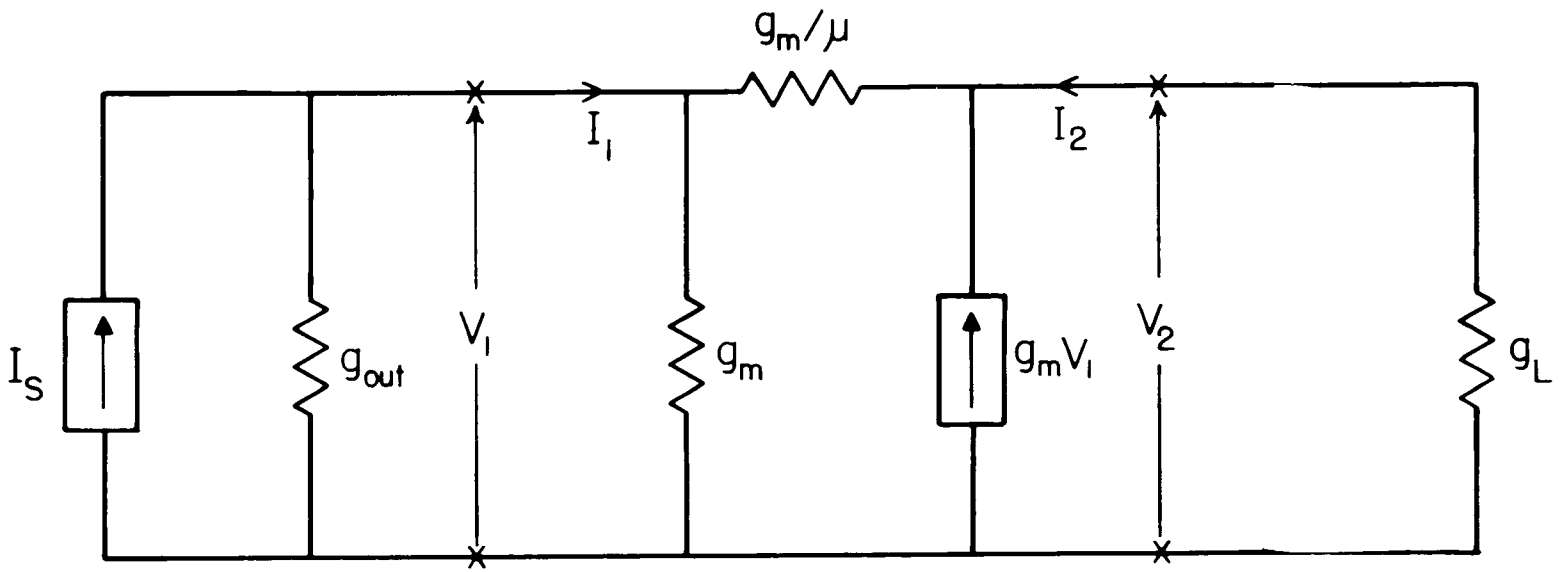

Equivalent Circuit of the Tunnel Diode Mixer Plus the Grounded Grid Amplifier. The Interelectrode Capacitances Are Neglected.

Fig. 9

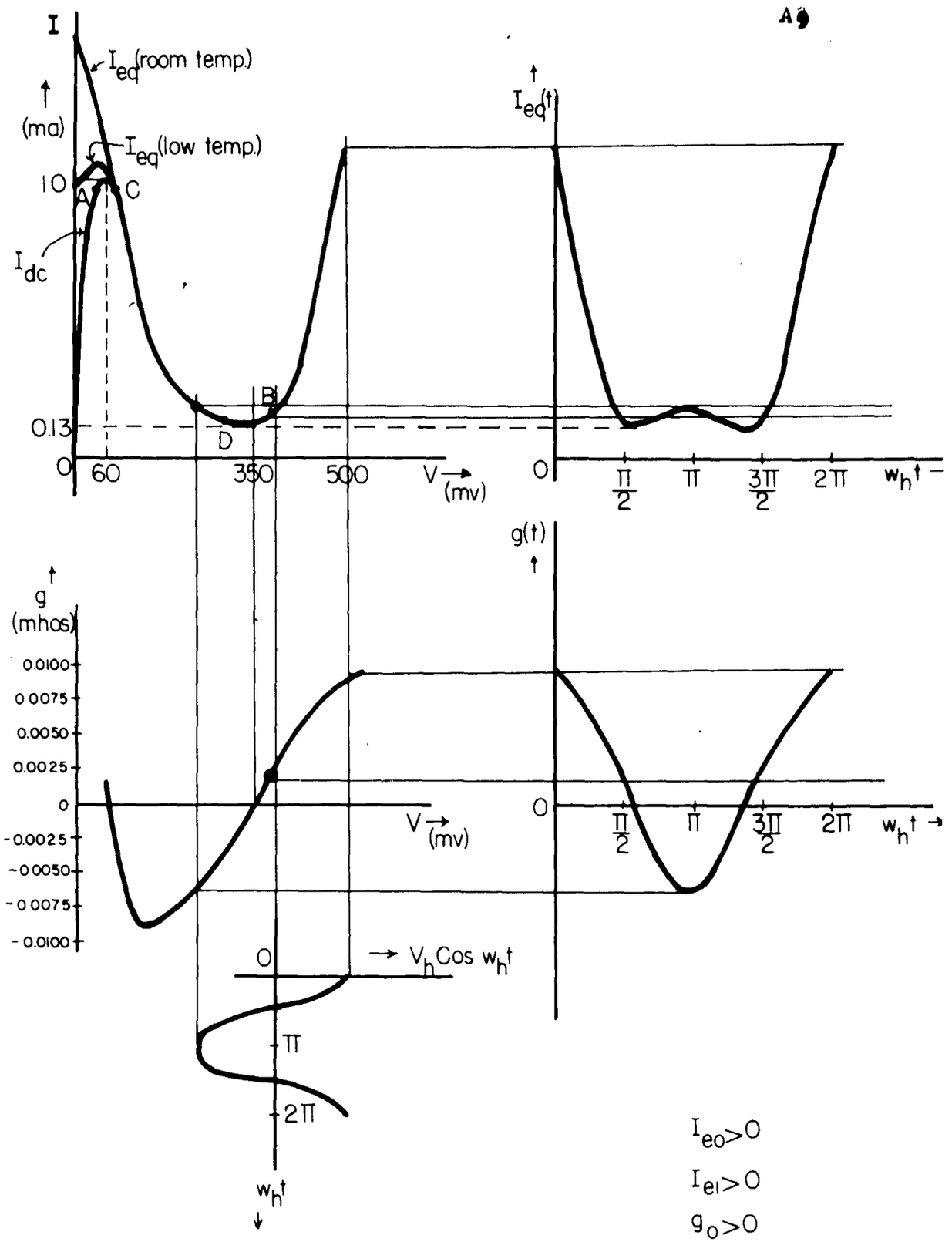

Typical I-V Characteristic of Germanium Tunnel Diode GE IN3218A

Graphical Method For The Operation Of A Tunnel Diode Mixer

Fig. 10

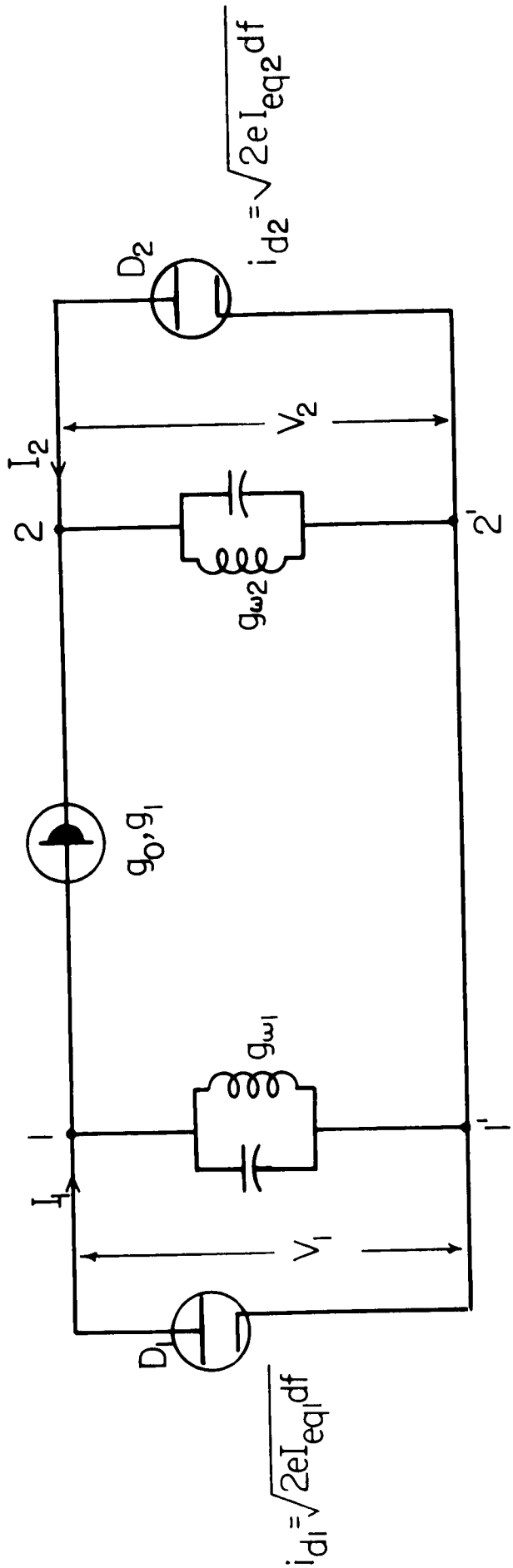

Fig. 11 Circuit for Measuring Current Amplification in Tunnel Diode Mixer

Fig. 12

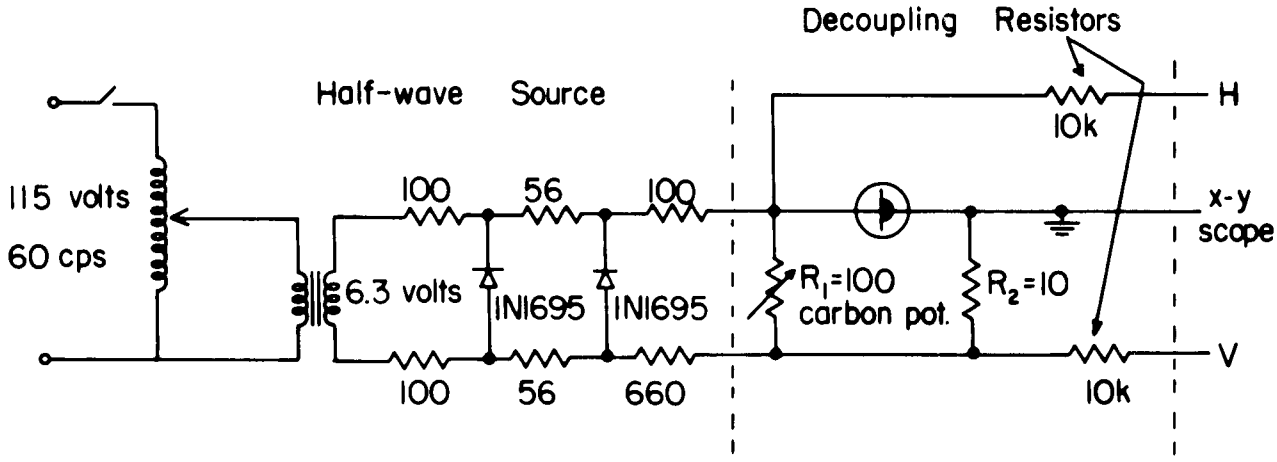

All Resistances in Ohms.

Tunnel Diode I-V Curve Tracer

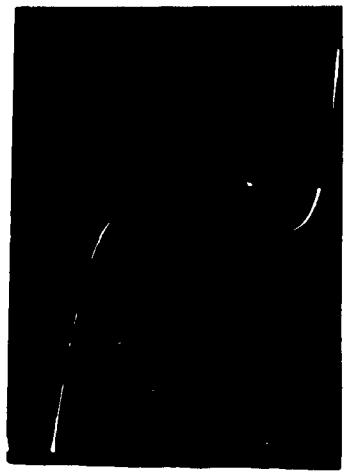

(a) GE IN2939

I_p = 1.000 ma

I_v = 0.118 ma

(b) GE 4JF2-BD-2

I_p = 0.290 ma

I_v = 0.026 ma

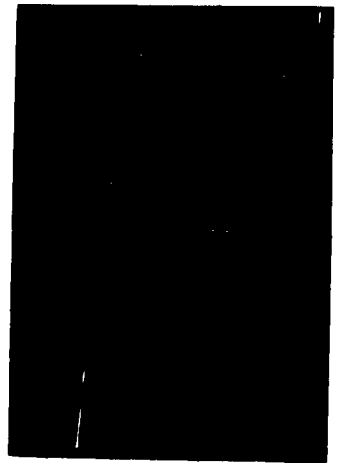

(c) GE 4JF2-BD-3

I_p = 0.124 ma

I_v = 0.011 ma

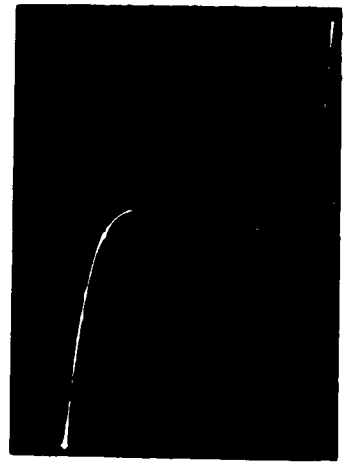

(d) Philco IN3353

I_p = 0.093 ma

I_v = 0.020 ma

Vertical Scale = (a) 1 ma/div ; (b),(c),(d) 0.1 ma/div

Horizontal Scale = 50 mv/div

Fig. 13 Current - Voltage characteristics of tunnel diodes

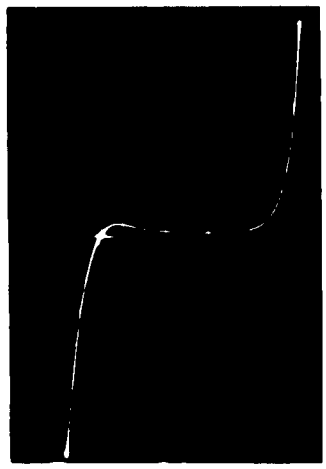

(a) GE 4JF2-BD-4

I_p = 0.040 ma

I_v = 0.006 ma

(b) GE 4JF2-BD-5

I_p = 0.018 ma

I_v = 0.003 ma

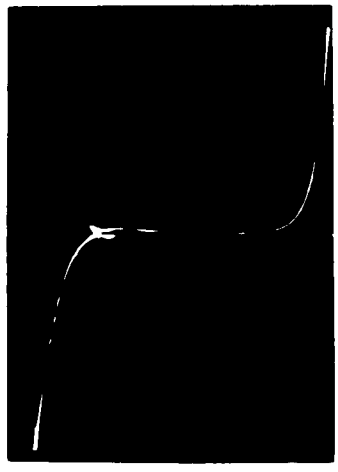

(c) GE 4JF2-BD-6

I_p = 0.013 ma

I_v = 0.002 ma

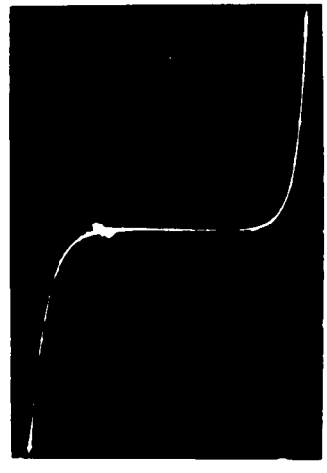

(d) GE 4JF2-BD-7

I_p = 0.002 ma

I_v = 0.0006 ma

Vertical Scale = 0.1 ma / div

Horizontal Scale = 50 mv / div

Fig. 14 Current - Voltage characteristics of tunnel diodes

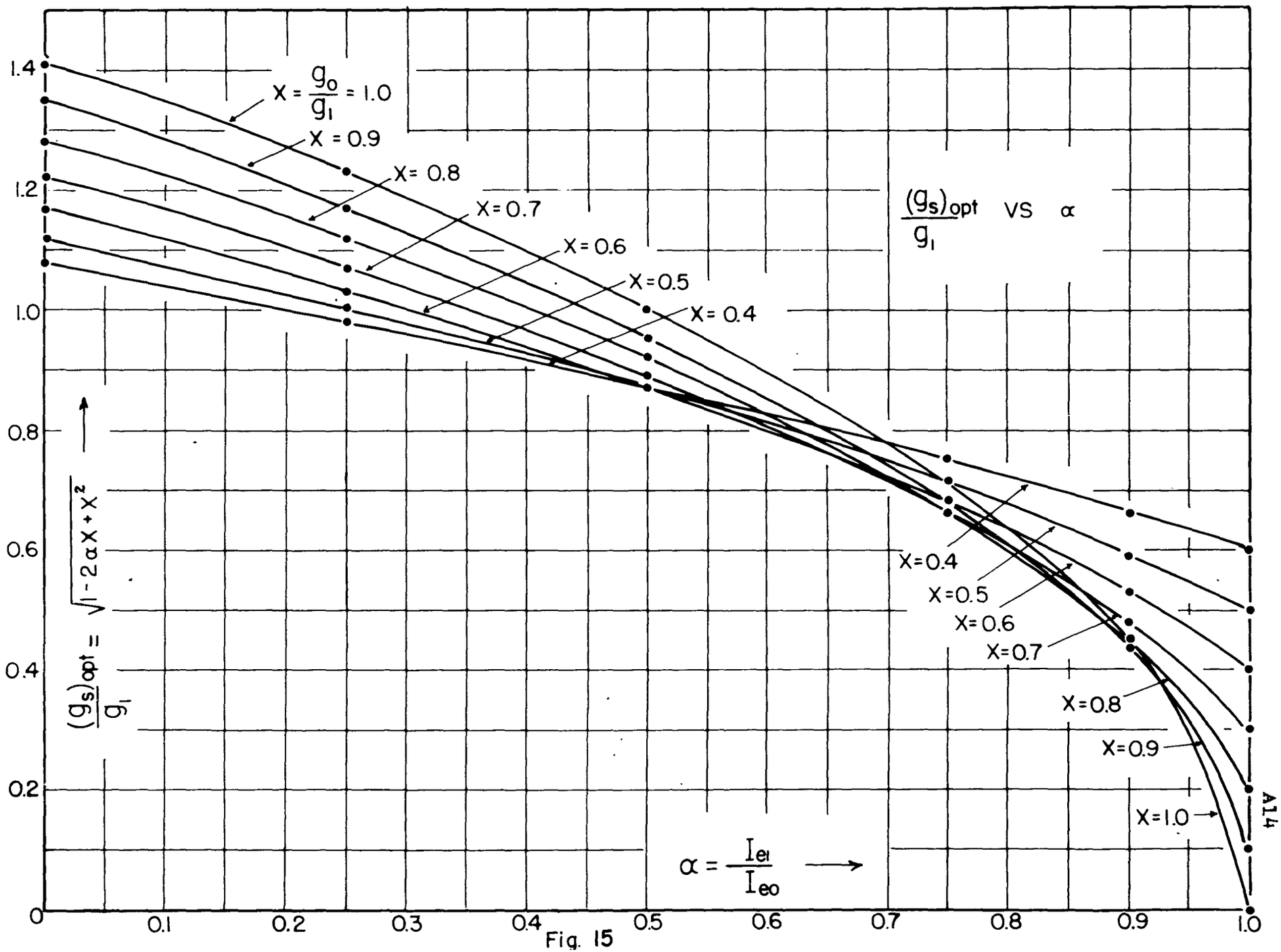
$X = \frac{g_0}{g_1} = 1.0$
X = 0.9
X= 0.8
X= 0.7
X= 0.6
X=0.5
X= 0.4
$\frac{(g_s)_{opt}}{g_1}$ VS α
X=0.4
X=0.5
X=0.6
X=0.7
X=0.8
X=0.9
X=1.0
$\frac{(g_s)_{opt}}{g_1} = \sqrt{1-2\alpha X+X^2}$
$\alpha = \frac{I_{e1}}{I_{e0}}$
1.4
1.2
1.0
0.8
0.6
0.4
0.2
0
0.1
0.2
0.3
0.4
0.5
0.6
0.7
0.8
0.9
1.0

Fig. 15

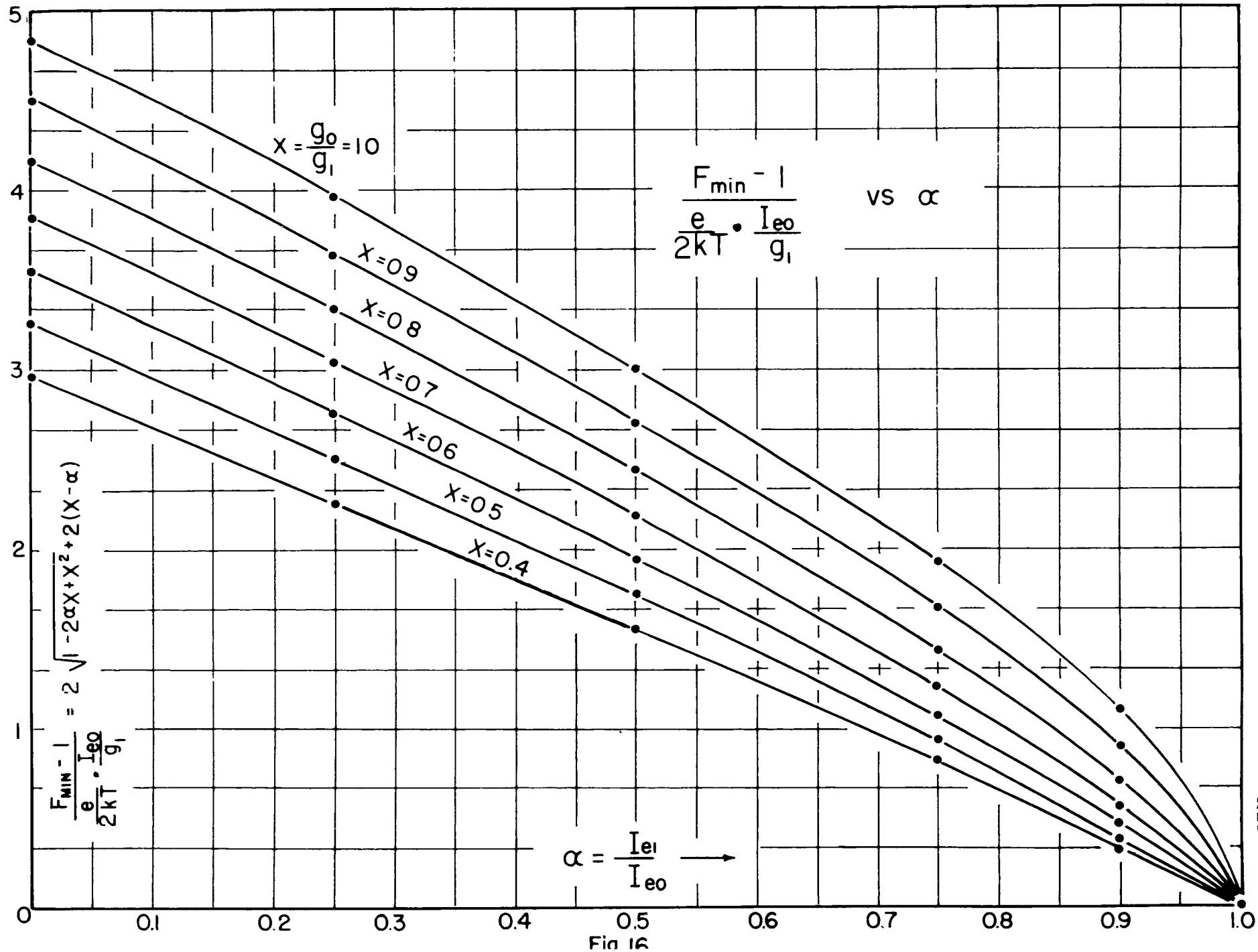
$X = \frac{g_o}{g_1} = 10$
X=0.9
X=0.8
X=0.7
X=0.6
X=0.5
X=0.4
$\frac{F_{min} - 1}{\frac{e}{2kT} \cdot \frac{I_{eo}}{g_1}}$ vs α
$\frac{F_{MIN} - 1}{\frac{e}{2kT} \cdot \frac{I_{eo}}{g_1}} = 2\sqrt{1 - 2\alpha X + X^2} + 2(X - \alpha)$
$\alpha = \frac{I_{e1}}{I_{eo}}$
0
1
2
3
4
5
0.1
0.2
0.3
0.4
0.5
0.6
0.7
0.8
0.9
1.0

Fig 16

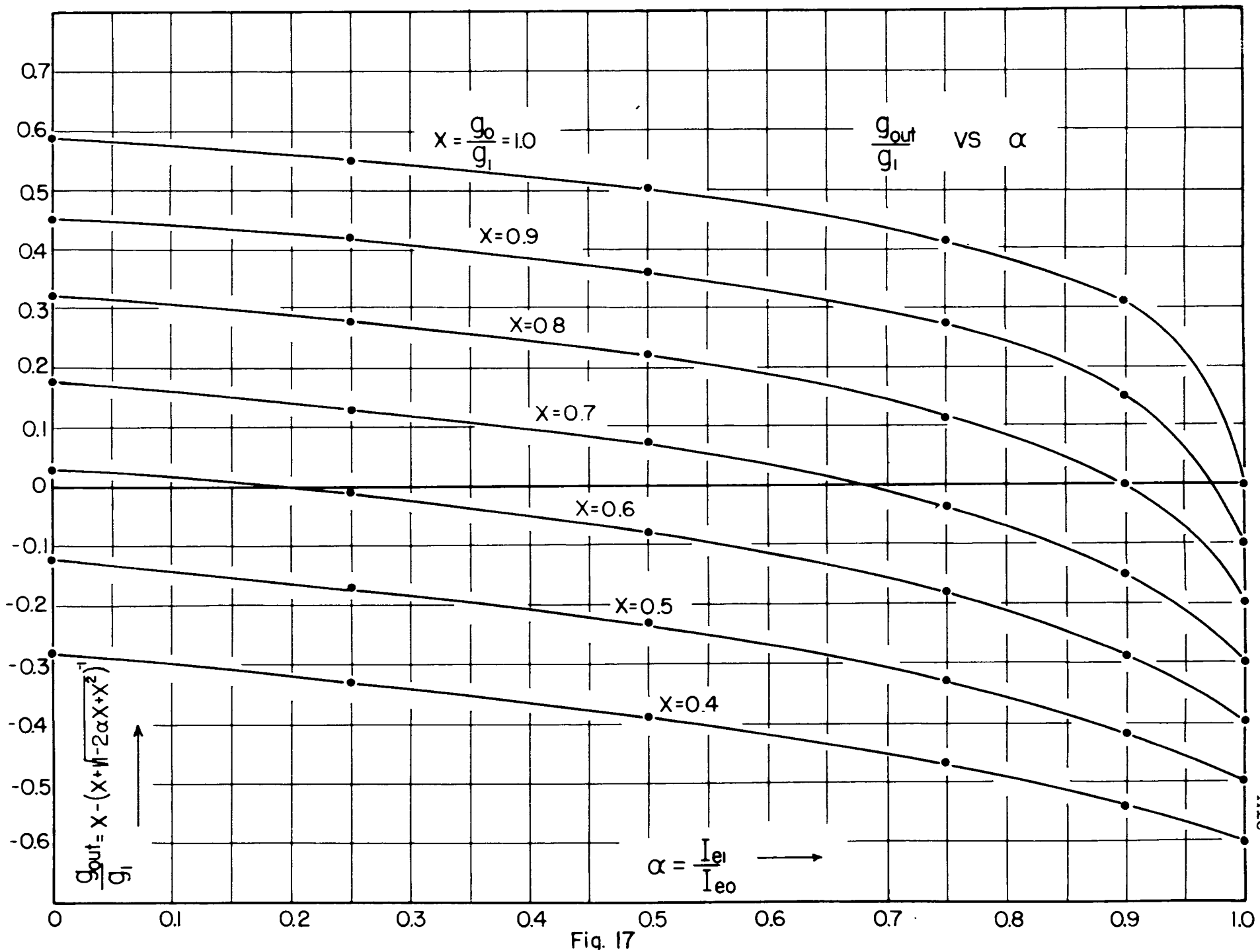
$\frac{g_{out}}{g_1}$ vs α
$X = \frac{g_0}{g_1} = 1.0$
X=0.9
X=0.8
X=0.7
X=0.6
X=0.5
X=0.4
$\frac{g_{out}}{g_1} = X - (X + \sqrt{1-2\alpha X+X^2})^{-1}$
$\alpha = \frac{I_{e1}}{I_{eo}}$
0.7
0.6
0.5
0.4
0.3
0.2
0.1
0
-0.1
-0.2
-0.3
-0.4
-0.5
-0.6
0
0.1
0.2
0.3
0.4
0.5
0.6
0.7
0.8
0.9
1.0

Fig. 17

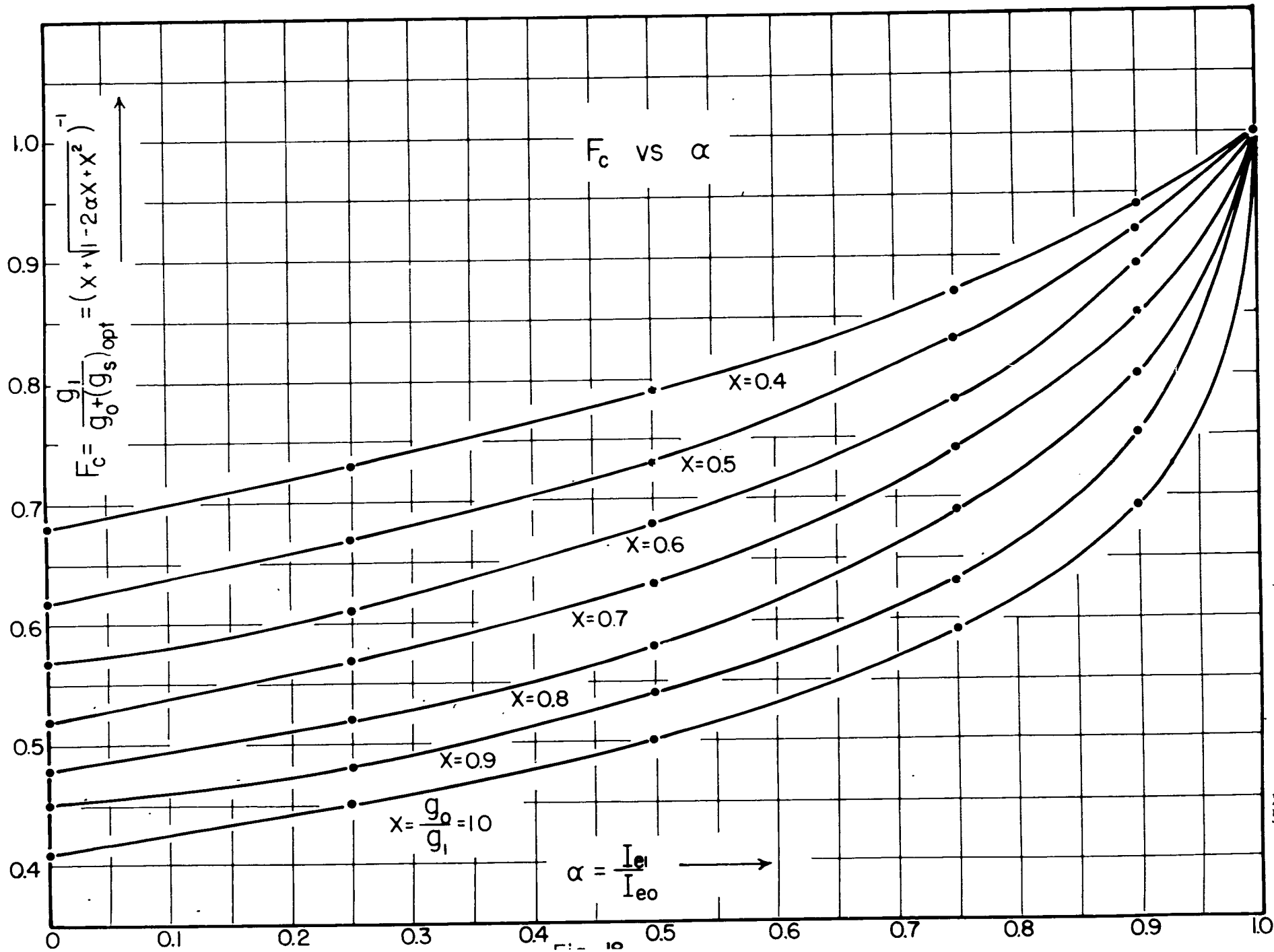
F_c vs α
$F_c = \frac{g_1}{g_o+(g_s)_{opt}} = (x+\sqrt{1-2\alpha x+x^2})^{-1}$
X=0.4
X=0.5
X=0.6
X=0.7
X=0.8
X=0.9
$X = \frac{g_o}{g_1} = 10$
$\alpha = \frac{I_{e1}}{I_{eo}}$
1.0
0.9
0.8
0.7
0.6
0.5
0.4
0
0.1
0.2
0.3
0.4
0.5
0.6
0.7
0.8
0.9
1.0

A17

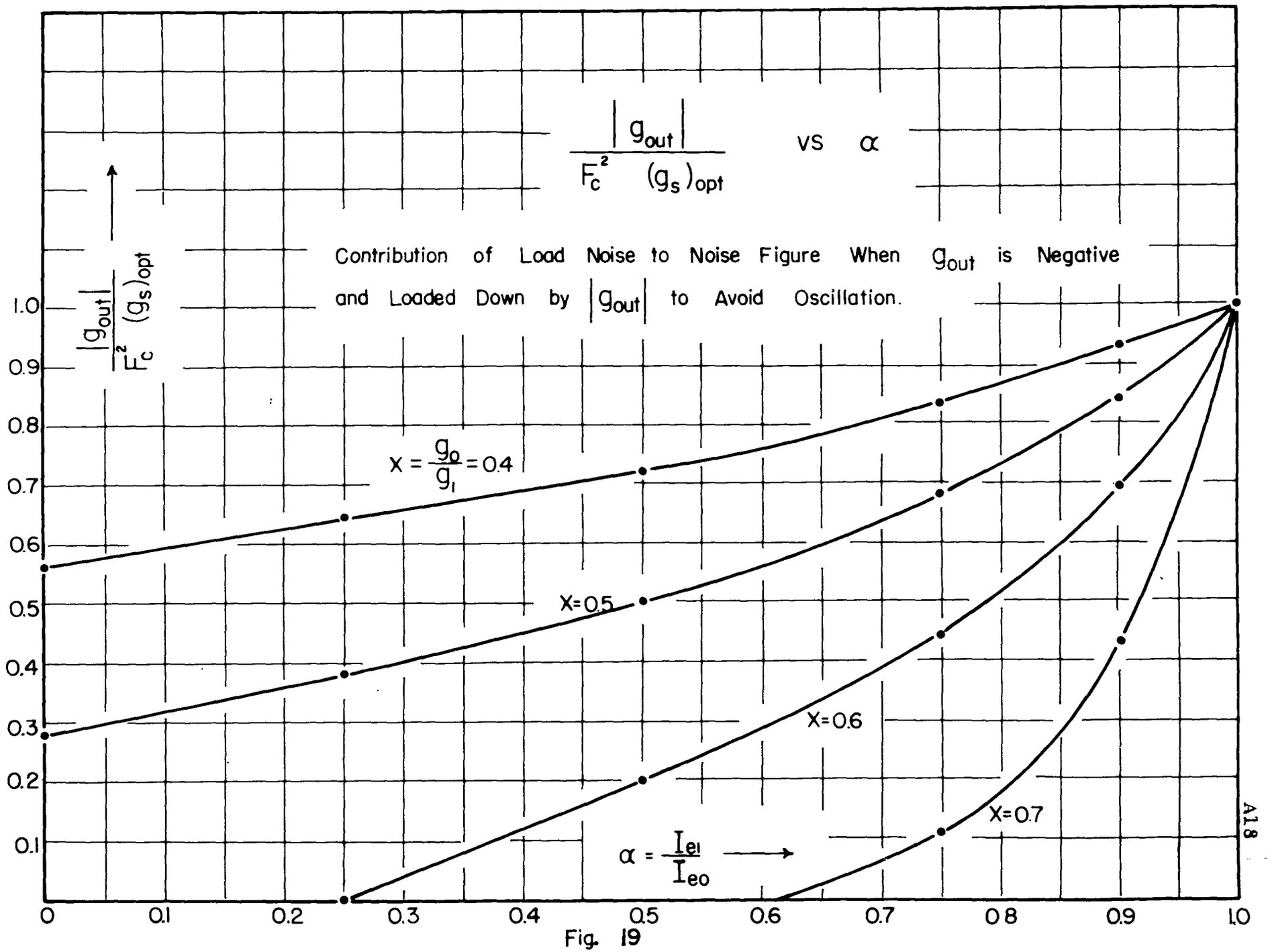
$\frac{|g_{out}|}{F_c^2 (g_s)_{opt}}$ vs α
Contribution of Load Noise to Noise Figure When g_{out} is Negative and Loaded Down by $|g_{out}|$ to Avoid Oscillation.
$\frac{|g_{out}|}{F_c^2 (g_s)_{opt}}$
1.0
0.9
0.8
0.7
0.6
0.5
0.4
0.3
0.2
0.1
$X = \frac{g_o}{g_i} = 0.4$
X=0.5
X=0.6
X=0.7
$\alpha = \frac{I_{ei}}{I_{eo}}$
0
0.1
0.2
0.3
0.4
0.5
0.6
0.7
0.8
0.9
1.0
A1.8
Fig. 19

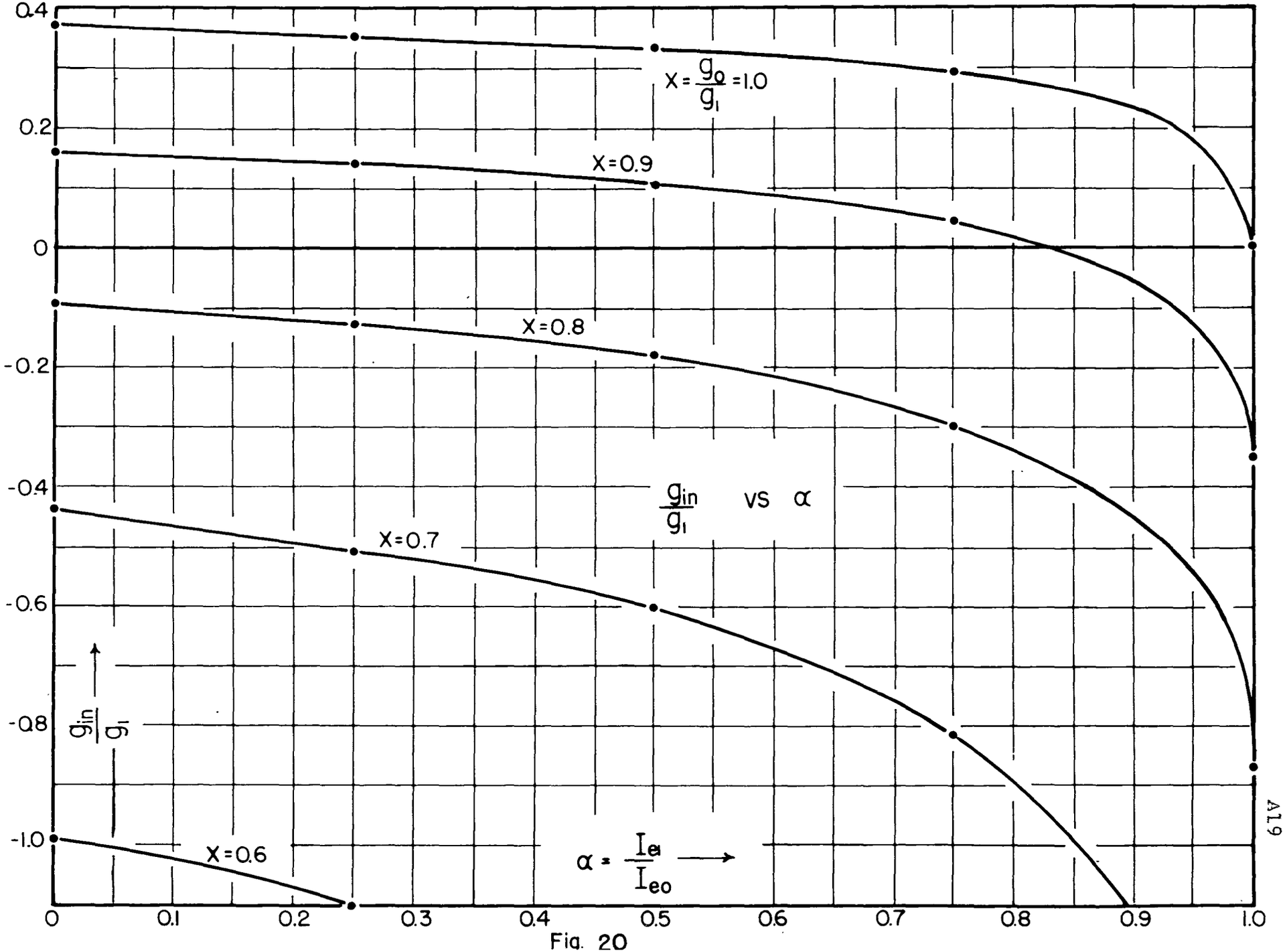
0.4
0.2
0
-0.2
-0.4
-0.6
-0.8
-1.0
0
0.1
0.2
0.3
0.4
0.5
0.6
0.7
0.8
0.9
1.0
X = g0/g1 = 1.0
X=0.9
X=0.8
X=0.7
X=0.6
gin/g1 vs α
gin/g1
α = Iei/Ieo

Fig. 20

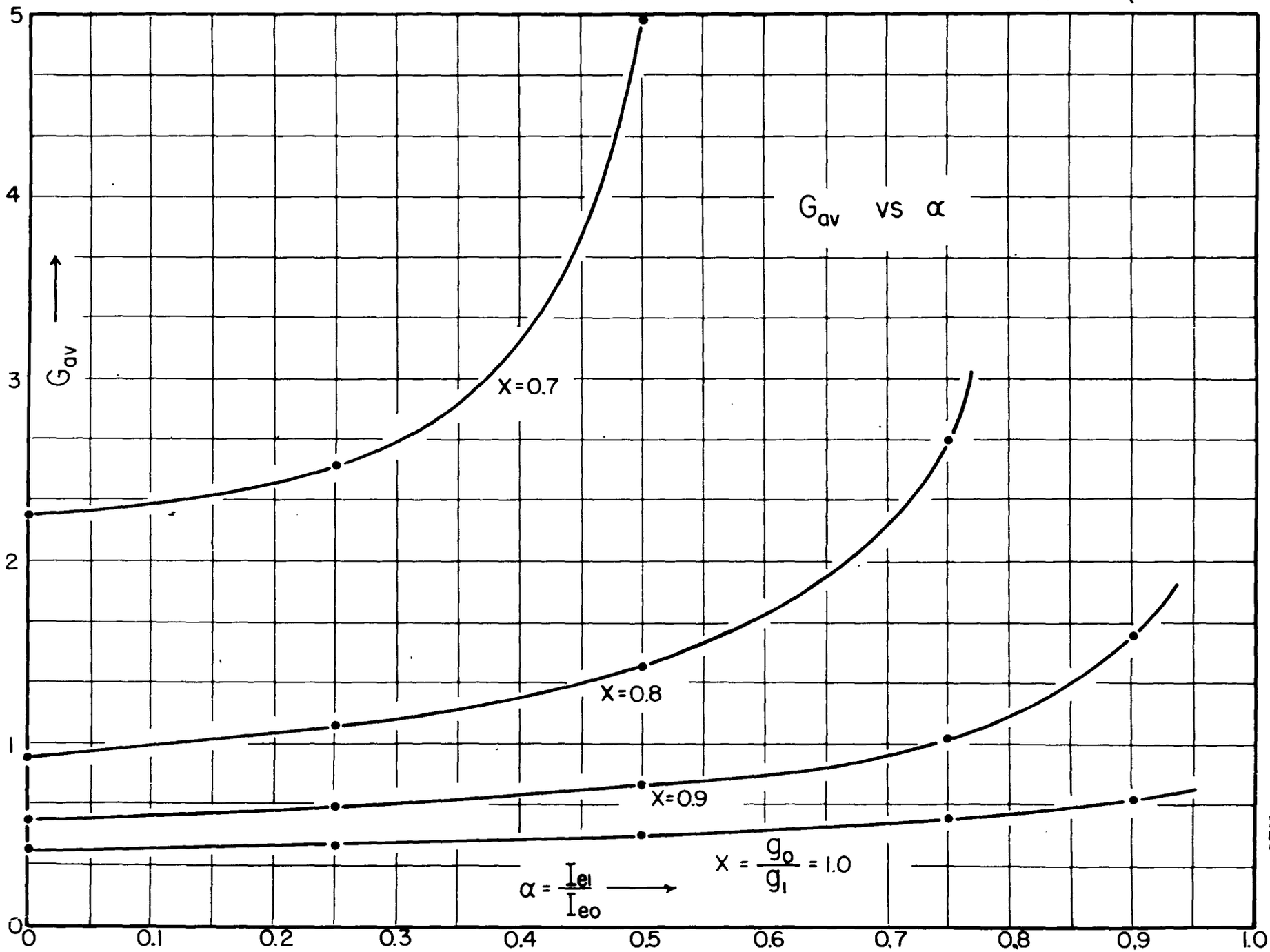
G_{av} vs α
G_{av}
X=0.7
X=0.8
X=0.9
$X = \frac{g_o}{g_1} = 1.0$
$\alpha = \frac{I_{e1}}{I_{eo}}$
0
1
2
3
4
5
0
0.1
0.2
0.3
0.4
0.5
0.6
0.7
0.8
0.9
1.0

Fig. 21

A20

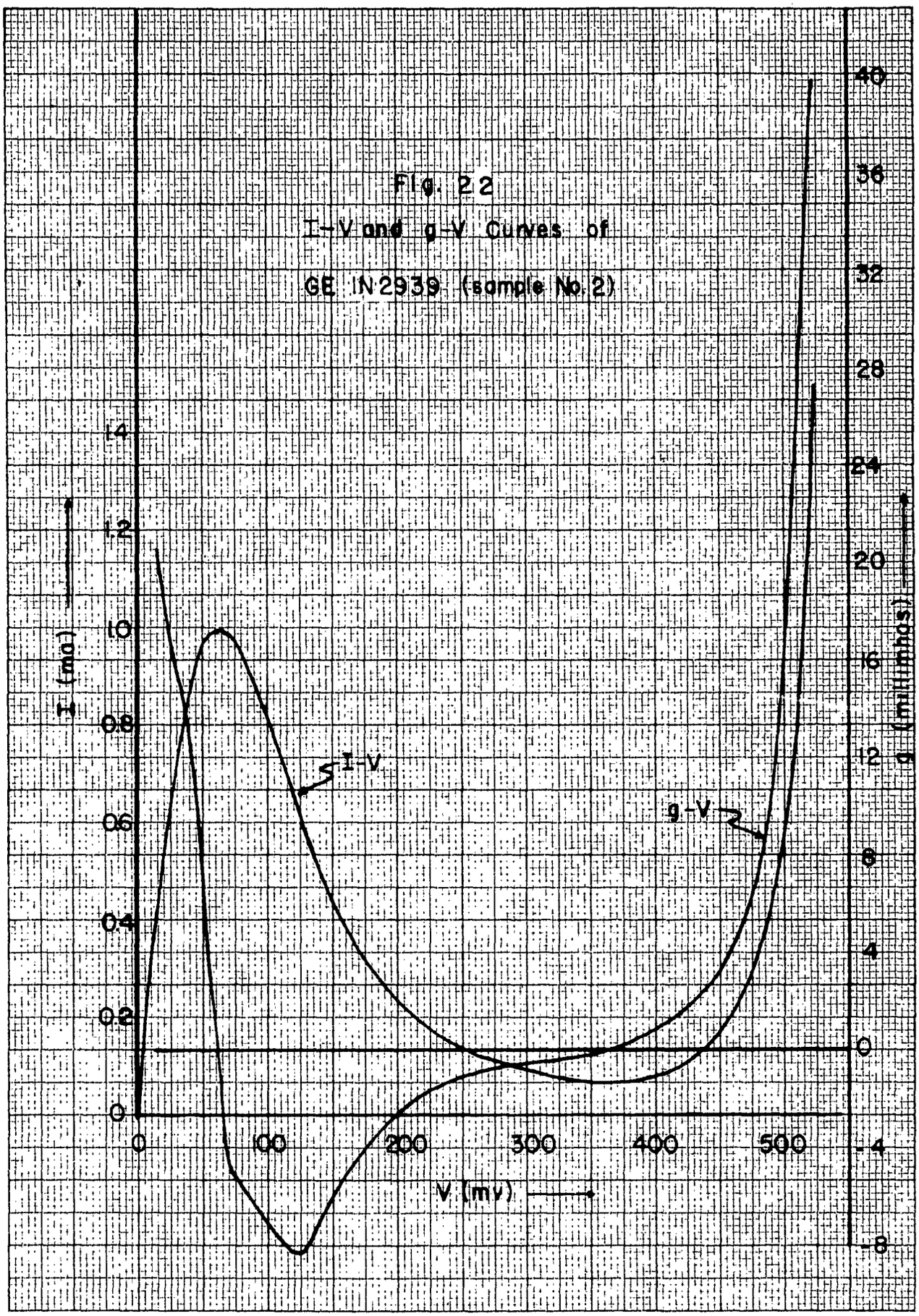

Fig. 22

I-V and g-V Curves of

GE IN2939 (sample No. 2)

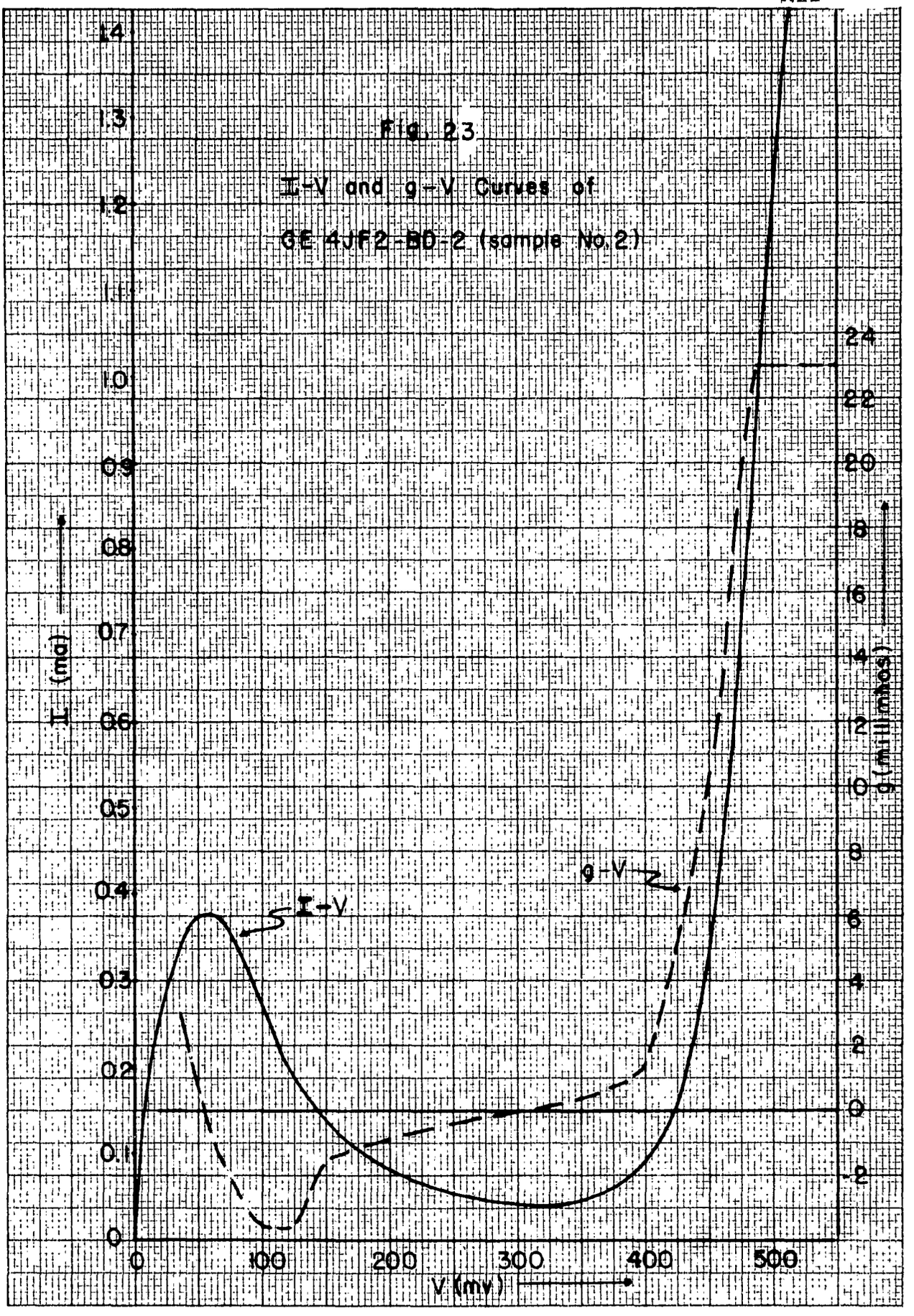

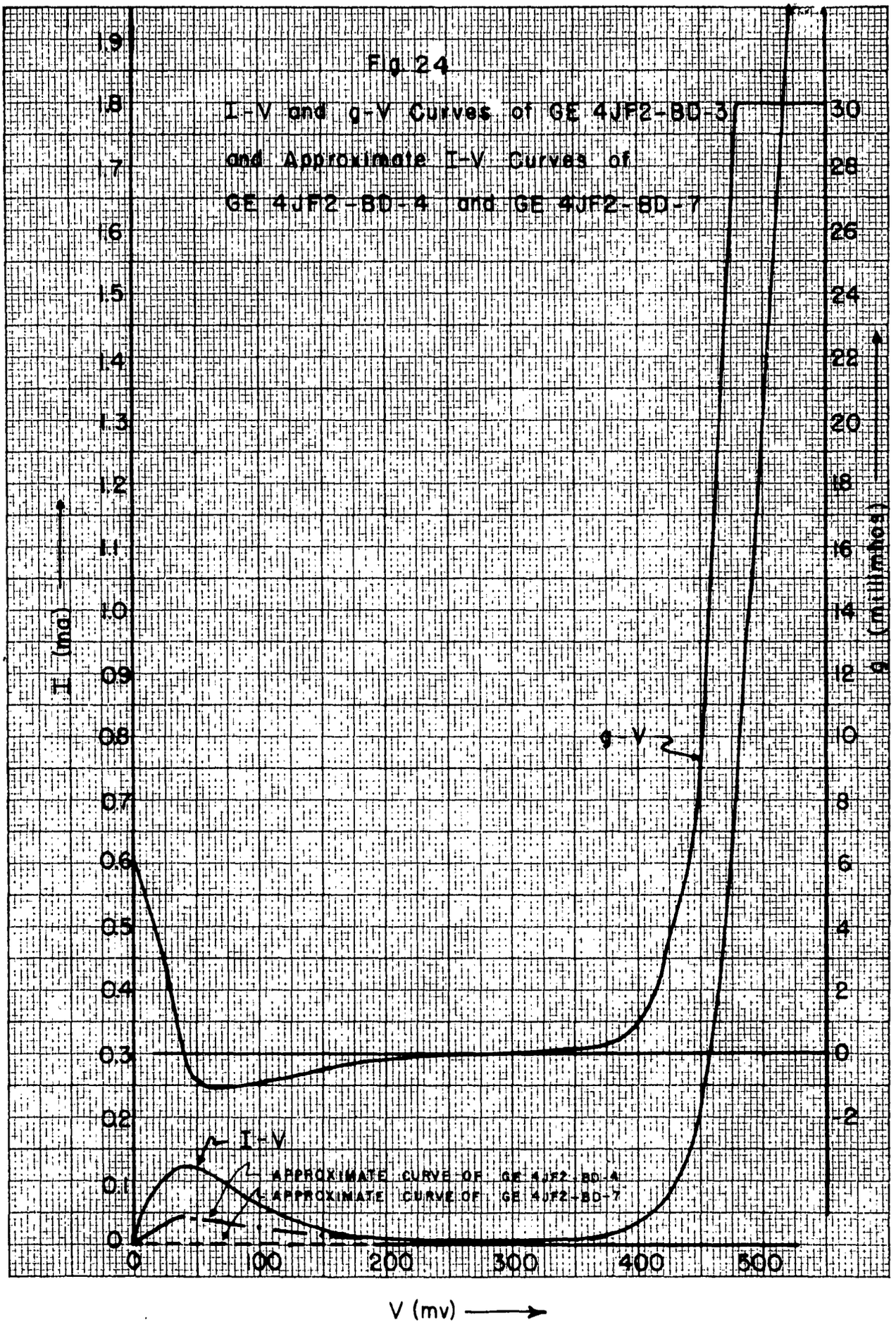

Fig 24

I-V and g-V Curves of GE 4JF2-BD-3

and Approximate I-V Curves of

GE 4JF2-BD-4 and GE 4JF2-BD-7

Fig. 25

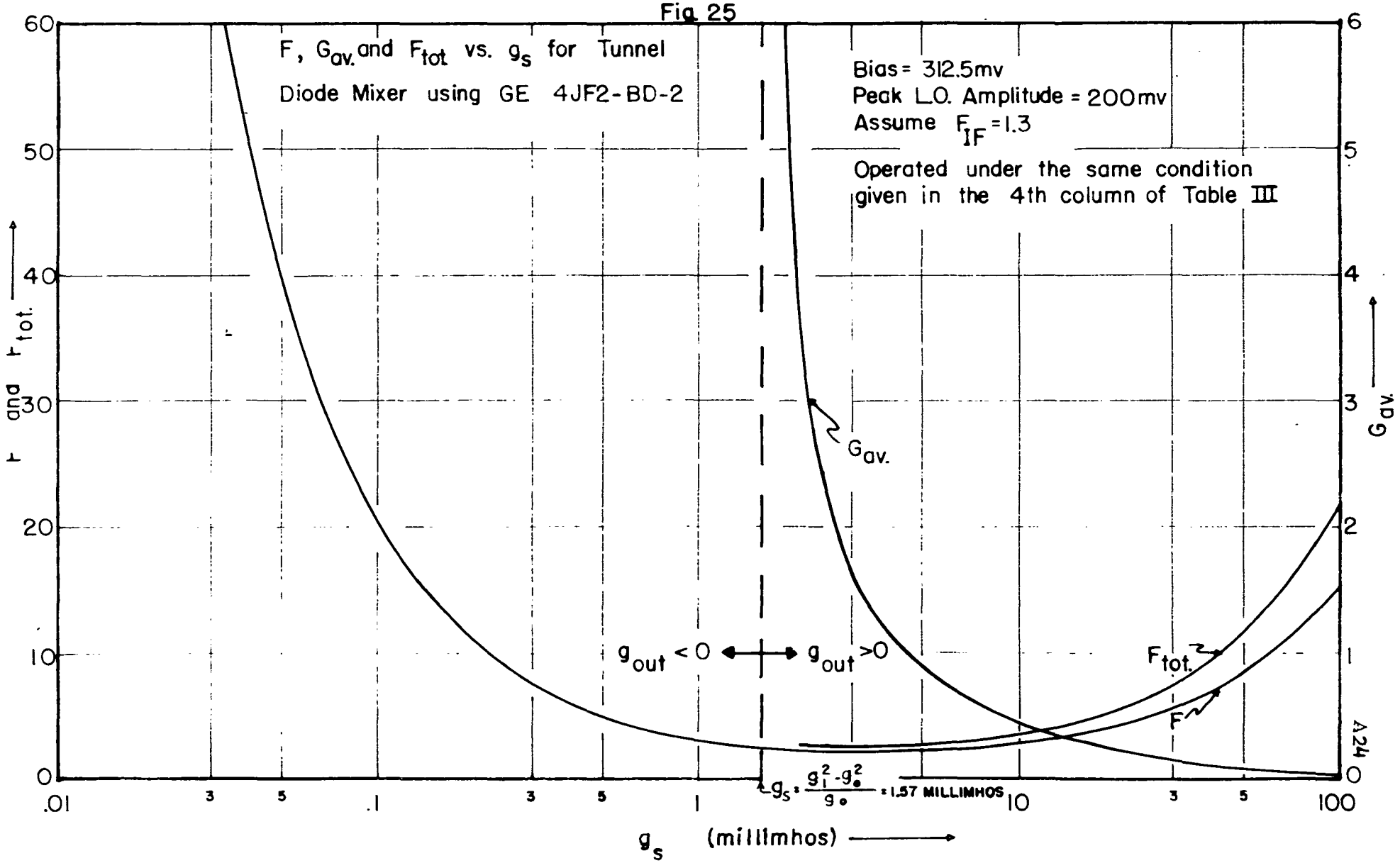
F, $G_{av.}$ and F_{tot} vs. g_s for Tunnel Diode Mixer using GE 4JF2-BD-2
Bias = 312.5mv
Peak L.O. Amplitude = 200mv
Assume F_{IF} = 1.3
Operated under the same condition given in the 4th column of Table III
F and $F_{tot.}$
$G_{av.}$
$G_{av.}$
$g_{out} < 0$
$g_{out} > 0$
$F_{tot.}$
F
$g_s = \frac{g_1^2 - g_o^2}{g_o}$ = 1.57 MILLIMHOS
g_s (millimhos)
60
50
40
30
20
10
0
6
5
4
3
2
1
0
.01
3
5
.1
3
5
1
10
3
5
100
A24

Fig. 26

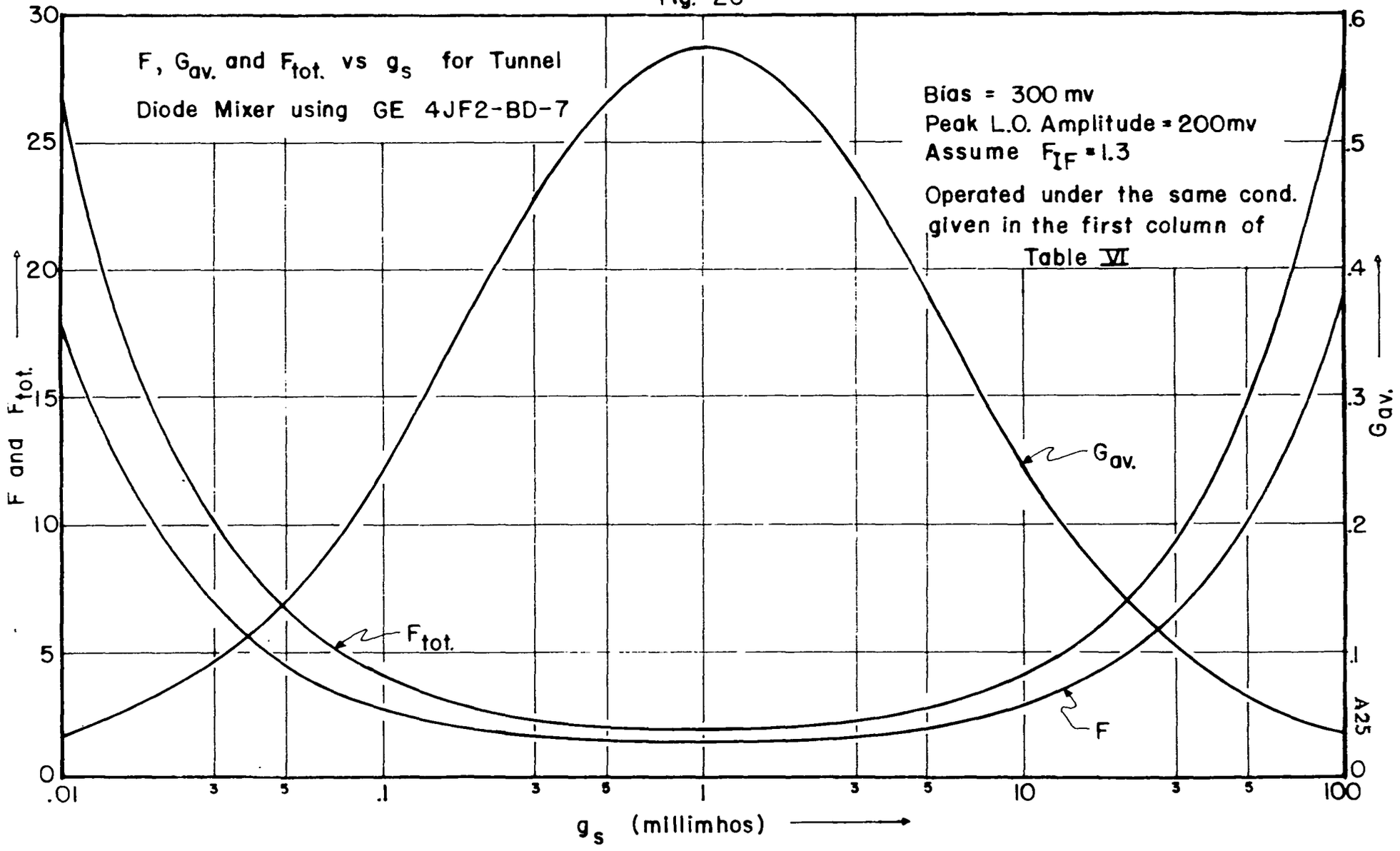
F, $G_{av.}$ and $F_{tot.}$ vs g_s for Tunnel Diode Mixer using GE 4JF2-BD-7
Bias = 300 mv
Peak L.O. Amplitude = 200mv
Assume F_{IF} = 1.3
Operated under the same cond. given in the first column of Table VI
$G_{av.}$
$F_{tot.}$
F
F and $F_{tot.}$
$G_{av.}$
A25
g_s (millimhos)
30
25
20
15
10
5
0
.6
.5
.4
.3
.2
.1
0
.01
3
5
.1
3
5
1
3
5
10
3
5
100

Fig. 27

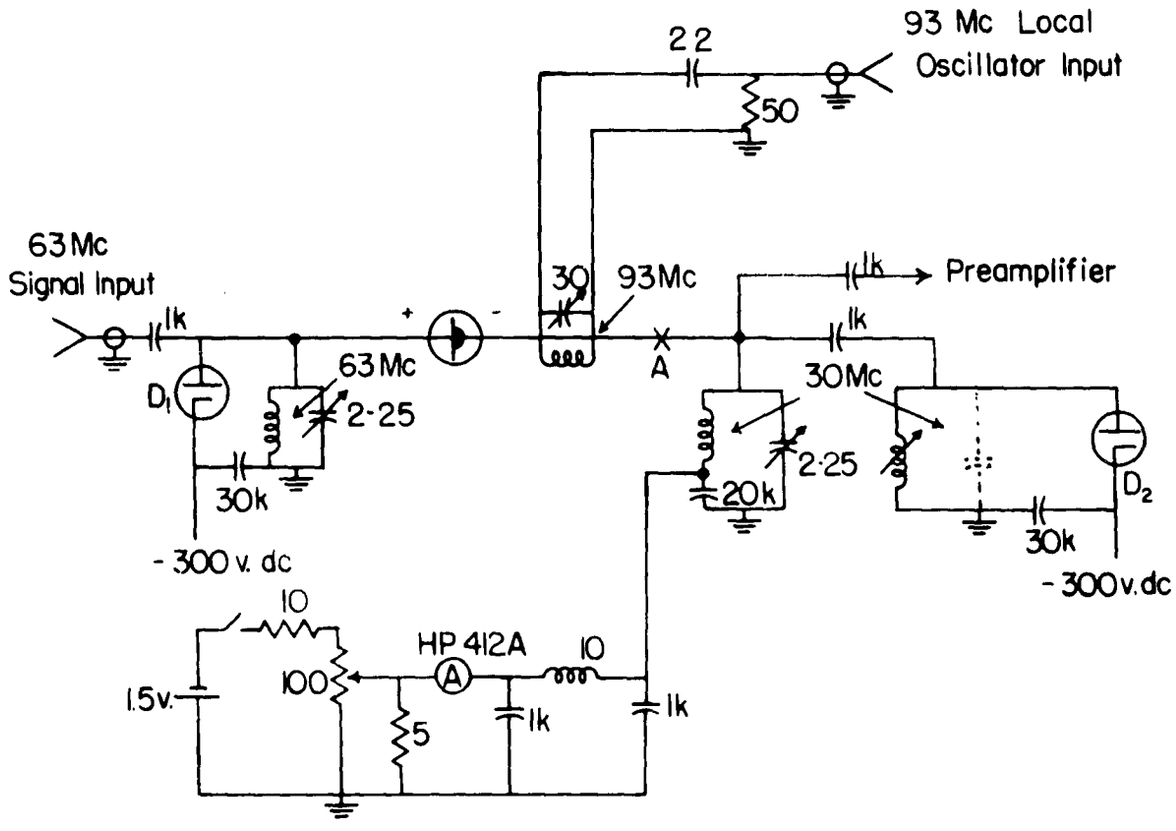

Resistor values are given in ohms.
Capacitor values are given in μμf.
Inductor values are given in μh.

Experimental Tunnel Diode Mixer With Noise Diodes at Both the Input and the Output

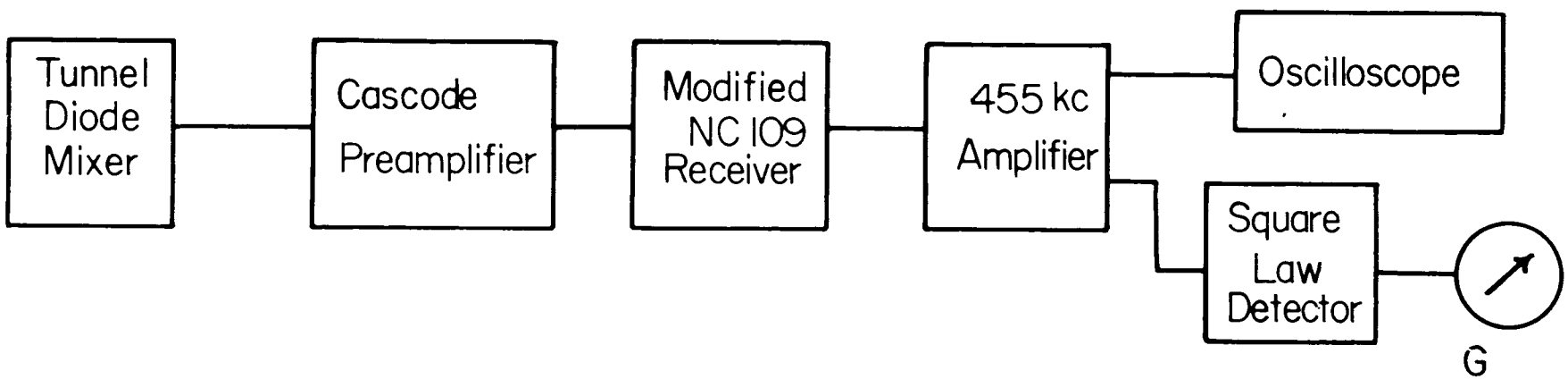

Block Diagram for Tunnel Diode Mixer Noise Measurement

A27

Fig. 28

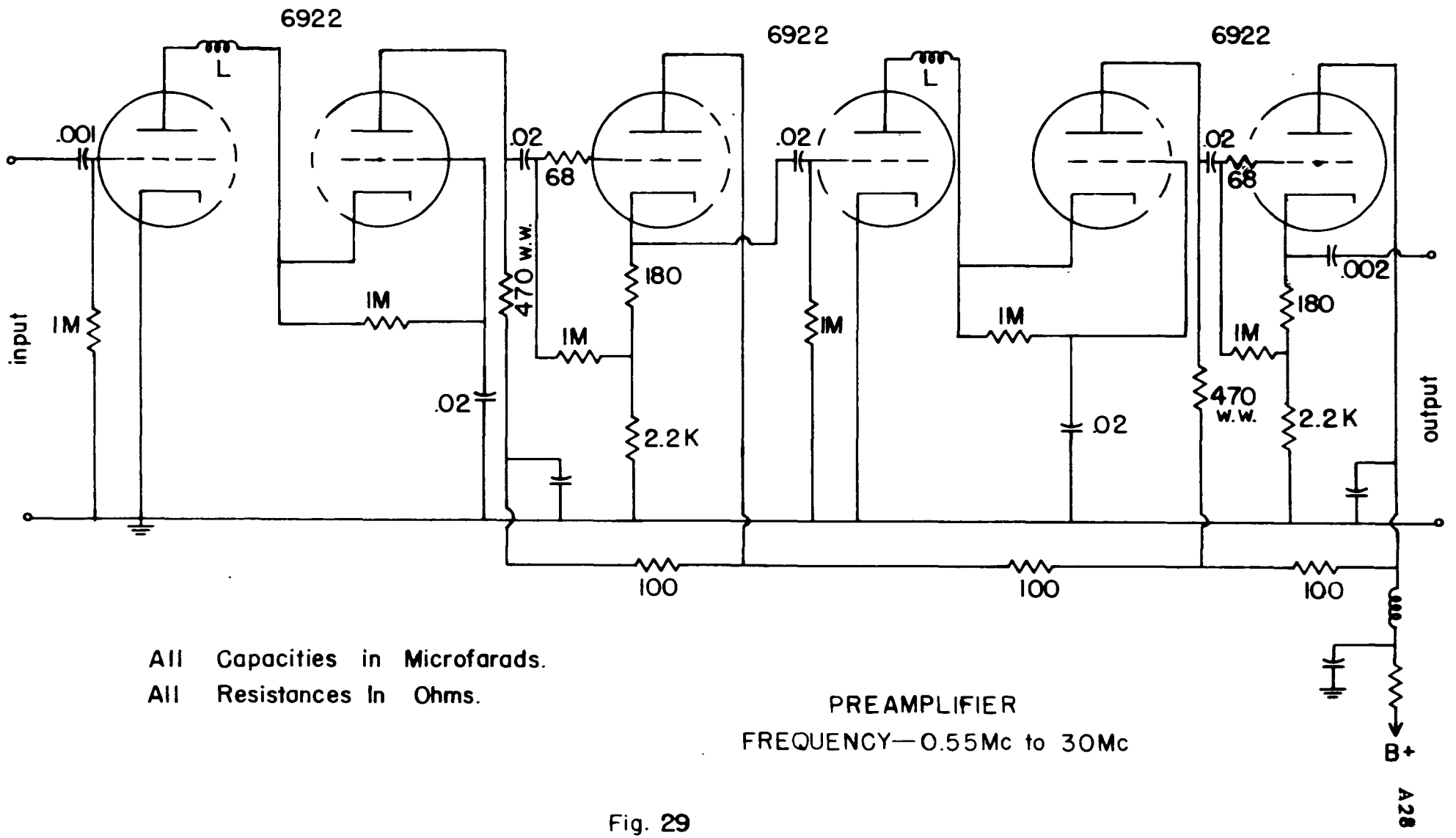

All Capacities in Microfarads.
All Resistances In Ohms.

PREAMPLIFIER
FREQUENCY—0.55Mc to 30Mc

Fig. 29

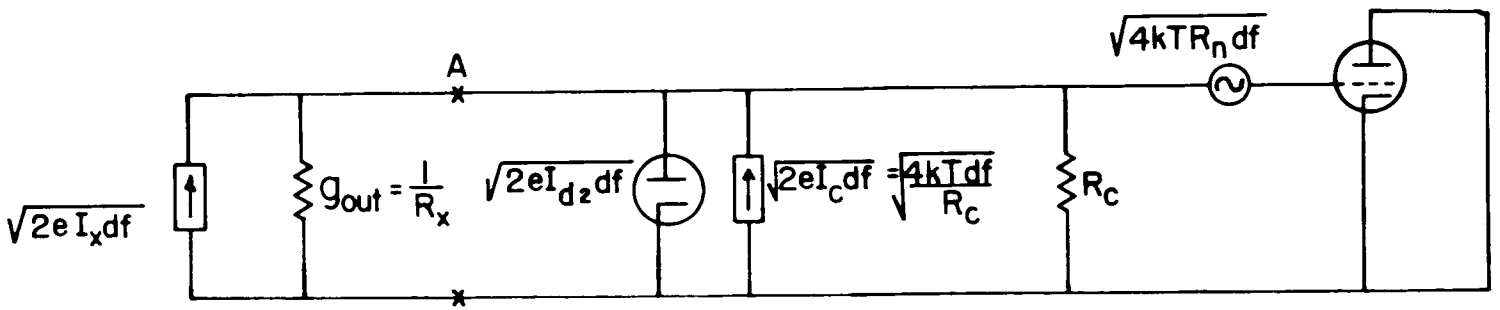

$\sqrt{2eI_x df}$ = Noise Current Generator Representing the Tunnel Diode Mixer.

$\sqrt{2eI_{d_2} df}$ = Noise Current Generator Representing the Noise Diode at the Output of the Mixer.

$\sqrt{2eI_c df}$ = Noise Current Generator Representing the Tuned Circuits at the Output of the Mixer

$\sqrt{4kTR_n df}$ = Electromotive Force Representing the Noise of the Equipment for Noise Measurement

Fig. 30

Equivalent Noise Circuit For Noise Measurement

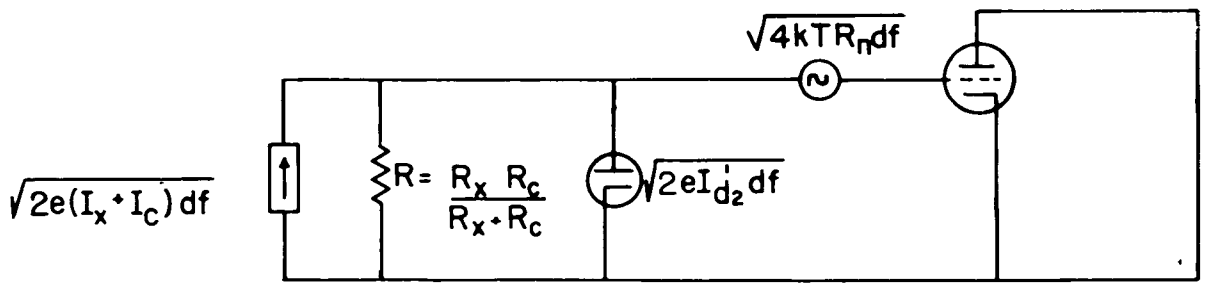

$\sqrt{2eI'_{d_2} df}$ = Noise Current Generator Representing the Noise Diode at the Output of the Mixer. Other Symbols are Defined in the Previous Figure.

Fig. 31

Equivalent Noise Circuit for Noise Measurement **(Modified)**

Fig. 32

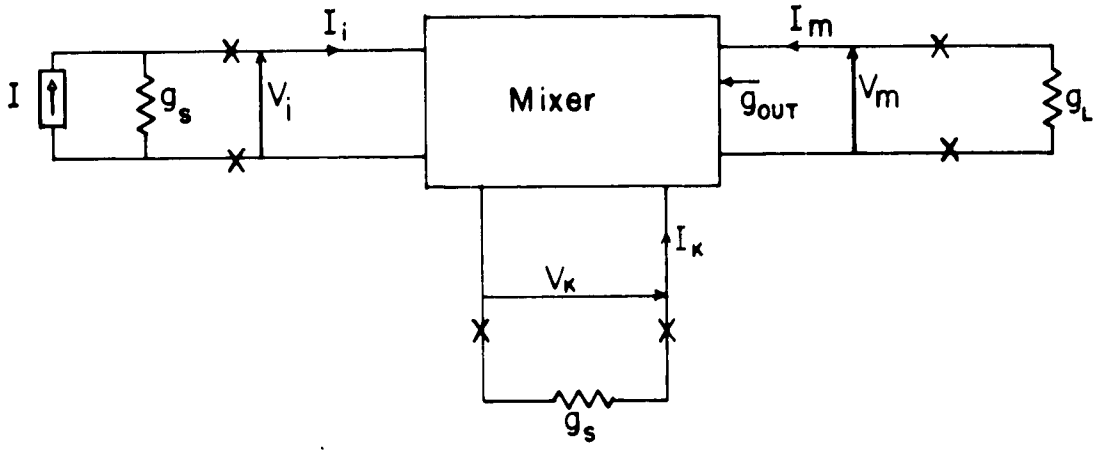

Mixer-terminal Conditions in the Broadband Case

Distribution List	# of Copies
Commanding Officer U. S. Army Electronics Material Support Agency Fort Monmouth, New Jersey Attn: SELMS-ADJ	1
Commanding General U. S. Army Electronics Command Attn: AMSEL-CG Forth Monmouth, New Jersey	1
Commanding Officer, 9560th TSU U. S. Army Electronics Research Unit P. O. Box 205 Mountain View, California	1
Director, U. S. Naval Research Laboratory Code 2027 Washington 25, D. C.	1
Commanding Officer and Director U. S. Navy Electronics Laboratory San Diego 52, California	1
Commander Wright Air Development Division Wright-Patterson Air Force Base, Ohio Attn: WCOSI-3	2
Commander Air Force Cambridge Research Center L. G. Hanscom Field Bedford, Massachusetts Attn: CROTLR-2	1
Commander Rome Air Development Center Griffiss Air Force Base, New York Attn: RAALD	1
Commander Armed Services Technical Information Agency Arlington Hall Station Arlington 12, Virginia	10
Advisory Group on Electron Tubes 346 Broadway New York 13, New York	2
Commanding Officer Frankford Arsenal Philadelphia 37, Pennsylvania Attn: ORDBA-FEL	1

DA36-039 sc-85374

# of Copies

Commanding Officer
Diamond Ordnance Fuze Laboratories
Connecticut Avenue and Van Ness Street
Washington 25, D. C.
Attn: T. T. Liimatainen — 1

Chief of Ordnance
Washington 25, D. C.
Attn: ORDTX-AR — 1

Technical Library
OASD (R and E)
Rm 3E1065, The Pentagon
Washington 25, D. C. — 1

Chief of Research and Development
OCS, Department of the Army
Washington 25, D. C. — 1

Department of the Navy
Bureau of Ships
Semiconductor Unit, Code 691A
Washington 25, D. C.
Attn: A. H. Young — 1

Commanding Officer
U. S. Naval Ordnance Laboratory
Corona, California — 1

General Electric Company
Electronics Park
Syracuse, New York
Attn: H. M. Sullivan — 1

University of Illinois
Urbana, Illinois
Attn: Dr. J. Bardeen — 1

Minneapolis-Honeywell Regulator Company
2753 Fourth Avenue, South
Minneapolis, Minnesota
Attn: Mr. L. Griffith — 1

Brown University
Providence 12, Rhode Island
Attn: John Truell — 1

Sprague Electric Transistor Laboratory
Marshall Street, Building 4
North Adams, Massachusetts
Attn: Mr. Kurt Lehovec — 1

H. R. B. Singer Co.
State College, Pennsylvania
Attn: Mr. S. Chaffee — 1

DA36-039 sc-85374

	# of Copies
Semiconductor Components Library Texas Instruments, Inc. P. O. Box 5012 Dallas 22, Texas	1
Western Electric Company 120 Broadway New York, New York Attn: Mr. J. Tweeddale	1
Battelle Memorial Institute 505 King Avenue Columbus, Ohio Attn: Librarian	1
Pacific Semiconductors, Inc. Research and Development Department 10451 West Jefferson Boulevard Culver City, California Attn: H. Q. North	1
Prof. John G. Linvill Electronics Laboratory Stanford University Stanford, California	1
U. S. Naval Research Laboratory Code 6451 Washington 25, D. C.	1
Director National Bureau of Standards Washington 25, D. C. Attn: Chief, Section 1.6 (Engineering Electronics)	1
Purdue University Lafayette, Indiana Attn: Prof. H. Y. Fan	1
Raytheon Company Semiconductor Division 150 California Street Newton 58, Massachusetts Attn: Semiconductor Division Library	1
Lincoln Laboratory Box 390 Massachusetts Institute of Technology Cambridge 39, Massachusetts Attn: A. L. McWhorter	1
Radio Corporation of America Princeton, New Jersey Attn: D. O. North	1

DA36-039 sc-85374

	# of Copies
Bell Telephone Laboratories Murray Hill, New Jersey Attn: H. C. Montgomery	1
Physics Dept. Syracuse University Attn: Dr. H. Levenstein Syracuse 10, New York	1
Motorola, Inc. 5005 East McDowell Avenue Phoenix, Arizona Attn: Dr. Bottom	1
The Ohio State University Antenna Laboratory 2024 Neil Avenue Columbus 10, Ohio	1
Commanding General U. S. Army Electronic Material Agency 225 South 18th Street Philadelphia 3, Pennsylvania	1
New York University College of Engineering University Heights, New York Attn: Dr. K. Cadoff	1
Directo National Bureau of Standards Boulder, Colorado Attn: Radio Library	1
Purdue University Physics Library Lafayette, Indiana	1
Marine Corps Liaison Office U. S. Army Electronics R and D Laboratory Fort Monmouth, New Jersey	1
The Moore School University of Pennsylvania Philadelphia 4, Pennsylvania Attn: Library	1
Hughes Aircraft Company Semiconductor Division P. O. Box 278 New Port Beach, California	1

DA36-039 sc-85374 # of Copies

Philco Corporation
Lansdale Division
Lansdale, Pennsylvania
Attn: J. R. Bordon 1

Commanding Officer
U. S. Army Electronics R and D Laboratory
Fort Monmouth, New Jersey
Attn: Director of Research 1
Attn: Chief, Technical Documents Center 1
Attn: Chief, Technical Information Division 3
Attn: Rpts Distribution Unit, Solid State and Frequency Control Div., (Record Copy) 1
Attn: Mr. T. Krueger, Solid State and Frequency Control Division 1
Attn: Mr. W. Dravneek, Surveillance Department 1
Attn: Ch. Microwave and Quantum Electronics Br., Solid State and Frequency Control Div. 1
Attn: K. Fischer, Solid State and Frequency Control Division 1

Chief, U. S. Army Security Agency
Arlington Hall Station
Arlington 12 Virginia 2

Deputy President
U. S. Army Security Agency Board
Arlington Hall Station
Arlington 12, Virginia 1

Total number of copies to be distributed - 70

This contract is supervised by the Solid State and Frequency Control Division, Electronic Components Depar ment, USAELRDL, Forth Monmouth, New Jersey. For further technical information contact Mr. Konrad H. Fischer, Project Advisor, Telephone 59-61792.